Facultad de Medicina
Clínica Alemana - Universidad del Desarrollo
Centro de Medicina Regenerativa

EVALUATION OF THE PROMOTION OF PRO-METASTATIC CAPACITIES MEDIATED BY sEVs SECRETED BY MDA-MB-231 METASTATIC BREAST CANCER CELLS AND IDENTIFICATION OF “EMT-PROMOTER” sEV-miRs PRESENT IN THEIR CARGO

BY: EDUARDO DURÁN JARA

Thesis presented to the Faculty of Medicine of Universidad del Desarrollo, to opt the academic degree of Doctor in Science and Innovation in Medicine

ADVISOR:
Mrs. LORENA DE LOURDES LOBOS-GONZÁLEZ, PhD

CO-ADVISOR:
Mr. MARCELO EZQUER, PhD

April 2023
SANTIAGO, Chile

To my beloved ones...and to myself

ACKNOWLEDGEMENTS

Fondap ACCDiS 15130011, Fondecyt 1211223, Fondef ID21I10210, Basal Funding Center for Regenerative Medicine ICIM UDD, Fondequip EQM160157 (Nanosight NS3000), Fondequip EQM190110 (QuantStudio 12K), Internal Grant UDD 23400174, UDD Internship Abroad Scholarship, PhD Scholarship UDD, National PhD Scholarship ANID, Operational Expenses National PhD Scholarship ANID.

TABLE OF CONTENTS

I. INDEX OF FIGURES ..... **x**

II. INDEX OF TABLES ..... **xii**

III. ABBREVIATURES ..... **xiii**

1. ABSTRACT ..... **xiv**

2. INTRODUCTION **1**

2.1 Breast cancer epidemiology (BC) 1

2.2 Small extracellular vesicles (sEVs) 2

2.2.1 sEVs as promoters of pro-metastatic capacities in recipient cells 3

2.3 miRNAs 4

2.3.1 Cellular dysregulation of miRNAs in cancer 5

2.3.2 Tumorigenic and pro-metastatic roles of miRNAs in BC 6

2.4 Epithelial-mesenchymal transition (EMT) 7

2.4.1 EMT importance in BC progression and metastasis 7

2.4.2 "EMT-promoter" miRNAs 9

2.5 sEVs as vehicles for miRNAs (sEV-miRs) 10

2.5.1 sEV-miRs as promotors of EMT, tumorigenesis and metastasis 11

2.5.2 sEV-miRs as promotors of EMT in BC 12

3. HYPOTHESIS AND AIMS **13**

3.1 Hypothesis 13

3.2 General aim 13

3.3 Specific aims 14

4. METHODOLOGY **14**

4.1 Antibodies 14

4.1.1 Primary antibodies 15

4.1.2 Secondary antibodies 15

4.2 Cell lines and cell culture 15

4.3 Animals 16

4.4 Statistical analyses 16

4.5 Specific aim 1 materials and methods 17

4.5.1 Isolation of sEVs 17

4.5.2 Characterization of sEVs 18

4.5.3 Transwell migration assay 20

4.5.4 Anchorage-independent growth evaluation. Colony formation 20

4.5.5 Tumoroid formation assay 21

4.6 Specific aim 2 materials and methods 22

4.6.1 miRNA-enriched RNA purification 23

4.6.2 small RNA sequencing 23

4.6.3 miRNA alignment and annotation 24

4.6.4 "Differential expression" analysis of sEV-miRs 25

4.6.5 Definition of candidate "EMT-promoter" sEV-miRs 25

4.6.6 Validation of candidate "EMT-promoter" sEV-miRs through miQPCR 26

4.6.7 Determination of sEV-miRs normalizers 29

4.7 Specific aim 3 materials and methods 30

4.7.1 Transfection of candidate sEV-miRs mimics 30

4.7.2 Evaluation of EMT markers in recipient cells treated with sEV-MDA231 or transfected with sEV-miR mimics 32

4.8 Specific aim 4 materials and methods 36

4.8.1 Evaluation of 3D migration mediated by "EMT-promoter" sEV-miRs mimics transfection by transwell assay 36

5. RESULTS 37

5.1 Specific aim 1 results 37

5.1.1 Isolation and characterization of sEVs secreted by MDA-MB-231 metastatic BC cells (sEV-MDA231) 37

5.1.2 sEV-MDA231 enhance in vitro 3D migration of tumorigenic non-metastatic BC cells 39

5.1.3 sEV-MDA231 increase the anchorage-independent growth potential of ductal carcinoma-derived BC cells 41

5.1.4 sEV-MDA231 enhance tumoroid formation of non-tumorigenic and BC cells in vitro . 43

5.1.5 sEV-MDA231 greatly promotes the formation of malignant ascites and tumor micronodules in a peritoneal carcinomatosis mice model 45

5.2 Specific aim 2 results 47

5.2.1 Characterization of BC cells-secreted sEVs 48

5.2.2 sRNA-seq analysis of BC cell-secreted sEVs shows different sRNAs profiles 50

5.2.3 Different/Several miRNAs are enriched in sEVs compared with parental cells 57

5.2.4 Several sEV-miRs are differentially enriched in sEV-MDA231 59

5.2.5 Validation of candidate "EMT-promoter" sEV-miRs using miQPCR 67

5.3 Specific aim 3 results 72

5.3.1 Evaluation of EMT-related genes in MCF10A and T47D cells after co-transfection of validated "EMT-promoter" sEV-miRs 72

5.3.2 Analysis of EMT-related markers after co-transfection of MCF10A and T47D BC cells with "EMT-promoter" sEV-miRs mimics 77

5.3.3 Evaluation of the expression of direct mRNA targets of co-transfected "EMT-promoter" sEV-miRs mimics 89

5.4 Specific aim 4 results 94

5.4.1 "EMT-promoter" sEV-miR mimics promote the 3D migration capacity of "normal" mammary epithelial MCF10A cells and tumorigenic non-metastatic T47D BC cells 95

6. DISCUSSION AND CONCLUSIONS 97

6.1 sEV-MDA231 promotes pro-metastatic capacities of recipient cells and greatly enhance the metastatic behavior of MDA-MB-231 TNBC cells *in vivo* 97

6.2 Characterization of the sRNA profile of sEV-MDA231 show the enrichment of several oncomiRs, participating in processes related with cell migration and EMT 102

6.3 The "EMT-promoter" sEV-miRs slightly promotes the expression of some EMT-markers in MCF10A "normal" mammary epithelial cells but not in T47D tumorigenic BC cells 107

6.4 The "EMT-promoter" sEV-miRs increase the migration capacity of MCF10A and T47D cells 112

7. BIBLIOGRAPHY 119

I. INDEX OF FIGURES

Figure 1: Characterization of sEVs secreted by MDA-MB-231 metastatic TNBC cells (sEV-MDA231). 38

Figure 2: Effect of sEV.MDA231 treatment on the migratory capacity of different BC recipient cells. 40

Figure 3: Effect of sEV-MDA231 treatment on the anchorage-independent growth potential of different BC recipient cells. 42

Figure 4: Effect of sEV-MDA231 treatment on the tumoroid formation capacity of different BC recipient cells. 44

Figure 5: Effect of sEV-MDA231 treatment on the formation of malignant ascites and tumor micronodules in a peritoneal carcinomatosis mouse model. 46

Figure 6: Characterization of sEVs secreted by different BC cell lines. 49

Figure 7: Characterization of the smallRNA profile of sEVs secreted by BC cells. 52

Figure 8: Identification of unique and common miRNAs in BC cell-secreted sEVs (sEV-miRs). 55

Figure 9: Identification of sEV-miRs differentially enriched in sEV-MDA231. 63

Figure 10: GO and pathway (KEGG) analysis summary of enriched sEV-miRs present in sEV-MDA231. 67

Figure 11: Validation of the presence and levels of “EMT-promoter” sEV-miRs in sEV-MDA231 through miQPCR. 69

Figure 12: Pathway (KEGG) and GO analysis summary of the six experimentally validated sEV-miRs present and enriched in sEV-MDA231. 71

Figure 13: Evaluation of miRNA mimic transfection efficiency in MCF10A cells. 74

Figure 14: Evaluation of sEV-miRs overexpression after co-transfection of “EMT-promoter” sEV-miRs mimics and treatment with sEV-MDA231 in MCF10A cells. 76

Figure 15: Evaluation of sEV-miRs overexpression after co-transfection of “EMT-promoter” sEV-miRs mimics and treatment with sEV-MDA231 in T47D BC cells. 77

Figure 16: Evaluation of the expression of EMT-markers after the co-transfection of “EMT-promoter” sEV-miRs mimics in MCF10A cells. 79

Figure 17: Evaluation of the expression of stemness and EMT-TFs after the co-transfection of “EMT-promoter” sEV-miRs mimics in MCF10A cells. 80

Figure 18: Evaluation of the expression of EMT-markers after the co-transfection of “EMT-promoter” sEV-miRs mimics in T47D BC cells. 82

Figure 19: Evaluation of the expression of stemness and EMT-TFs after the co-transfection of “EMT-promoter” sEV-miRs mimics in T47D BC cells. 83

Figure 20: Co-transfection of “EMT-promoter” sEV-miRs mimics in MCF10A cells. EMT-proteins evaluation by Western blot. 86

Figure 21: Co-transfection of “EMT-promoter” sEV-miRs mimics in T47D BC cells. EMT-proteins evaluation by Western blot. 88

Figure 22: Effect of “EMT-promoter” sEV-miRs mimic co-transfection on the expression of predicted mRNA targets in MCF10A cells. 92

Figure 23: Effect of “EMT-promoter” sEV-miRs mimic co-transfection on the expression of predicted mRNA targets T47D cells. 94

Figure 24: Evaluation of MCF10A and T47D cell migration after co-transfection with “EMT-promoter” sEV-miRs. 96

Figure 25: Research graphical summary. 117

II. INDEX OF TABLES

Table 1: Method for cDNA preparation from miRNA-enriched RNA from BC cells and sEVs 27

Table 2: Primers and oligonucleotides sequences used for miQPCR reaction 28

Table 3: qPCR protocol and method for the detection of enriched/overrepresented sEV-miRs. 29

Table 4: Final concentration of sEV-mIRs mimics transfected in MCF10A and T47D cells 32

Table 5: qPCR reagents and concentration used 34

Table 6: qPCR program, performed in a StepOne Plus or QuantStudio 12K thermalcycler 34

Table 7: Quality control and filtering of the raw data (input reads) of the sRNA-seq of BC and BC cells-secreted sEVs..... 50

Table 8: Reads aligned corresponding to mature or hairpin sequences of human miRNAs annotated 53

Table 9: Unique sEV-miRs detected in sEV-MCF10A, sEV-T47D, sEV-ZR75 and sEV-MDA231 56

Table 10: Enriched miRNAs loaded in sEVs compared with their parental cell of origin 58

Table 11: Total number of dysregulated sEV-miRs. Enriched and decreased sEV-miRs between each sEVs secreted by the different cell lines are indicated..... 62

Table 12: List of the twenty-two sEV-miRs identified as enriched in sEV-MDA231 compared with every other BC cells-secreted sEVs analyzed 62

Table 13: KEGG analysis of the 27 sEV-miRs enriched or selectively present in sEV-MDA231 64

Table 14: GO analysis of the 27 sEV-miRs enriched or selectively present in sEV-MDA231 64

Table 15: Stoichiometry and final concentration of each sEV-miR for the co-transfection assays 73

Table 16: Predicted mRNA targets for the six "EMT-promoter" sEV-miRs enriched in sEV-MDA231 89

III. ABBREVIATURES

BC: breast cancer

sEVs: small extracellular vesicles

RNA: ribonucleic acid

miRNAs: microRNAs

EMT: epithelial-mesenchymal transition

ECM: extracellular matrix

DMEM/F12: Dulbecco's modified essential medium/F12

FBS: fetal bovine serum

UC: ultracentrifugation

NTA: nanotracking analysis

TEM: transmission electron microscopy

WB: western blot

PBS: phosphate buffer saline

sRNA-seq: small RNA sequencing

sRNAs: small RNAs

tRNAs: transfer RNAs

piwiRNAs: piwi-associated RNAs

snoRNAs: small nucleolar RNAs

snRNAs: small nuclear RNAs

vRNAs: vaultRNA

sEV-miRs: small extracellular vesicle-associated miRNAs

PEG 8000: polyethylene glycol 8000

GO: Gene Ontology

KEGG: Kyoto Encyclopedia of Genes and Genomes

1. ABSTRACT

Breast cancer (BC) is one of the most common and deathly cancers worldwide. However, despite the improvements in screening and treatment, there is a high probability of local recurrence and distant metastasis to occur; the latter being the main cause of the patient's death. Communication between heterogeneous tumor cells mediated by small extracellular vesicles (sEVs) is essential to promote tumorigenesis and metastasis. sEVs are nanosized vesicles secreted by all cell types that mediate intercellular communication through their cargo, which include nucleic acids, proteins and other biomolecules. However, the mechanisms and specific molecules involved in these phenomena are still not completely defined and vary between different cancer types. Among the molecules described in the cargo of sEVs are microRNAs (sEV-miRs); small non-coding, single-stranded RNA molecules of approximately 20 nucleotides, which are master regulators of gene expression. It is widely demonstrated that cellular miRNA dysregulation can promote tumor growth, progression and metastasis. These findings have positioned miRNAs, and particularly sEV-miRs as a new research focus worldwide. Epithelial-mesenchymal transition (EMT) is a complex and dynamic process that involves many cellular and molecular changes. Cells undergoing EMT can increase their tumorigenic and pro-metastatic capacities, such as cell migration and invasion, cytoskeleton remodeling, increased anchorage-independent growth, among others. Some miRNAs have been implicated in the regulation of EMT in BC, such as members of the let-7 and miR-200 family, as

well as miR-105, miR-21 and miR-10b. However, to date there are very few studies that consider BC tumor cells-secreted sEVs as vehicles for “EMT-promoter” sEV-miRs, favoring the EMT and EMT-related phenotypic and functional changes (such as increased migration), promoting the tumorigenic and/or metastatic potential of recipient cells. Therefore, we hypothesize that the EMT and the migration of cells with no metastatic potential is favored by specific sEV-miRs in the cargo of metastatic BC cell-secreted sEVs. The aim of this project is to characterize the sEV-miRs profile of metastatic BC cells and identify specific sEV-miRs that could induce EMT and/or migration in cells with no metastatic potential. The findings of this thesis could be relevant in order to identify new possible BC biomarkers in sEVs, as well as the possible use of specific sEV-miRs as therapeutic options to treat this disease.

RESUMEN

El cáncer de mama (CM) es uno de los cánceres más comunes y mortales en todo el mundo. Sin embargo, pese a las mejoras en monitoreo, detección y tratamientos tempranos del tumor primario, existe una alta probabilidad de recurrencia local y metástasis a distancia; siendo esta última la principal causa de muerte de las pacientes. La comunicación entre células tumorales heterogéneas mediada por vesículas extracelulares pequeñas (sEVs; del inglés *small extracellular vesicles*) es esencial para promover el crecimiento tumoral y la metástasis. Las sEVs son nanovesículas secretadas por todas las células y median la comunicación intercelular a través de su cargo, el cual incluye ácidos nucleicos, proteínas y otras biomoléculas. Sin embargo, los mecanismos y moléculas específicas involucradas en estos fenómenos aún no están completamente definidos y varían entre diferentes tipos de cáncer. Entre las moléculas descritas en el cargo de las sEVs se encuentran los microRNAs (sEV-miRs); pequeñas moléculas de RNA monocatenario no codificante, de aproximadamente 20 nucleótidos, cuya función es la de reguladores maestros de la expresión génica. Se ha demostrado ampliamente que la desregulación de miRNAs celulares puede promover el crecimiento, la progresión y la metástasis del tumor. Estos hallazgos han posicionado a los miRNAs, y particularmente a los sEV-miRs, como un nuevo foco de investigación a nivel mundial. La transición epitelio-mesenquimal (EMT; del inglés *epithelial-mesenchymal transition*) es un proceso complejo y dinámico que involucra muchos cambios celulares y

moleculares. Las células que sufren una EMT pueden aumentar sus capacidades tumorigénicas y pro-metastásicas, como la migración e invasión celular, la remodelación de su citoesqueleto, el aumento de su capacidad de crecimiento independiente de anclaje, entre otras. Particularmente en CM, algunos miRNAs han sido implicados en la regulación de la EMT, tales como algunos miembros de las familias let-7 y miR-200, así como los miR-105, miR-21 y miR-10b. Sin embargo, hasta la fecha existen muy pocos estudios que consideren las sEVs secretadas por células tumorales de CM como vehículos para los sEV-miRs promotores de EMT, favoreciendo los cambios relacionados con EMT (como el aumento de la migración) y promoviendo el potencial tumorigénico y/o metastásico de células receptoras. Por lo tanto, planteamos la hipótesis de que la EMT y la migración de células sin potencial metastásico se ven favorecidas por sEV-miRs específicos en el cargo de sEVs secretadas por células de CM metastásicas. El objetivo de esta tesis es caracterizar el perfil de sEV-miRs de células de CM metastásicas e identificar sEV-miRs específicos que podrían inducir EMT y/o migración en células sin potencial metastásico. Los hallazgos de esta tesis podrían ser relevantes para identificar nuevos posibles biomarcadores de CM en sEVs, así como el posible uso de sEV-miRs específicos como opciones terapéuticas para tratar esta enfermedad.

2. INTRODUCTION

2.1 Breast cancer epidemiology (BC)

Breast cancer (BC) is one of the most relevant diseases in Chile and worldwide. According to the World Health Organization, in 2020 BC was the second most common cause of death worldwide. The latest GLOBOCAN data estimated more than 19 million new cases and more than 10 million deaths due to this disease during 2020 (1). In this context, BC is the most common cause of death associated with cancer in women (second considering both sexes) and the second with the highest incidence worldwide (1). In Chile, according to data from the Clinical Cancer Center of Clínica Las Condes, three women die every day from BC. In addition, 25% of new cases correspond to this type of cancer. On the other hand, despite the enormous scientific effort and advancements, current therapeutic strategies against BC are not effective. These alternatives include surgery, hormone-, chemo-, radio-, immunotherapy, or combination therapy. Their choice depends on various factors, including the clinical diagnosis, mutational burden, hormone receptors expression, tumor invasion, among others (2) (www.cancer.gov/about-cancer/treatment). However, despite being able to detect, treat and/or resect the primary tumor, there is a high probability of local recurrence and/or the formation of metastatic foci in distant tissues; these being the main responsible for causing patients' death (3–7).

2.2 Small extracellular vesicles (sEVs)

The presence of secreted vesicles in the extracellular space is known till the 60s' (8,9). However, it was not until 2011 when the term "extracellular vesicle" was proposed to define extracellular structures enclosed by a lipid bilayer (10). Extracellular vesicles (EVs) mainly includes plasma membrane-derived vesicles (i.e. microvesicles, oncosomes, and apoptosomes) and multivesicular bodies-derived vesicles (i.e. exosomes). EVs can be classified by their biogenesis machinery, molecular cargo, or even by their size (11–14); this case being classified as large EVs and small EVs (sEVs). On the other hand, communication between different and heterogeneous tumor cells is essential to promote tumorigenic capacities in less aggressive cells and for metastasis to occur efficiently. This intercellular crosstalk is largely mediated by EVs, particularly by sEVs (15–19). sEVs are 40-200 nm diameter nanovesicles secreted by virtually all cells types (12,20–22), and their cargo, which can include proteins, lipids, nucleic acids (DNA, mRNA, miRNAs and other non-coding RNAs (ncRNAs)) and other metabolites defines what changes will generate in a recipient cell. For instance, when a neighbor/target recipient cell incorporates tumor cell-secreted sEVs, this cell can undergo a "reprogramming". Examples of this reprogramming include the preparation of the pre-metastatic niche (when the recipient cells are in distant tissues) or the promotion of the migration and invasion capacities of other tumor cells in the same primary tumor; changes that ultimately can favor the metastatic process (17,23–25). However, the mechanisms by which sEVs

promote these phenomena are still not well understood and the specific responsible molecules involved have not been fully defined. Moreover, they can vary depending on the EVs subpopulation analyzed or the cancer type that is being studied (26–33).

2.2.1 sEVs as promoters of pro-metastatic capacities in recipient cells

Intercellular communication via sEVs can be auto-, para-, endo- or juxtracrine. Hoshino and colleagues have shown that the integrin profile in sEVs' cargo (mainly exosomes) secreted by different types of tumor cells, including BC cells, defines, in part, the site of metastasis (34). These sEVs are taken up by endothelial and epithelial cells from distant tissues, preparing the pre-metastatic niche and promoting the expression of pro-tumor and pro-metastatic proteins in tissues such as lungs and bone. On the other hand, it has been shown that exosomes secreted by BC cells contain transforming growth factor β (TGF-β), which in a paracrine manner, modulates the transformation of fibroblasts into myofibroblasts, favoring the growth of the primary tumor, increasing its vascularization and promoting its migration and invasion capacity (35,36). This paracrine action of exosomes is particularly relevant considering the great cellular heterogeneity in the primary tumor and the direct contact between cells with different degrees of transformation and aggressiveness, which can increase their tumorigenic and metastatic potential when receiving exosomes or sEVs secreted by other, more aggressive tumor cells. Recent studies have shown that sEVs

secreted by the metastatic TNBC cells, MDA-MB-231 (sEV-MDA231), promote the invasion capacity and anchorage-independent growth potential of two cell lines with no metastatic potential, such as MCF7 and T47D BC cells (37,38). Similar studies have described this phenomenon also in murine models (39). Considering this background, understanding the mechanisms by which sEVs secreted by BC tumor cells promote the gain of tumorigenic and pro-metastatic capacities, knowing their role and identifying the molecules responsible for increasing those properties in recipient cells would generate new biomarker candidates and possibilities of therapeutic targets against this disease.

2.3 miRNAs

One of the main components of the EVs' cargo corresponds to miRNAs (EV-miRs). miRNAs are small single-stranded, ncRNA molecules of 18-25 nucleotides in length, which are master regulators of gene expression through inhibiting translation and/or directly promoting the degradation of a target mRNA (40–45). To date, an enormous number of miRNAs has been described; most of them showing a specific expression pattern for each cell type (46–51) (https://www.mirbase.org/index.shtml). As the miRNA profile reflect the physiologic or pathophysiological state of a cell, the dysregulation of the cellular miRNA profile has been associated with the development and severity of several pathologies, including BC (52–57). However, the mechanisms by which this occurs and the implications it may have on the development and severity of the

disease are still not completely understood. Therefore, knowing the role of miRNAs in the regulation of tumor progression and metastasis is an area of great importance to better understand these phenomena and to discover new therapeutic targets.

2.3.1 Cellular dysregulation of miRNAs in cancer

As mentioned before, miRNAs are master regulators of gene expression. miRNAs exert their actions by complementarity and union of their 5' seed sequence with the 3' UTR of a target mRNA (58,59). Due to this mechanism of action, a single miRNA can target several different mRNAs. Similarly, a unique target mRNA can be targeted by several miRNAs. This promiscuity or versatility support the fact that the cellular miRNA profile can be used as a surrogate of the metabolic/physiologic/pathophysiological state of a cell. Notably, it has been shown that the miRNAs can act as better biomarkers than proteins or mRNAs (60), and even can better identify and classify different BC subtypes (50,52,55,57). On the other hand, it has been demonstrated that the dysregulation of the cellular miRNA profile (or dysregulation of specific miRNAs) is associated with tumor growth, progression, therapy resistance and metastasis (54–56,60). For instance, upregulation of miR-200c and miR-141 and down regulation of miR-124a and miR-26b promotes metastasis by indirectly increasing SerpinB2 or c-Jun expression (61). In another studies, it was shown that upregulation of miR-21 is associated with resistance several treatments (62,63), and increase BC cells

invasion (64). On the other hand, downregulation of tumor suppressor miRNAs is far most common. Several studies have shown that downregulation of tumor suppressor miRNAs such as miR-101, miR-497, miR-143, miR-340, miR-34a or miR-138 can regulate tumor cell apoptosis, increase tumor cell proliferation, migration, invasion and EMT (56).

2.3.2 Tumorigenic and pro-metastatic roles of miRNAs in BC

There is a significant number of miRNAs involved in tumorigenesis and metastasis, both oncogenic (oncomiRs) and tumor-suppressor miRNAs (46,65,66). The dysregulation of the cellular miRNA profile, being a tumor cell or a healthy neighbor cell, can trigger the overexpression of oncogenic proteins or the downregulation of tumor suppressor proteins, which ultimately leads to primary tumor growth, progression and the consequent development of metastases. Particularly in BC, the most studied miRNAs are members of the miR-200 and let-7 families, as well as miR-105, miR-10b, among others (60,67–70). However, most of these studies have been focused on the dysregulation of miRNAs in the tumor cell itself or in cells of the tumor microenvironment, but do not address cellular communication mechanisms that could be triggering these changes, for example, transport and delivery through sEVs. Within the few studies involving sEV-miRs, it has been suggested that some of these (miR-26a-5p, miR-181b-5p, miR-487b-3p), secreted by lung cancer cells exposed to TGF-β, are responsible for increasing the tumorigenic potential of neighboring cells, for

example, promoting tumor cell migration and epithelial-to-mesenchymal transition (EMT) (71). On the other hand, there are recent reports indicating that the transfer of some sEV-miRs promotes resistance to radio- or chemotherapy in BC tumor cells (72–75). Although there are studies focused on the sEV-miRs profile in various types of cancer, there is no further evaluation of their specific role promoting tumorigenic or metastatic capacities in the context of BC. For this reason, interest arises in studying the specific effect of the sEV-miRs secreted by metastatic BC cells on the pro-tumorigenic and pro-metastatic phenotypic changes that it could cause when incorporated by another recipient cell (tumor or healthy).

2.4 Epithelial-mesenchymal transition (EMT)

EMT is a complex cellular and molecular process, essential for tissue remodeling and metastases development (76). Cells undergoing EMT can increase their invasive and migratory capabilities, promotes cytoskeleton and extracellular matrix remodeling, increase their anchorage-independent growth capacity, upregulate the expression of molecules and transcription factors characteristics of a mesenchymal stage, among others (76–79).

2.4.1 EMT importance in BC progression and metastasis

As in most of cancers, the mechanisms behind BC progression and subsequent metastasis are still not fully elucidated. Moreover, new molecular and

epidemiological players are discovered every day. The EMT is an important process by which tumor cells adapt and develop new ways to increase their migratory and invasive potential in order to spread and colonize new distant tissues (76,78). Importantly, the EMT is a dynamic and not categorical process in which a cell gains mesenchymal properties and lose their epithelial characteristics (76). In this context, the EMT is not the same in every cancer type; molecules and transcription factors (TFs) involved, as well as functions and capacities gained are different between different cancer (76,80). Particularly in BC, there are contradictory results regarding the importance of the EMT in the metastatic cascade, especially in the *in vivo* context (76). For instance, in BC mouse models, it has been shown that EMT, mediated by the activation of Snail1 TF, occurs in the primary tumor and it is important for tumor cell invasion and formation of CTCs, but not for metastatic colonization (81,82). In 2016, an elegant and interesting study in mice showed that a small pool of BC tumor cells undergoes spontaneous EMT. This results in increased motility and dissemination capacity, which finally increased metastasis (83). Other reports had associated the activity of other TFs in the regulation of EMT in BC such as Zeb1 (84,85), Twist1 (86,87), or Notch family members (88). In addition, other TFs associated with tumor cell stemness have been associated with the EMT, tumor cell renewal and therapy resistance, such as Nanog or Oct4 in BC and others (89–91). Furthermore, “effector” molecules are equally important mediating the functional effects of an EMT, such as Vimentin (92), N-Cadherin (93,94) or ECM proteins such as

fibronectin (95,96), modulating cytoskeleton remodeling and tumor cell adhesion loss, increasing cell migration and invasion. As the importance of EMT in the metastatic cascade is getting clearer, and the number of molecules contributing to this process increase, authors have tried to set guidelines and strict definitions to better understand this area, and to draw reproducible and impactful conclusion (80). One of those molecules not so recently involved with the acquisition of the EMT are miRNAs, which also need to be carefully considered when studying this phenomenon.

2.4.2 "EMT-promoter" miRNAs

As master regulators of gene expression, it is not weird that miRNAs can modulate the acquisition of the EMT. It has been largely demonstrated that miRNAs can promotes or inhibit the EMT in different contexts (65,97–99). However, considering tumor heterogeneity and miRNAs versatility of action, the study of the effect of miRNAs modulating the EMT is not so straightforward. In a cancer context, several cellular miRNAs are or may be dysregulated, causing that blaming only one miRNA for an effect is very difficult. The appearance and apogee of next generation sequencing technologies, such as that to sequences miRNAs, has generated incredible growth in the study of this process (57,100) (see elsewhere in the TCGA or GEO databases). Particularly in BC, several studies have implicated several different miRNAs in the acquisition and development of the EMT. For instance, members of the miR-200 and let-7 family of miRNAs have

been widely implicated in the inhibition of the EMT. On the other hand, oncomiRs such as miR-9, miR-34a, miR-23a, miR-10b or miR-21 have been shown to promote the EMT by different mechanisms. The following reviews and articles clearly describe several miRNAs involved in the regulation of the EMT in BC, and highlights their importance in the progression of the disease (56,67,69,101–105). The problem is that most studies consider just one dysregulated miRNA, and use strategies to increase or knock out the expression of that miRNA to evaluate its effect, greatly altering its expression and excluding other dysregulated miRNAs that may be working together to cause the final effect and give rise to an EMT phenotype. Other important thing to take into consideration is that, as mentioned. miRNAs can be transported and delivered by secreted sEVs. This topic is even harder to test, because several issues such as miRNA abundance in sEVs (not only in BC, but also in other contexts) (106–109), or miRNA functional delivery mediated by these vesicles. Thus, the study of miRNAs, either in the cellular context or within a sEVs, is of great importance to better understand their implications in the development of the EMT.

2.5 sEVs as vehicles for miRNAs (sEV-miRs)

The delivery of functional sEV-miRs in different disease settings is nowadays a hot research topic. Furthermore, since the cargo of sEVs can reflect the metabolic and physiological state of a tumor cell, the transport and delivery of sEV-miRs in the context of cancer is increasingly important as they can act as cancer

biomarkers (progression, metastasis, recurrence, therapy resistance) (100,110–114), or they can exert a functional effect in neighbor or distant recipient cells in the organism (115–120). All this offers the possibility of using sEV-miRs as biomarkers and/or therapeutic targets (direct or indirect) to treat cancers (121).

2.5.1 sEV-miRs as promotors of EMT, tumorigenesis and metastasis

Recent evidence suggests a fundamental role of EVs (including sEVs and exosomes) as “EMT-promoters” (122–125). Furthermore, some studies have shown that exosomes secreted by invasive tumor cells are capable of inducing EMT in healthy recipient cells (123). To date, most studies have focused on the analysis of the EVs proteome during the EMT process (126–129). On the other hand, references in the literature focused on the analysis and identification of sEV-miRs and their effect on this process are scarce, despite the biological importance of these oligonucleotides (and also that of sEVs) in tumor progression and metastasis development. Recently, exosomes from melanoma cells have been shown to promote EMT in melanocytes through a miR-191 and let-7a-dependent mechanism (125). In another study published in 2018, the authors identify the exo-miRs profile of lung cancer cells before and after undergoing EMT, induced by TGF-β. The profile of exo-miRs secreted by A549 lung cancer epithelial cells was found to be different from that of these same cells after EMT. Furthermore, these exosomes (M-exosomes; from *mesenchymal exosomes*) were capable of

inducing EMT in tumor and non-tumor epithelial recipient cells, which demonstrates the importance of sEV-miRs in this process (71).

2.5.2 sEV-miRs as promotors of EMT in BC

In the context of BC, the results are quite scant. Although there are reports that show the action of sEVs on the EMT of a tumor recipient cell, only a few molecules, mostly proteins, have been directly involved in this process (for example TGF-β). In the case of miRNAs, recent studies suggest the participation of miR-137 in the induction of EMT in BC models (130), however the participation of EVs in this phenomenon was not directly addressed in that study. Other reports suggest the participation of other cells of the tumor microenvironment as exosomes or EVs-producers, such as endothelial cells, immune cells or fibroblasts (117,119,131,132). For instance, Donnarumma and coworkers showed the participation of EV-miR-21, -378 and -143 secreted by cancer-associated fibroblast as promoters of EMT in BC tumor cells was described (119). Finally, Singh et al., reported an increase in the invasion capacity of mammary epithelial cells (one of the typical EMT characteristics) mediated by EV-miR-10b secreted by metastatic BC cells (133).

In summary, it has recently been suggested that specific molecules in the cargo of EVs could function as markers of tumorigenicity and metastasis in BC (15,113,134,135), however, most are focused on the proteome of these

nanovesicles. Research focused on the effects and specific roles of sEV-miRs on the phenotypic changes, from their involvement in EMT to the development of metastasis, are scarce. Existing studies are limited to the characterization of the sEV-miRs profile of metastatic cells, but they do not go deep investigating the specific role of different sEV-miRs on the EMT of a tumor recipient cell in the context of BC. Therefore, this thesis seeks to identify and characterize the complete sEV-miRs profile of metastatic BC cells and assess their role on EMT and the enhancement of metastatic potential of non-metastatic, less aggressive BC cells.

3. HYPOTHESIS AND AIMS

3.1 Hypothesis

The promotion of epithelial-mesenchymal-related pro-metastatic capacities in non-metastatic recipient cells is favored by specific miRNAs present in metastatic MDA-MB-231 breast cancer cell-secreted small extracellular vesicles.

3.2 General aim

To identify specific miRNAs in metastatic BC cell-secreted sEVs and to evaluate their role in the promotion of EMT-related pro-metastatic capacities in non-metastatic recipient cells.

3.3 Specific aims

1. To evaluate the effect of metastatic sEV-MDA231 over the acquisition/promotion of tumorigenic and pro-metastatic capacities of non-tumorigenic and non-metastatic recipient cells.

2. To characterize the miRNA profile of sEVs (sEV-miRs) secreted by metastatic and non-metastatic BC cells and to define candidate EMT-promoters.

3. To evaluate the role of candidate sEV-miRs overrepresented/enriched in metastatic sEV-MDA231 on the expression of EMT molecular markers in non-metastatic BC cells.

4. To evaluate the role of candidate sEV-miRs overrepresented/enriched in metastatic sEV-MDA231 on the migration capacity of non-tumorigenic and non-metastatic BC cells (as a surrogate of the EMT).

4. METHODOLOGY

4.1 Antibodies

4.1.1 Primary antibodies

Rabbit anti-human CD63 (Abcam ab68418), mouse anti-human TSG101 (Santa Cruz sc-7964), rabbit anti-human Flotillin 1 (Cell Signaling #18634S), mouse anti-human Calnexin (Santa Cruz sc-46669), rabbit anti-human Vimentin (Cell Signaling #5741S), mouse anti-human E-Cadherin (Santa Cruz sc-8426), mouse anti-human N-Cadherin (Santa Cruz sc-8424), rabbit anti-human Zeb1 (Cell Signaling #70512S), rabbit anti-human Twist1 (Cell Signaling #69366S), rabbit anti-human Snail1/Slug (Abcam ab85931), mouse anti-human GAPDH (Santa Cruz sc-47724), mouse anti-human β-actin (Santa Cruz sc-47778).

4.1.2 Secondary antibodies

Anti-mouse IgG-HRP (Cell Signaling #7076), anti-rabbit IgG-HRP (Cell Signaling #7074), goat anti-mouse 680LT (Licor #925-68020) and goat anti-rabbit 800CW (Licor #92532211).

4.2 Cell lines and cell culture

Human BC cell lines T47D, ZR75 and MDA-MB-231 were obtained from ATCC (ATCC® HTB133TM, ATCC® CRL1500TM, and ATCC® HTB-26TM, respectively) and cultured in DMEM/F12 medium (Gibco #12400-024), supplemented with 10% fetal bovine serum (FBS; Capricorn Scientific #FBS-HI-12A) and 100 UI/mL penicillin, 0.1 mg/mL streptomycin and 0.05 mg/mL

gentamicin. MCF10A immortalized normal mammary epithelial cell line were kindly donated by Dr. Flavia Bruna (Instituto de Medicina y Biología Experimental de Cuyo (IMBECU), CONICET, CCT-Mendoza, Argentina), and cultured in DMEM/F12 medium supplemented with Brain Pituitary Extract, hEGF, Insulin, Hydrocortisone, and GA-1000 according with the instructions (MEGM™ Mammary Epithelial Cell Growth Medium SingleQuots™ Kit; Lonza #CC-4136). All cell lines were cultured/incubated at 37 °C, 5% CO_2.

4.3 Animals

Animal studies were conducted in accordance with the guidelines of the Ethical Committee of Clínica Alemana Universidad del Desarrollo. Immune-compromised NOD/SCID mice were obtained from Jackson Laboratories (Bar Harbor, ME). Mice were maintained in the animal facility of Facultad de Medicina, Clínica Alemana Universidad del Desarrollo, in an exclusive, temperature-controlled environment, conditioned with HEPA filters, with a 12/12 h light/dark schedule, and sterile food and water ad libitum.

4.4 Statistical analyses

Graphs and statistical analysis were performed in GraphPad Prism v8 software. Parametric student t test was used to compare 2 groups. Two tailed parametric ANOVA or non-parametric Kruskal-Wallis test were used when comparing 3 or

more groups. Tukey's or Dunn's correction were used for multiple comparisons as correspond. All differences were considered statistically significant if $p < 0.05$.

4.5 Specific aim 1 materials and methods

To evaluate the effect of metastatic sEV-MDA231 over the acquisition/promotion of tumorigenic and pro-metastatic capacities of non-tumorigenic and non-metastatic recipient cells.

4.5.1 Isolation of sEVs

Cell culture conditioned medium was used for sEVs isolation. When used for this purpose, FBS was previously depleted of extracellular vesicles (EV-depleted FBS) by ultracentrifugation at 100,000 × g for 16 h at 4 °C. The supernatant was then filtered through 0.22 μm syringe filters (GE Healthcare) and use to prepare complete culture medium. For sEVs isolation, 1.5-2.0 x 10^6 cells were seeded in complete culture medium (supplemented with 10% regular FBS and antibiotics as described). *Twenty-four hours later, cell culture medium was discarded, the cells were washed 1-2 times with 1X sterile PBS and culture medium was replaced with EV-depleted FBS-supplemented DMEM/F12 (plus antibiotics) cell culture medium until it reached 80-90% confluence. After 48 h, the supernatants were collected. Conditioned medium obtained from each cell line was centrifuged first at 3,000 x g for 10 min to eliminate cell debris and then at 10,000 x g for 15 min to eliminate bigger vesicles (mainly apoptotic bodies). The supernatants were then filtered

through 0.22 µm filters and centrifuged at 100,000 x g for 2 h at 4 °C (Ultracentrifuge Hanil 5, Korea; fixed rotor #9). sEVs pellets were washed, suspended in cold PBS and stored at -80 °C until use. *Note: As an alternative protocol, twenty-four hours after cell seeding, cell culture medium was discarded and replaced with 10 mL Optimem (Gibco #22600-050) per 100 mm plate and supplemented with antibiotics as described. Cell culture supernatant was collected 48 h later to isolate sEVs. Cell culture supernatants were centrifuged first at 3,000 x g for 10 min to eliminate cell debris and then at 10,000 x g for 15 min to eliminate bigger vesicles (mainly apoptotic bodies). The supernatants were then filtered through 0.22 µm filters and concentrated using Amicon 100 MWCO tubes (Merck Millipore #UFC910024). Finally, sEVs were obtained through precipitation and size-exclusion columns using Exo-Spin™ exosome purification kit according to manufacturer instructions (Cell Guidance #EX01-25).*

4.5.2 Characterization of sEVs

sEVs were characterized through three different techniques: nanotracking analysis (NTA), transmission electron microscopy (TEM), and western blot (WB). For NTA, cell culture supernatant-isolated sEVs were diluted 1:100 with filtered sterile PBS and injected into Nanosight NS300 instrument (NanoSight NTA 2.3 Nanoparticle Tracking and Analysis Release Version Build 0033; Malvern Instruments. Fondequip EQM160157) to measure particle concentration and size distribution. Camera was set to capture three videos of 30 s each per sample.

Videos were then analyzed to determine the size distribution plus an approximation to the quantity of particles (Camera level 11-12; Gain 5). *Note: for a more reliable quantification, samples should be diluted to show >10 particles per frame in every video. If there are less particles, it is not recommended to use those concentration values*. For TEM characterization, sEVs were deposited on Formvar-carbon coated grids (TED Pella. Mountains Lake, CA, USA). After 1-2 min of adsorption, the excess was removed with absorbent paper and contrasted with uranyl acetate pH 7.0 for 1 min; excess was removed and dried for 1-2 additional min at room temperature. The samples were observed using a Talos F200C G2 electron microscope at 80 kV (Unidad de Microscopía Avanzada UC (UMA). Pontificia Universidad Católica de Chile, Santiago, Chile). Finally, for WB analysis, 15 µg of sEVs total protein extracts were lysed with RIPA buffer and sonicated twice in a bath sonicator (Power Sonic 405; LabTech) for 10 min at medium potency. Total protein extracts were mixed with Laemmli loading buffer (BioRad #1610747), heated at 95 °C for 5 min and loaded in 10-12% SDS-acrylamide gels. Proteins were transferred to nitrocellulose membranes which were blocked (Intercept TBS blocking buffer; Licor #927-70001) for 1 h and probed with antibodies against EV markers (CD63, TSG101) and negative markers (Calnexin) to evaluate possible cellular contamination. Finally, bound antibodies were detected with anti-IgG 680LT/800CW secondary antibodies (1:10,000 dilution) and revealed in an Odyssey Clx imaging system (Licor).

4.5.3 Transwell migration assay

To evaluate the effect of sEV-MDA231 over the 3D migration capacity of BC cells we used transwell assay. Briefly, Boyden chambers were previously hydrated with DMEM/F12 culture medium for 1 h. 2.5 x 10^4 cells were seeded on the upper chamber of 24-well transwell plates. After that, ~5,000 particles per seeded cell (generally 5 µg total protein) were added to the cells to evaluate the effect over 3D migration capacity of BC cells. After 16 h, transwell inserts/membranes were collected, fixed with 4% PFA and stained with DAPI (Sigma Aldrich D9542). Cells on the other side of the inserts were visualized on an inverted fluorescence microscope and counted in at least 10 fields.

4.5.4 Anchorage-independent growth evaluation. Colony formation

Anchorage-independent cell growth capacity was determined by colony formation in soft agar as previously described (136). Briefly, MCF10A (5.0 X 10^3), MCF7 (7.5 X 10^3), T47D (5.0 X10^3), ZR75 (5.0 X10^3) and MDA-MB-231 (3.5-4.0 X 10^3) cells were seeded in 12-well plates suspended in soft agar (UltraPure™ Agarose Invitrogen™; #16500-100) and incubated for 24 h. After that time, cells were treated with 10 µg of total protein sEVs (or the equivalent to ~5,000 particles/per cell), 2 µg of anti-lactadherin antibody or left untreated. Formation of colonies >50 µm or >100 µm in diameter was scored 1 and 2 weeks respectively, after treatments under a phase-contrast microscope at 10X as described (136). At least 10 fields per condition were counted (Durán-Jara, E. et al., 2023. In revision).

4.5.5 Tumoroid formation assay

BC cells (5.0 x 10^5 MCF10A, 7.5 x 10^4 MCF7 or MDA-MB-231) were seeded on sterile 2% agar-covered plates (6 well-plates), supplemented with Mammary Epithelial Cell Growth culture medium (at least 1.5 mL of MEGM™ (Lonza, cat. CC-3151) supplemented with EGF 25 ηg/mL, hydrocortisone 0.5 g/mL, insulin 5 µg/mL (Lonza, cat. CC-4136) and bFGF 25 ηg /mL (Invitrogen; cat PHG0026). To evaluate the effect of sEV-MDA231 on tumoroid/spheroid formation, 5 µg of sEV-MDA231 were added to each well at the same day of cell seeding. Tumoroids/spheroids were grown at 37 °C, 5% CO_2 for 14 d. Cell culture medium was not renewed during the 14 d of the experiment and the formation of spheres was visually recorded by photography using Micrometrics SE Premium 4 software in a Nikon Eclipse TS100 inverted microscope. After 14 d, cell culture medium with the spheres was extracted from the well and passed through a 70 µm filter (BD Falcon, cat.352350). The spheres retained on the filter were recovered and plated onto a 12-well adhesion plate (Corning, cat. 3512). After 24 h, the adhered spheres were fixed with 4% PFA in 1X PBS for 10 min, washed and stained with DAPI 1:300 for 10 min. Finally, spheres were washed 3 times with 1X PBS and visualized and recorded under the same microscope to confirm that the recovered spheres remain viable.

4.5.6 Peritoneal carcinomatosis murine model

Two groups of seven NOD/SCID mice (two separate experiments) were inoculated intraperitoneally (ip) with 2.0×10^6 MDA-MB-231 cells in 200 µL saline, either alone (saline group) or together with sEV-MDA231 (10 µg sEV-MDA231; 1st dose). Seven days after tumor cell inoculation, the mice were treated again with sEV-MDA231 (2nd dose). The mice were treated on days 7, 9, 11, 15, 17, and 19 (six doses). The animals were euthanized 21 days after cell injection. The mesenteric tissue and retroperitoneal tumor masses were excised and fixed in 4% PFA. Malignant ascites were collected and the total cell number was determined by trypan blue exclusion assay. For tumor micronodule measurements, the tumor tissues were fixed and paraffin-embedded. Histological sections of mesenteric tissue were first stained with hematoxylin and eosin (HE). Images of the HE-stained sections were gray-scale-transformed to define a hyperdense area. The number of tumor micronodules in the mesenteric tissues of the peritoneal cavity was evaluated using purple hyperchromia. Tumor area was also measured by gray range density/intensity, which coincides with denser nuclear staining of tumor cells. The final *in vivo* evaluation was performed in a double-blind manner.

4.6 Specific aim 2 materials and methods

To characterize the miRNA profile of sEVs (sEV-miRs) secreted by metastatic and non-metastatic BC cells and to define candidate EMT-promoters.

4.6.1 miRNA-enriched RNA purification

Cellular and sEV-RNA were purified using miRNeasy kits (Qiagen #217004) according to the manufacturer instructions. As the obtained sEV-RNA is a very small amount, the final elution volume for sEV-RNA was 10-15 µL. On the other hand, for cellular RNA, the elution volume was 30 -40 µL.

4.6.2 small RNA sequencing

The sequencing of sRNAs was carried out by the company Novogene (https://en.novogene.com/). Basically, miRNA-enriched RNA samples (both cells and sEVs) were subjected to quality control prior to the sequencing. Cellular RNA samples had to have a RIN >7.5 and sEVs RNA samples had to have a sharp peak of small RNAs between 25-200 nt and no peaks >2,000 nt. Library preparation was performed using the NEBNext kit (New England Biolabs®, UK). Sequencing was performed on the NovaSeq6000 (Illumina. San Diego, CA, USA) with the following specifications: single-end 50 bp and >20 million reads per sample. The adapters used were:

5’ adapter: 5’-GTTCAGAGTTCTACAGTCCGACGATC-3’

3’ adapter: 5’-AGATCGGAAGAGCACACGTCT-3’

4.6.3 miRNA alignment and annotation

To perform the alignment and annotation of miRNAs, the fastq files obtained after the sequencing were uploaded to the sRNAbench (137,138) (https://arn.ugr.es/srnatoolbox/) web platform and aligned against the GRCh38_p10 version of the human genome. The parameters were set as follow:

5' adapter: 5'-GTTCAGAGTTCTACAGTCCGACGATC-3'

3' adapter: 5´-AGATCGGAAGAGCACACGTCT-3'

Library preparation: NEBnext protocol (preloaded, matches the 3' adapter)

Phred score threshold: 33

Low quality reads filter method: minimum mean quality score (a read is accepted if the average Phred score is above a certain threshold)

Low quality reads filter threshold: 20

Alignment type: bowtie seed alignment (only mismatches in seed region)

Seed length for alignment: 20 nt

Minimum read count: 10 nt

Minimum read length: 16 nt

Allowed mismatches: 1 nt

Maximum number of multiple mapping: 10 nt

Reference annotation database: human miRBase v22

4.6.4 "Differential expression" analysis of sEV-miRs

For differential expression (DE) analysis, the sRNAtoolbox platform was also used, using the sRNAde tool (138). sRNAde allows DE analysis to be performed through different known software/packages such as DESeq2, edgeR and NOISeq. As we do not have biological replicates, the edgeR package was used for this analysis. We performed the DE analyzes comparing miRNA profiles of MDA-MB-231 vs MCF10A cells (metastatic vs non-tumorigenic) and between different sEVs, i.e sEV-MDA231 vs sEV-MCF10A (metastatic vs non-tumorigenic) and sEV-MDA231 vs sEV-T47D/sEV-ZR75 (metastatic vs tumorigenic but non-metastatic). DE was defined as a fold change ≤0.5 and ≥2, with a significant p value <0.05. More information about edgeR statistical analysis can be found here (139).

4.6.5 Definition of candidate "EMT-promoter" sEV-miRs

As MDA-MB-231 breast cancer cells are highly metastatic and have a marked mesenchymal phenotype, we used sEVs secreted by this cell line to identify candidate sEV-miRs that could be implicated in the promotion of EMT. We compared the overrepresented DE sEV-miRs (fold change ≥2, p value <0.05) in sEV-MDA231 versus every other cell line-secreted sEVs (sEV-MCF10A, sEV-T47D, sEV-ZR75). We used the venny v2.0.2 tool (https://bioinfogp.cnb.csic.es/tools/venny/index2.0.2.html) to generate lists and Venn diagrams to find sEV-miRs overrepresented always in sEV-MDA231,

independent of the comparison made. We also included sEV-miRs only detected in sEV-MDA231 as candidates (not detected in the other sEVs). Subsequently, using webtools such as miRWalk (140,141) (http://mirwalk.umm.uni-heidelberg.de/), STRING (142) (https://stringdb.org/), and Panther (143–145) (http://www.pantherdb.org/), candidate "EMT-promoter" sEV-miRs secreted by sEV-MDA231 were subjected to mRNA target prediction, interaction, gene ontology (GO) and pathway analyses to evaluate their possible biological, oncogenic and metastatic function.

4.6.6 Validation of candidate "EMT-promoter" sEV-miRs through miQPCR

In order to validate the presence and levels of the candidate "EMT-promoter" sEV-miRs we used a specific qRT-PCR approach called miQPCR, developed by Benes and coworkers (146) with minor modifications. Briefly, the protocol/method includes a first step of universal ligation at the 3' end of a miLinker oligonucleotide and the elongation of all miRNAs present in the sample. Then, a reverse transcription step of all elongated miRNA in the sample is performed to obtain cDNA. Finally, a qPCR step, where a specific forward primer is used to amplify the desired miRNA. Briefly, 10 ng of RNA (or miRNA), quantified by Qubit™ fluorometric assay (Invitrogen #Q32881), was used to link the miLinker oligonucleotide and reverse transcribed to prepare the cDNA. In the first step, the RNA was mixed and incubated with miLinker (final concentration 0.05 mM) and 50% PEG 8000 (final concentration 3.875%) (**Table 1**; mix 1). The second step

consist of the ligation of the miLinker using the T4 RNA ligase 2, truncated K227Q (T4 Rnl2tr K227Q) from bacteriophage T4 (New England Biolabs® UK #M0351S) (**Table 1**; mix 2). The T4 RNA ligase 2 specifically ligates the pre-adenylated 5´ end of DNA or RNA to the 3´ OH end of RNA. The enzyme does not use ATP for ligation, but requires pre-adenylated linkers, so the miLinker oligo is synthesized to be adenylated at their 5' end. Finally, the elongated miRNAs are reverse transcribed using a universal miQRT primer against a miLinker region and the Superscript II reverse transcriptase enzyme (Invitrogen #18064022) in the presence of DTT (final concentration 16.5 mM) (**Table 3**; mixes 3 and 4). **Tables 1 and 2** show the complete program and reagent concentrations, besides the list of all primers and sequences used to the preparation of the cDNA.

Table 1: Method for cDNA preparation from miRNA-enriched RNA from BC cells and sEVs

Mix 1	**Volume for 1 rx (µL)**	**1X Conc**
miLinker (stock 5 mM)	0.2	0.05 mM
50% PEG 8000	1.55	3.875%
Total volume	1.75	-
	1.5 per tube	-
Step 1: 3 min at 75 °C, then hold at 10 °C		
Mix 2	**Volume for 1 rx (µL)**	**1X Conc**
NEB 10X T4 ligase buffer	0.60	-
MgCl2 (stock 50 xM)	1.60	4 mM
RNase Inhibitor (40 U/uL)	0.11	4.4 U/rx
T4 RNA ligase 2 (200000 U/mL)	0.11	22000 U/rx
Nuclease-free ddH_2O	0.30	-
Total volume	2.72	-

	2.75 per tube	
Step 2: 30 min at 25 °C, 3 min at 85 °C, then hold at 10 °C		
Mix 3	**Volume for 1 rx (µL)**	**1X Conc**
dNTPs (stock 10 µM)	0.50	0.25 µM
miQRT primer (stock 10 µM)	0.25	0.125 µM
Nuclease-free ddH_2O	4.50	-
Total volume	5.25	-
	5.1 per tube	
Step 3: 3 min at 75 °C, then hold at 10 °C		
Mix 4	**Volume for 1 rx (µL)**	**1X Conc**
5X RT buffer	4.40	-
DTT (stock 0.1 M)	3.30	16.5 mM
Nuclease-free ddH_2O	2.20	-
Total volume	9.80	-
	9.60 per tube	
Step 4: 3 min at 45 °C, then add 0.3 µL of Superscript II RT (or water)		
Step 5: 30 min at 45 °C, 5 min at 85 °C, then hold at 10 °C		

Finally, each cDNA sample was diluted until 250 µL with nuclease-free ddH_2O to reach a final concentration of 0.04 ng/µL. For the qPCR step, the starting material was normalized according to the number of sEVs, not the amount of cDNA. So, considering the initial volume of sEVs required to have 10 ng of RNA, the initial sample volume of cDNA for qPCR reaction was adjusted to the volume corresponding to 1.0 x 10^5 sEVs, determined by NTA. The method and the concentrations of all reagents of the qPCR reaction are shown in **Table 3**.

Table 2: Primers and oligonucleotides sequences used for miQPCR reaction

Oligonucleotide	**Sequence (5' → 3')**
miLinker	pp (r) A. GGCCGAACTACGACCTGCATAAACGG. ddC
miQ-RT primer	CCCAGTTATGGCCGTTTATGCAGGT

Table 3: qPCR protocol and method for the detection of enriched/overrepresented sEV-miRs

qPCR mix preparation	
Reagent	**Volume for 1 rx (µL)**
2X Brilliant II SYBR Green MasterMIx	10
Forward specific miRNA primer (stock 10 µM)	0.5
Reverse universal primer (stock 10 µM)	0.5
Nuclease-free ddH_2O	Variable (to reach 20 µL)
Total PCR volume: 20 µL	
qPCR method	
1. Polymerase activation	10 min at 95 °C
2. cDNA denaturation	10 s at 95 °C
3. Primer annealing and extension	35 s at 60 °C
Steps 2 and 3 → 50 cycles	
4. Melting curve	

The list of specific miRNA primers is shown in **Table A** in the annexes.

4.6.7 Determination of sEV-miRs normalizers

As there are no housekeeping or standard miRNAs to normalize the detection in sEV-miRs, we needed to empirically define the best unique or best combination of sEV-miR to normalize our data using our own samples. According to the literature at that date, seven miRNAs were acquired and evaluated as possible normalizers for our samples. The miRNAs evaluated were miR-16-5p, miR-21-5p, miR-25-3p, miR-125a-5p, miR-148a-3p, miR-423-3p, miR-451a and miR-484 (**Table A**). NormFinder Microsoft Excel complement/add-in was used to

determine which unique sEV-miR or combination of sEV-miRs was/were the best normalizers of our sEV samples (https://moma.dk/normfinder-software) (147).

4.7 Specific aim 3 materials and methods

To evaluate the role of candidate sEV-miRs overrepresented/enriched in metastatic sEV-MDA231 on the expression of EMT molecular markers in non-metastatic BC cells.

4.7.1 Transfection of candidate sEV-miRs mimics

The mature sequence of candidate sEV-miRs mimics were acquired from Thermo Fisher Scientific (mirVana® miRNA mimic #4464066) and transfected with Lipofectamine 2000 reagent (Thermo Fisher Scientific #11668019) according to the manufacturer instructions with slight modifications. In brief, sEV-miRs mimics stocks were diluted with nuclease-free ddH_2O to reach a concentration of 100 µM. A 10 µM, 1 µM or 0.1 µM working solution for each mimic was then prepared with nuclease-free ddH_2O. One day before transfection, 5.0 x 10^5 MCF10A or 7.0 x 10^5 T47D cells were seeded on 6-well plates in complete DMEM/F12 culture medium. Twenty-four hours later (the day of transfection), cells had acquired ~70% confluence. Each sEV-miR mimic (or scramble control) was mixed with 125 µL of Optimem medium (miRNA volume varies depending on each miRNA). On a separate tube, 2.5-5.0 µL of Lipofectamine 2000 transfection reagent was also mixed with 125 µL of Optimem medium (for each well) at room temperature. After

that, mimics and transfection reagent were mixed by pipetting and incubated for 20 min at room temperature. In the meantime, cell culture medium was discarded; cells were washed with 1X PBS and replaced with 1.75 mL of fresh Optimem. After 20 min, 250 µL of mimic/Lipofectamine 2000 mix was added to each well drop by drop to reach a final volume of 2 mL per well. Based on the results of the sRNA-seq (read counts for each sEV-miR), the quantity of each sEV-miR mimic was calculated stoichiometrically proportional. So, sEV-miRs mimics concentration in each well varies depending on the miR transfected and are shown in **Table 4**. Non-transfected cells, transfection reagent-treated cells, and scramble mimic transfected cells were included as controls. Mimic transfection efficiency was evaluated after 24-48 h by miQPCR as described. In addition, we checked transfection efficiency by co-transfecting a fluorescently labeled antisense oligo (ASO-AF594). To optimize the level of over-expression after sEV-miR mimic transfection and to better reflect the over-expression acquired after the incubation of recipient cells with the entire sEV-MDA231, decreasing amounts of sEV-miR mimics were used to transfect MCF10A/T47D cells. Each candidate sEV-miR mimic was transfected from 25-10-5-2.5.1.0 pmol per well as described previously. sEV-miRs overexpression was evaluated through miQCR as described and compared against cells incubated with sEV-MDA231.

Table 4: Final concentration of sEV-mIRs mimics transfected in MCF10A and T47D cells

sEV-miR (MDA231)	Read count	RPM adjusted (total)	Proportion (vs RPM)	Volume (WS 10 µM)	Final Conc (nM)
miR-100-5p	31758	5579.14	1.000	2.5 µL	12.5
miR-122-5p	14949	2629.92	0.471	1.2 µL	6.0
miR-146a-5p	2329	406.13	0.073	1.8 µL (1 µM)	0.9
miR-223-3p	568	99.93	0.018	4.5 (0.1 µM)	0.225
miR-760	317	55.77	0.010	2.5 (0.1 µM)	0.125
let-7d-5p	116	20.41	0.004	1.0 (0.1 µM)	0.05

RPM: reads per million; WS: working solution

4.7.2 Evaluation of EMT markers in recipient cells treated with sEV-MDA231 or transfected with sEV-miR mimics

4.7.2.1 Evaluation of gene expression of EMT-associated genes

For mRNA evaluation (genes associated with EMT), transfected cells (or incubated with sEV-MDA231) were carefully washed twice with 1X PBS and detached from the well using trypsin (Gibco #25200-056). Cell suspensions were collected in 15 mL conical tubes and centrifuged at 500 x g for 5 min. Cell pellets were lysed using 400 µL of TRIzol™ Reagent (Invitrogen #15596026) for each well (6-well plate) and RNA was isolated for each condition according to the manufacturer instructions. Briefly, lysed cells were incubated for 5 min at room temperature to allow complete dissociation of the nucleoproteins complex. Then, 0.2 mL of chloroform per 1 mL of TRIzol™ Reagent used for lysis were added to

each tube, securely cap the tube and thoroughly mix by vigorous shaking. After a 3 min incubation, tubes were centrifuged for 15 min at 12,000 × g at 4°C. The mixture separated into a lower red phenol-chloroform, an interphase, and a colorless upper aqueous phase. Transfer the aqueous phase containing the RNA to a new tube. To precipitate RNA, 0.5 mL of isopropanol was added to the aqueous phase, per 1 mL of TRIzol™ Reagent used for lysis. We incubated the tubes for 10 min at 4 °C and then centrifuged them for 10 min at 12,000 × g at 4 °C. Total RNA pellets were washed/suspended with 1 mL of 75% ethanol per 1 mL of TRIzol™ Reagent used for lysis, then centrifuged for 5 min at 7,500 × g at 4 °C. Finally, the supernatant of each tube was discarded and RNA pellets were air-dried the for 5–10 min. RNA pellets were suspended in nuclease-free H_2O and incubated in a water bath or heat block set at 55–60 °C for another 10–15 min. Finally, each RNA sample was quantified in a Nanodrop equipment and stored at -80 °C until use. For cDNA preparation, 1 µg of RNA was treated with DNAse I (Invitrogen #18068-015) and then reverse transcribed using M-MLV reverse transcriptase (Invitrogen #28025-013) according to the manufacturer's instructions. The cDNA (20 µL final volume each sample) was diluted 1:2 – 1:10 with nuclease-free H_2O and 1-2 µL of diluted cDNA was used for each qPCR reaction. The qPCR reaction and program are detailed in **Tables 5 and 6**. Specific primers for each gene are detailed in **Table B** in the annexes.

Table 5: qPCR reagents and concentration used

Reagent	Volume for 1 rx (µL)	Final Conc
2X Brilliant II SYBR® Green QPCR Master Mix (#600828 Agilent Technologies)	10	1X
Forward specific primer (10 µM)	0.5	0.25 µM
Reverse specific primer (10 µM)	0.5	0.25 µM
Nuclease-free water	7	-
cDNA template	2.0	-
Final PCR volume: 20 µL		

Table 6: qPCR program, performed in a StepOne Plus or QuantStudio 12K thermocycler

qPCR method	
1. Polymerase activation	10 min at 95 °C
2. cDNA denaturation	15 s at 95 °C
3. Primer annealing	45 s at 60 °C
4. Extension	60 s at 72 °C
Steps 2 and 3 → 40 cycles	
5. Melting curve	

4.7.2.2 Evaluation of proteins associated with EMT

Non-tumorigenic MCF10A or tumorigenic non-metastatic T47D BC cells were incubated with sEV-MDA231 or transfected with sEV-miRs mimics as described in previous sections. For protein markers evaluation, after 24-48 h cell culture medium was discarded, cells were washed twice with 1X PBS and then lysed with RIPA buffer (150-200 µL per well in a 6-well plate). Lysed cells were collected with a cell scraper in 1.5 eppendorf tubes and 1X protease inhibitor cocktail (Pierce. Thermo Scientific #78430) was added to each tube. Cell lysates were

sonicated (three 5 s pulses with 5 s between each pulse in a stem sonicator) carefully in order to not generate bubbles or foam (or two 10 min incubations in a bath sonicator). After that, resuspensions were centrifuged for 15 min at 14,000 x g and 4 °C and supernatants were collected in new tubes. Total protein extracts were quantified using the microBCA kit (Pierce. Thermo Fisher Scientific #23252) according to the manufacturer instructions and stored at -80 °C until use. Twenty µg total protein extract of each sample was mixed with Laemmli loading buffer (Biorad) and denatured at 95 °C for 5 min. Denatured proteins were loaded in 10-12% acrylamide gels and SDS-PAGE electrophoresis was performed. Before transfer, gels were washed and incubated/activated with Trans-blot turbo 5X transfer buffer (Biorad #10026938) briefly. Separated proteins were transferred from the gel to a nitrocellulose membrane (GE) in a semi-wet transfer blot system (Biorad) for 20-25 min at 25 V, 2.5 A. Membranes were washed once with 1X PBS, blocked with Intercept TBS blocking buffer (Licor #927-70001) for 1 h at room temperature with agitation and probed with antibodies against EMT markers (e.g. Vimentin, E-Cadherin, N-Cadherin, Snail, Slug, Zeb1, Twist). Finally, bound antibodies were detected with anti-IgG 680/800 GW secondary antibodies (1:10,000 dilution) and revealed in an Odyssey Clx imaging system (Licor).

4.8 Specific aim 4 materials and methods

To evaluate the role of candidate sEV-miRs overrepresented/enriched in metastatic sEV-MDA231 on the migration capacity of non-tumorigenic and non-metastatic BC cells (as a surrogate of the EMT).

4.8.1 Evaluation of 3D migration mediated by "EMT-promoter" sEV-miRs mimics transfection by transwell assay

Twenty-four hours before the assay, MCF10A cells and T47D BC cells were transfected with "EMT-promoter" sEV-miRs mimics as described or treated with 3 µg proteins sEV-MDA231 (~3000 particles per seeded cell). The day of the experiment, Boyden chambers were hydrated with DMEM/F12 culture medium for 1 h. Twenty-four hours after the transfection, 2.5 x 10^4 MCF10A or T47D cells previously transfected with "EMT-promoter" sEV-miRs mimics or treated with sEV-MDA231 were seeded on the upper chamber of 24-well transwell plates to evaluate the effect over 3D migration capacity of BC cells. Cells previously treated with sEV-MDA231 were re-incubated (or not) with sEV-MDA231. After 16 h, transwell inserts/membranes were carefully collected, fixed with 4% PFA for 10 min, and stained with DAPI (1:300 dilution). Cells on the other side of the inserts were visualized on an inverted fluorescence microscope and counted in at least 10 fields.

5. RESULTS

5.1 Specific aim 1 results

To evaluate the effect of metastatic sEV-MDA231 over the acquisition/promotion of tumorigenic and pro-metastatic capacities of non-tumorigenic and non-metastatic recipient cells.

5.1.1 Isolation and characterization of sEVs secreted by MDA-MB-231 metastatic BC cells (sEV-MDA231)

The first step to test our hypothesis was to isolate and characterize sEV-MDA231. sEVs secreted by these cells were isolated using differential centrifugation and UC and characterized by NTA, TEM and WB. NTA showed that sEV-MDA231 had a narrow distribution, with a peak at ~112 nm and a mean size of ~130 nm (**Figure 1a**; left). TEM analysis showed round and cup-shaped structures/vesicles, characteristic of enveloped nanovesicles, with sizes ranging that of sEVs (**Figure 1a**; right). Evaluation of markers using WB showed the presence of CD63, and TSG101 as characteristic markers of EVs. All sEVs isolated also contained the EV marker Flotillin-1, however there is a marked difference in the abundance of that protein between the different sEVs, being much more abundant in sEV-T47D and sEV-MDA231 than sEV-MCF10A and sEV-ZR75 (**Figure 1b**). The negative markers Calnexin was not detected, discarding RER contamination in our sEVs (**Figure 1b**). The presence of these makers, along with their size distribution and

structure strongly suggest that the isolated sEV-MDA231 are mainly composed by exosomes.

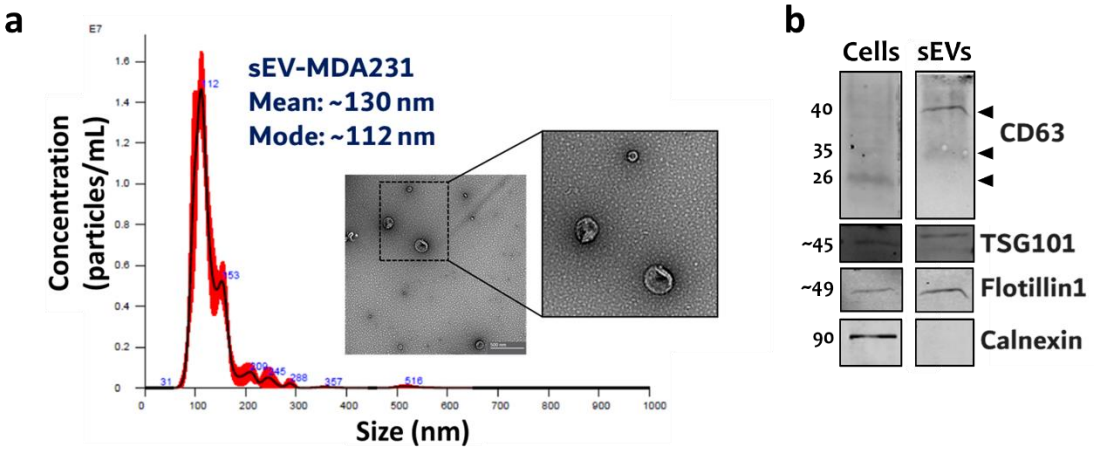

Figure 1: Characterization of sEVs secreted by MDA-MB-231 metastatic TNBC cells (sEV-MDA231).

sEVs secreted by MDA-MB-321 TNBC cell line were obtained through cell culture conditioned medium ultracentrifugation and the number, size and integrity were analyzed by **(a)** Nanotracking analysis (left), transmission electron microscopy (right); **(b)** Detection of sEVs markers in human BC cell-secreted sEVs by western blot. Total protein extracts were loaded in 10-12% acrylamide gels and transferred to nitrocellulose membranes. CD63, TSG101 and Flotillin-1 were used as sEVs markers. Calnexin was used as intracellular contamination protein. Human normal mammary epithelial MCF10A cells was used as control. (a) In TEM image, the white size bar indicates 500 nm.

5.1.2 sEV-MDA231 enhance in vitro 3D migration of tumorigenic non-metastatic BC cells

We used transwell Boyden chambers to evaluate the effect of sEV-MDA231 over the migratory capacity of normal mammary epithelial MCF10A cells and different BC cell lines. MCF7 (breast adenocarcinoma; luminal A-like; ER+/PR+/HER2-), T47D (infiltrating ductal carcinoma; luminal A-like; ER+/PR+/HER2-), ZR75 (ductal carcinoma; luminal B-like; ER+/PR-/HER2-) and triple-negative MDA-MB-231 (breast adenocarcinoma; basal-like; ER-/PR-/HER2-) were seeded in transwell Boyden chambers with an 8 μm pore PET-membrane inserts, and treated or not with sEV-MDA231 for 16 h. Despite the different phenotype and aggressiveness inherent of each cell line, the incubation with sEV-MDA231 promoted approximately a two-fold increase in their migratory capacity (**Figure 2**). However, when multiple comparison analyses were performed, only, MCF7, T47D and ZR75 BC cells increased their migratory capacity when incubated/treated with sEV-MDA231 (**Figure 2b-d**). Remarkably, the use of sonicated (disrupted) sEV-MDA231 did not promote the migration of these cells, suggesting the need of the complete undisrupted sEVs. On the other hand, although a small increase was observed, treatment of MCF10A and MDA-MB-231 BC cells with sEV-MDA231 did not increase their migration capacity statistically (**Figure 2a and e**).

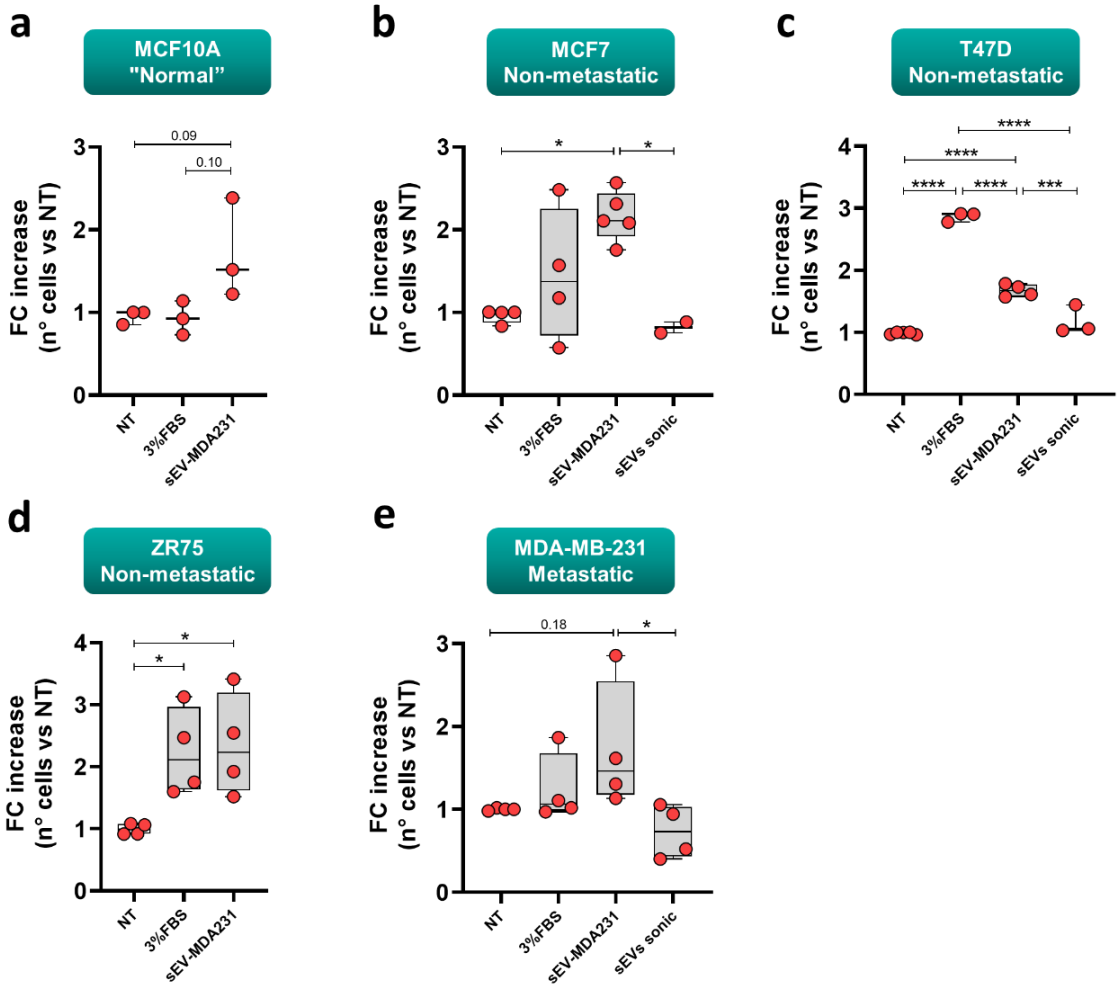

Figure 2: Effect of sEV.MDA231 treatment on the migratory capacity of different BC recipient cells.

Different human BC cells were incubated with metastatic sEV-MDA231 to evaluate its role in their migratory capacity by a transwell migration assay. **(a)** MCF10A, **(b)** MCF7, **(c)** T47D, **(d)** ZR75 and **(e)** MDA-MB-231 recipient cells were seeded on PET-membrane Boyden transwell chambers and treated once with sEV-MDA231 for 16 h. After that, membranes were collected, fixed with 4% PFA and stained with DAPI. Cells into the membrane were counted in 10 fields on an inverted fluorescence microscope and then quantified. Graphs show box plots displaying all points and

whiskers showing minimum and maximum. Each point represents mean FC of one experiment. (*) $p < 0.05$; (***) $p < 0.001$; (****) $p < 0.0001$.

5.1.3 sEV-MDA231 increase the anchorage-independent growth potential of ductal carcinoma-derived BC cells

The anchorage-independent growth assay, also known as clonogenic assay, evaluates the capacity of cells to survive without a solid surface, therefore extrapolating the results with their capacity to growth and survive in the bloodstream. We evaluated the clonogenic potential of the same previously mentioned BC cell lines (MCF7, T47D, ZR75 and MDA-MB-231), as well as of MCF10A normal mammary epithelial cells after their incubation with sEV-MDA231. Similar to what we saw in the transwell migration assay, sEV-MDA231 promotes the anchorage-independent growth potential only of some BC cell lines but not in others (**Figure 3**). First, sEV-MDA231 did not improve anchorage-independent growth of normal breast epithelial MCF10A cells (**Figure 3a**). Interestingly, sEV-MDA231 did promote the clonogenic potential of ductal carcinoma-derived BC cell lines, i.e. T47D and ZR75 BC cells (**Figure 3b,c**), however, the increment was just 25-40% approximately. On the other hand, neither MCF7 nor MDA-MB-231 BC cells increased their anchorage-independent growth capacity after their incubation/treatment with sEV-MDA231 (**Figure 3d,e**).

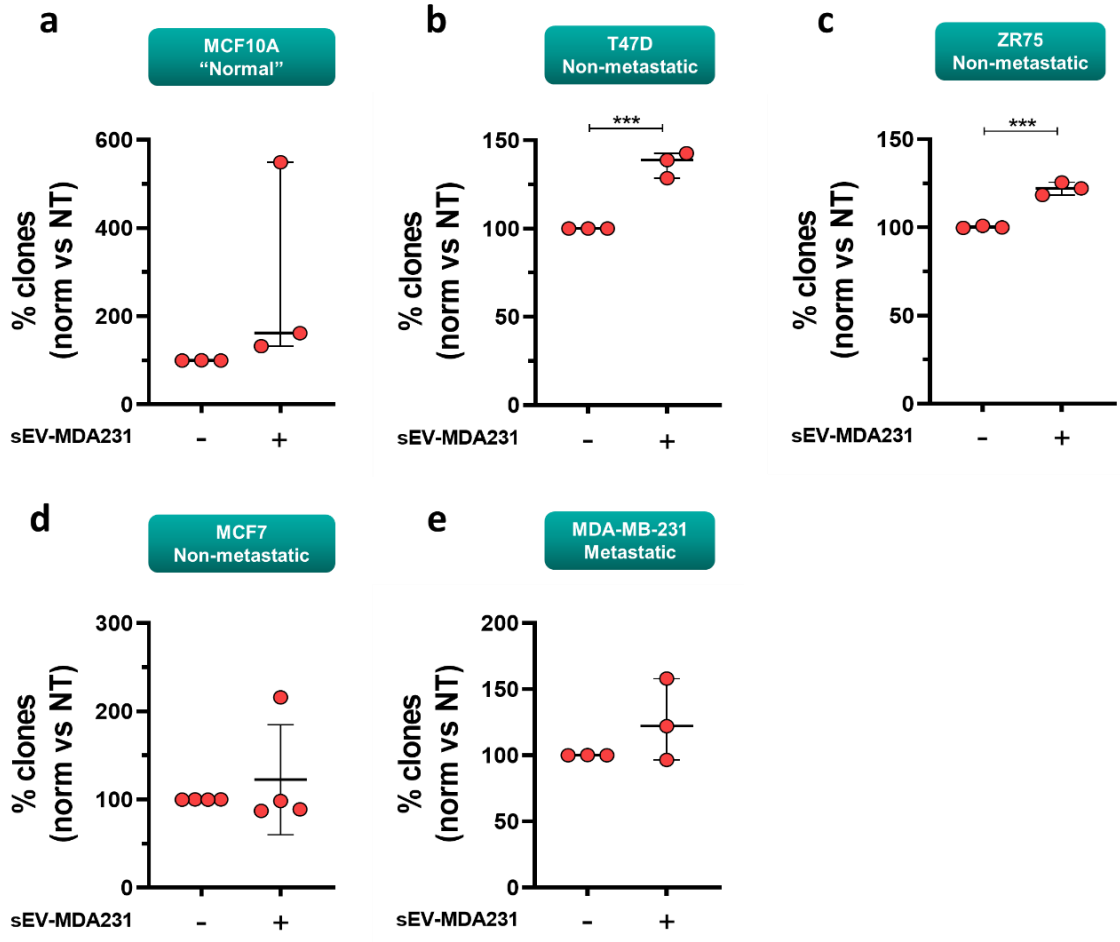

Figure 3: Effect of sEV-MDA231 treatment on the anchorage-independent growth potential of different BC recipient cells.

Anchorage-independent growth (clonogenic assay) was evaluated in recipient cells incubated with sEV-MDA231. 3.0-7.5 x 10^3 recipient cells were seeded in semisolid cell culture medium. Next day cells were treated with sEV-MDA231 (D1). Another supplement was added at day 8 (D8). The number of clones formed were evaluated at day 14 (D14), visualized under inverted optic microscope. Each condition was tested in duplicates and at least 10 fields per condition were evaluated. **(a)** MCF10A, **(b)** T47D, **(c)** ZR75, **(d)** MCF7 and **(e)** MDA-MB-231 recipient cells. Graphs show box plots displaying all points and whiskers showing minimum and maximum. All

data is representative of at least 3 independent experiments. Each point represents mean percentage of one experiment. (***) $p < 0.001$.

5.1.4 sEV-MDA231 enhance tumoroid formation of non-tumorigenic and BC cells in vitro

Tumoroids formation evaluates the stemness properties of a specific population of tumor cells. We evaluated the capacity of sEV-MDA231 to improve tumoroid formation of two BC cell lines (MCF7 and MDA-MB-231) and an immortalized, non-tumorigenic mammary epithelial cell line (MCF10A). The incubation of each BC cell line with sEV-MDA231 improve tumoroid formation by approximately 2-4-fold. First, sEV-MDA231 promoted spheroid formation in non-tumorigenic MCF10A cells (**Figure 4a**), On the other hand, despite the difference in total tumoroid numbers for each cell line (MDA-MB-231 cell line is much more aggressive than MCF7, and also have a high metastatic potential), sEV-MDA231 incubation slightly promoted tumoroid formation compared with untreated cells by almost 2-fold (**Figure 4b,c**). However, those changes were not statistically significant. Interestingly, we could not test the tumoroid formation capacity of T47D and ZR75 ductal BC cells since they were not able to form tumoroids with our protocol. Representative images of MDA-MB-231 tumoroids are shown in figure 4d (**Figure 4d**).

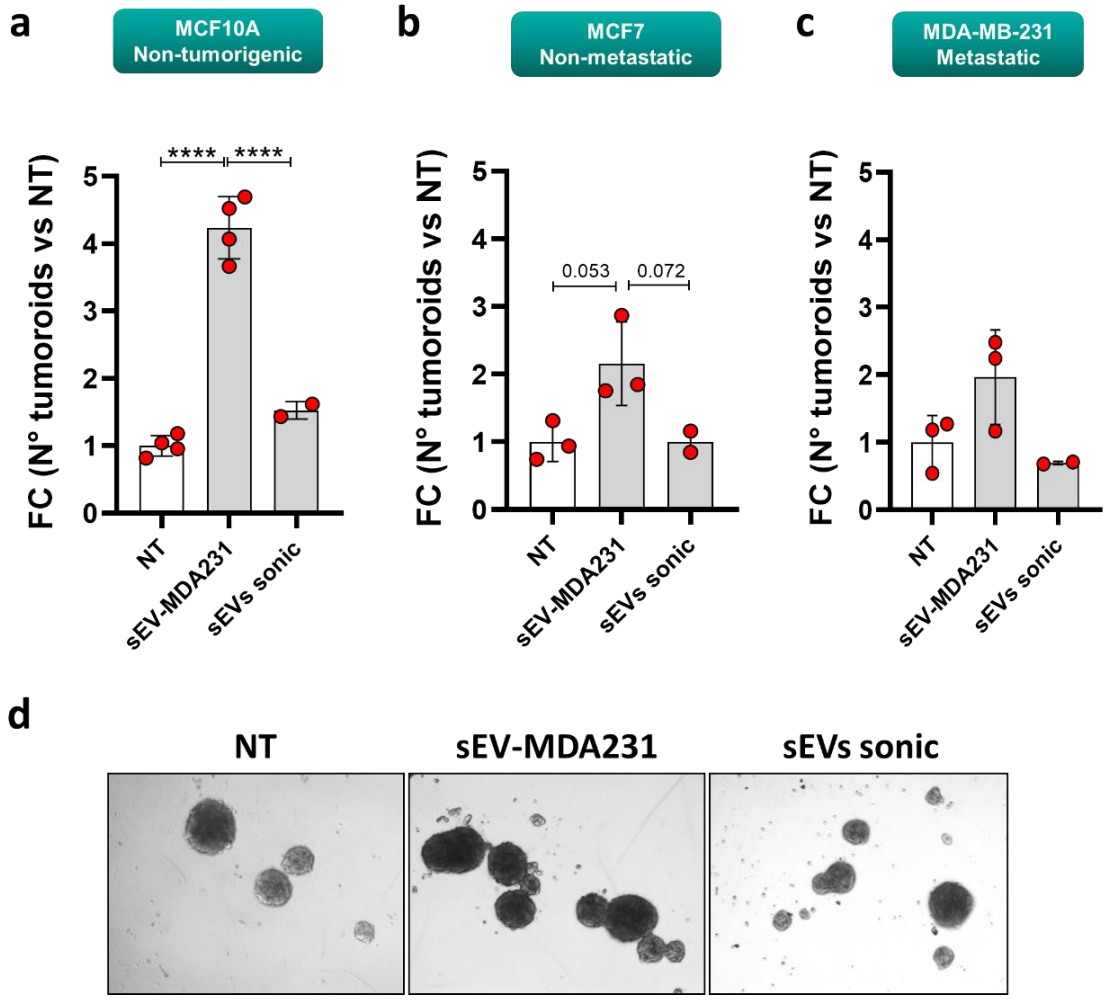

Figure 4: Effect of sEV-MDA231 treatment on the tumoroid formation capacity of different BC recipient cells.

Different human BC cells were incubated with metastatic sEV-MDA231 to evaluate its role in promoting spheroid/tumoroid formation. After 14 days, spheroids/tumoroids were visualized and photographed under an inverted microscope. Spheroids/tumoroids with a size ≥ 100 µm were quantified in **(a)** MCF10A cells, **(b)** MCF7 BC cells and **(c)** MDA-MB-231 TNBC cells. Representative images of spheroids/tumoroids formed in the different conditions after 14 days are shown **(d)**. Graphs show mean ± SD. All data is representative of 3 independent experiments. Each point represents mean FC of one experiment. (****) $p < 0.0001$.

5.1.5 sEV-MDA231 greatly promotes the formation of malignant ascites and tumor micronodules in a peritoneal carcinomatosis mice model

To evaluate whether the sEV-MDA231 plays a role in promoting metastasis *in vivo*, we used a peritoneal carcinomatosis mouse model in which we injected tumor cells directly into the peritoneal cavity of mice. We injected 2.0 x 10^6 highly metastatic MDA-MB-231 breast tumor cells on day 0 and, on the same day, treated mice with sEV-MDA231 (10 µg total protein (**Figure 5a**). With this model, we can evaluate metastasis by directly detecting tumor growth in retroperitoneal organs such as the spleen, liver, kidneys, and mesentery, and evaluate the formation of malignant ascites and the number of tumor nodules formed. We observed that treatment with sEV-MDA231 increased tumor growth; the total tumor mass was higher in mice treated with sEV-MDA231 versus those inoculated only with tumor cells (not shown). In addition, sEV-MDA231 treatment significantly promoted the formation of malignant ascites in the peritoneal cavity of mice (**Figure 5b,c**). In the same way, mice that received sEV-MDA231 developed more and larger mesenteric tumor nodules than untreated mice (**Figure 5d,e**). These results strongly suggest that sEV-MDA231 play an important/a major role in the development of peritoneal metastasis in our *in vivo* model.

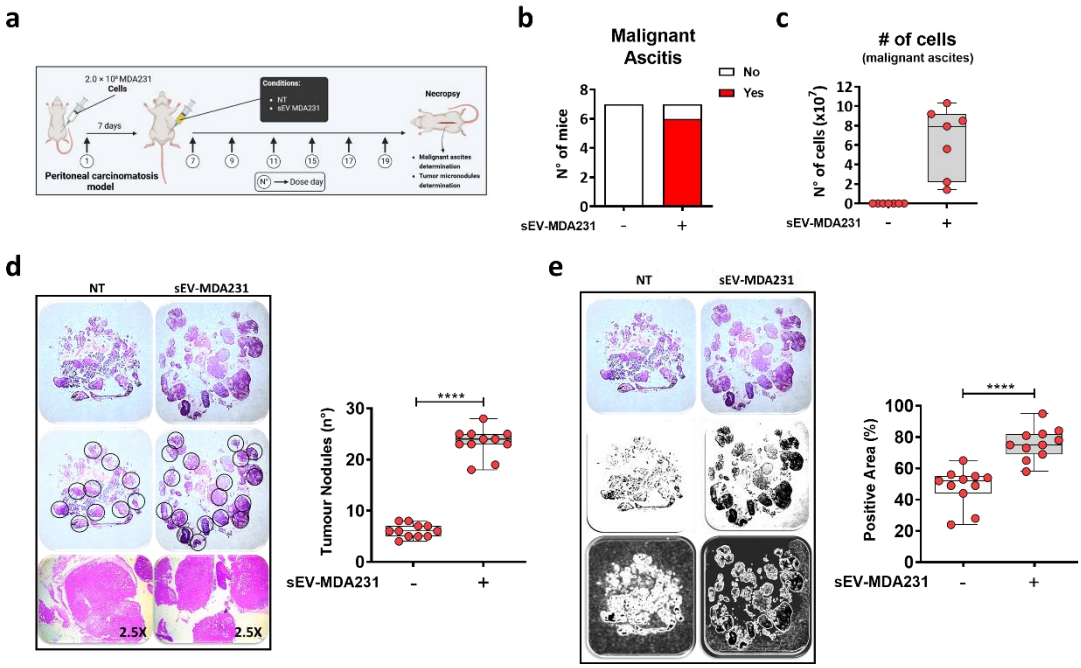

Figure 5: Effect of sEV-MDA231 treatment on the formation of malignant ascites and tumor micronodules in a peritoneal carcinomatosis mouse model.

NOD/SCID mice (two separated experiments) were inoculated intraperitoneally (ip) with 2.0 × 10^6 MDA-MB-231, either alone (saline group) or together with sEV-MDA231. Seven days after tumor cells inoculation, mice were treated again with sEV-MDA231 on days 7, 9, 11, 15, 17 and 19 (7 total doses). Mice were euthanized on day 21 post-cell injection and organs were collected in the necropsy **(a)**. When present, malignant ascites were also collected and total cell number was determined by trypan blue exclusion assay **(b,c)**. For tumor micronodules measurement, tumor tissues were fixed and paraffin-embedded. Histologic sections of mesenteric tissue were first stained with HE. Images of HE-stained sections were gray scale-transformed to define a hyperdense area. Tumor micronodules number in mesenteric tissues in the peritoneal cavity were evaluated by purple hyperchromia. Tumor area was also measured by gray range density/intensity, which coincides with the denser nuclear staining of tumor cells **(d,e)**. The final *in vivo* evaluation was performed in a double-blinded fashion and corroborated by anatomopathological analysis.

In summary, all these results suggest that sEVs secreted by a highly aggressive and metastatic BC cell line (sEV-MDA231) can promote tumorigenic and pro-metastatic capacities of less aggressive (tumorigenic, non-metastatic) recipient BC cell lines, such as migration, tumoroid formation and clonogenic potential. Moreover, sEV-MDA231 can even increase some of these capacities in an immortalized, normal mammary epithelial cell line (migration and spheroid formation) highlighting their tumorigenic and pro-metastatic effect. Interestingly, the treatment with sEV-MDA231 in a peritoneal carcinomatosis (metastatic) *in vivo* model have a striking effect promoting the formation of malignant ascites and tumor peritoneal micronodules.

5.2 Specific aim 2 results

To characterize the miRNA profile of sEVs (sEV-miRs) secreted by metastatic and non-metastatic BC cells and to define candidate promoters of the EMT.

Before starting, it is important to mention prior studies and preliminary results from our research group regarding the effect of sEVs secreted by “normal” and non-metastatic BC cells. It has been shown that sEVs secreted by non-tumorigenic mammary epithelial MCF10A cells (sEV-MCF10A) seems to have no pro-metastatic effects in recipient cells (148–150). Similarly, preliminary results from our lab have shown that sEV-MCF10A does not promote the tumoroid formation capacity of MCF7 and MDA-MB-231 recipient cells (**Figure S1a,b**). Moreover,

sEVs secreted by MCF7 BC non-metastatic cells (sEV-MCF7) does not promote the invasion and colony formation capacity of MDA-MB-231 recipient cells (**Figure S1c,d**). These literature and results support our experimental approach analyzing the effect of sEVs secreted by metastatic BC cells, and comparing them versus sEVs secreted by normal and non-metastatic BC cells.

5.2.1 Characterization of BC cells-secreted sEVs

In order to get insights on which molecules in sEVs cargo could be associated with the promotion of those tumorigenic and pro-metastatic capacities, more precisely, which miRNAs could be involved, we performed RNA sequencing of the small RNA fraction (small RNA-seq) present in sEVs secreted by the different BC cell lines used, with emphasis in the subsequent analysis of sEV-miRs. The NTA showed that both, the mean size and mode size of sEVs seemed to be similar in all isolated sEVs (**Figure 6a**). In addition, their size distributions were similar to those evaluated by NTA and TEM (**Figure 6b**). Finally, WB analysis showed that all sEVs contained typical sEVs markers such as CD63 and TSG101 (and Flotillin-1 in two out of four sEVs). Moreover, the isolated sEVs did not contained the endoplasmic reticulum marker calnexin, thus showing no contamination with RER components, but they contained the Golgi marker GM130, which suggest contamination with Golgi proteins in our sEVs preparations (**Figure 6c**).

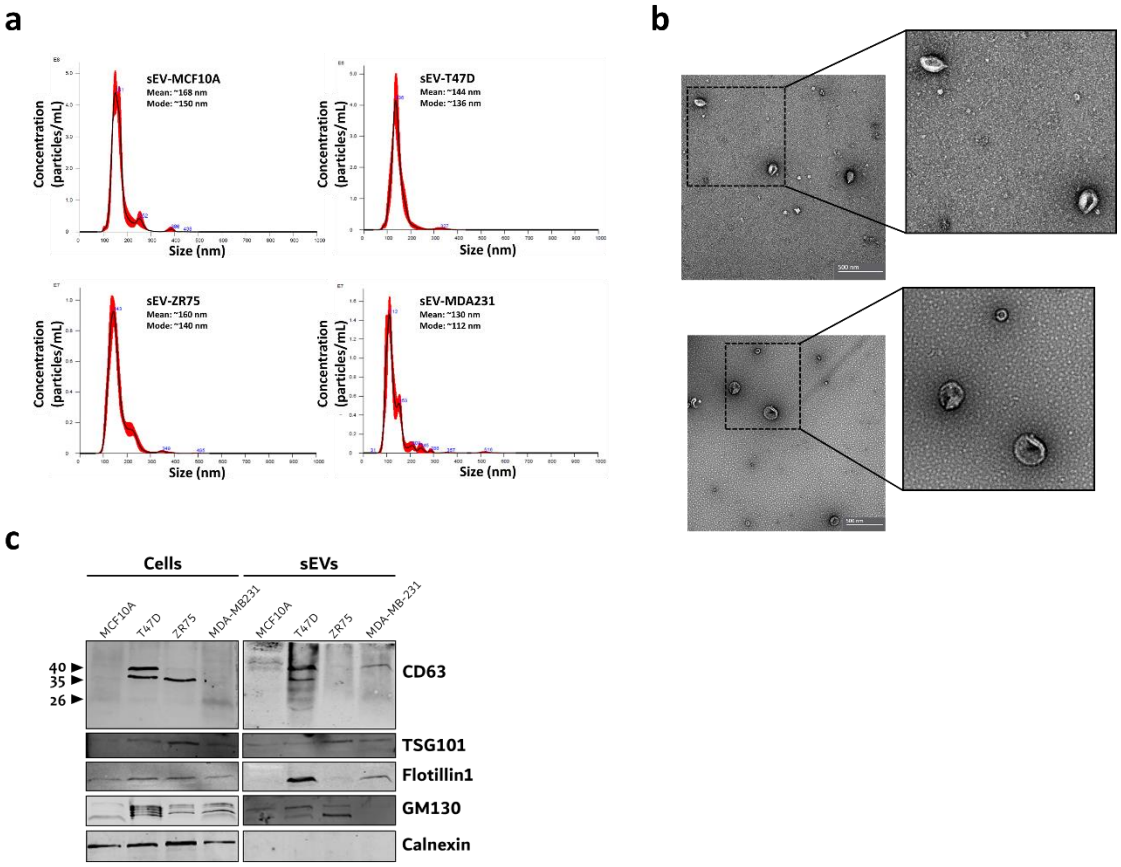

Figure 6: Characterization of sEVs secreted by different BC cell lines.

sEVs secreted by different human BC cell lines were obtained through cell culture conditioned medium ultracentrifugation and the number, size and integrity were analyzed by **(a)** nanotracking analysis and **(b)** transmission electron microscopy (representative images of sEV-MCF10A (up) and sEV-MDA231 (down)). **(c)** Detection of sEVs markers in human BC cell-secreted sEVs. Total protein extracts (~10 µg) were loaded in 10-12% acrylamide gels and transferred to nitrocellulose membranes. CD63, TSG101 and Flotillin-1 were used as sEVs markers. Calnexin was used as intracellular contamination protein. Human normal mammary epithelial MCF10A cells was used as control. (b) In TEM images, the white size bar indicates 500 nm.

5.2.2 sRNA-seq analysis of BC cell-secreted sEVs shows different sRNAs profiles

After the purification of miRNA-enriched RNA of sEVs secreted by T47D, ZR75 and MDA-MB-231 BC cell lines and of MCF10A normal/non-tumorigenic mammary epithelial cell line, we aimed to characterize their miRNA profile using a small RNA-seq approach. Due to the Covid 19 pandemics, the company Novogene performed the small RNA-seq, however, we did an in-house analysis of all the raw data using the sRNAbench web platform (https://arn.ugr.es/srnatoolbox/). As shown in **Table 7**, after the QC analysis and filtering, the total reads for subsequent analyses were between 11M-20M (54.1-96.3% of total initial reads). Filtering parameters include quality of reads, minimum number of a single read and minimum length of individual read. The alignment analysis against the human genome showed a differential composition of sRNAs in cells against sEVs, being mainly composed of miRNAs in cells and for tRNA fragments in sEVs (**Figure 7**).

Table 7: Quality control and filtering of the raw data (input reads) of the sRNA-seq of BC and BC cells-secreted sEVs

Sample	N° raw input reads	Quality filter reads (>20)	Reads below min count (>=10)	Reads below min length	Total, filtered reads	Reads in analysis (%)
MCF10A_cells	21557602	4060	2298621	3005904	5390804	16166798 (75.0)

MDA231_cells	20540061	3876	2785144	6591096	9428706	11111355 (54.1)
sEV-MCF10A	21440856	38425	2197596	1643262	3944379	17496477 (81.6)
sEV-T47D	20617889	37781	1131359	340095	1721353	18896536 (91.7)
sEV-ZR75	20319662	36725	1262640	447488	1832944	18486718 (91.0)
sEV-MDA231	20858146	38388	498608	177277	769080	20089066 (96.3)

As shown in figure 7, miRNAs are the main component of the sRNA profile of MCF10A and MDA-MB-231 cells (**Figure 7a**), ranging between 40-60% of all sRNAs. On the other hand, the main component of sEVs sRNAs are tRNAs, fragments of transfer RNAs in BC cell-secreted sEVs and yRNAs particularly in sEV-MCF10A. Interestingly, miRNAs correspond approximately to 1-3% of total sRNAs of BC cell-secreted sEVs, while are most abundant in MCF10A non-tumorigenic cells, reaching almost 20% of all sRNAs (**Figure 7b**). In addition, at the time of analysis, an important proportion of sRNA reads were unable to be aligned, resulting in unassigned reads. These sRNAs could correspond to piwiRNAs and other that were not included in the web-tool database. Other sRNAs detected and correctly aligned corresponded to snRNA, snoRNAs, vRNAs and other less abundant sRNA species.

After the characterization of the sRNA profile of the sEVs secreted by each cell line, we aimed to characterize specifically the miRNA profile of those vesicles.

miRNA annotation and analysis showed that 70.22% and 57.35% of all reads correctly mapped correspond to miRNAs in MCF10A cells and MDA-MB-231 cells respectively. On the other hand, when we analyzed sEVs, we saw that just 1.57, 2.86 and 2.46% of all reads correspond to sEV-miRs in sEV-T47D, sEV-ZR75 and sEV-MDA231, respectively. Interestingly, nearly 22% of the reads correspond to miRNAs in sEV-MCF10A, which are a non-tumorigenic breast epithelial cell line (**Table 8**).

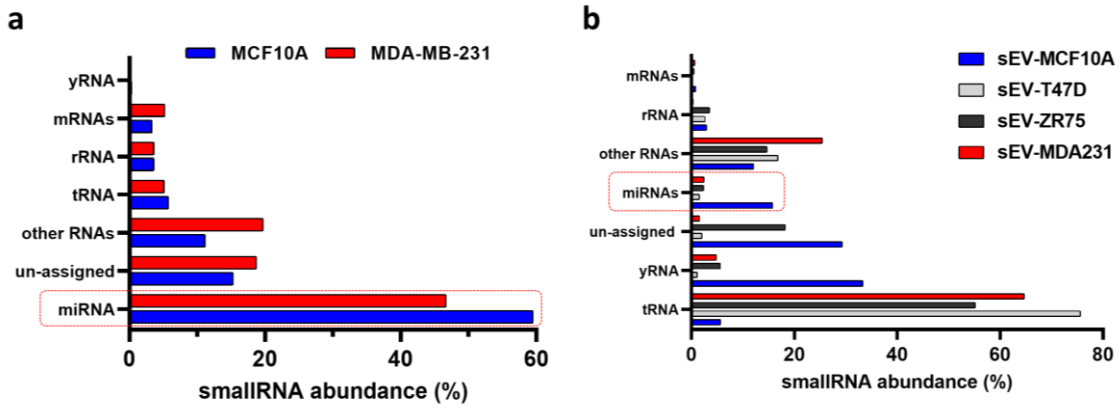

Figure 7: Characterization of the smallRNA profile of sEVs secreted by BC cells.

The fastq files after small RNA-seq were uploaded to the sRNAbench web platform and aligned against the GRCh38_p10 version of the human genome. The adapters used in the preparation of the library and the protocol setting parameters are detailed in the Methodology section. **(a)** Cellular sRNA profiling in "normal" MCF10A (blue) and MDA-MB-231 TNBC cells (red). **(b)** sRNA profiling in sEVs secreted by different BC cells. sEV-MCF10A (blue), sEV-T47D (light grey), sEV-ZR75 (grey), sEV-MDA231 (red). Y-axis denotes different sRNA species. X-axis indicates percentage abundance of each sRNA specie in y-axis.

Table 8: Reads aligned corresponding to mature or hairpin sequences of human miRNAs annotated

	Reads mapped to miRs (%)	Detected mature miRs (% total)	Detected hairpin miRs (% total)
MCF10A_cells	8376242 (70.22)	461 (17,35)	394 (20.55)
MDA231_cells	4793737 (57.35)	410 (15,44)	346 (18.05)
sEV-MCF10A	2448403 (22.36)	400 (15,06)	379 (19.77)
sEV-T47D	183284 (1.57)	212 (7,98)	212 (11.06)
sEV-ZR75	356776 (2.86)	275 (10,35)	266 (13.88)
sEV-MDA231	137516 (2.46)	153 (5,76)	167 (8.71)

We were able to detect less miRNAs in sEVs than in the cells of origin. Total miRNAs detected 400 in MCF10A and MDA-MB-321 cells; however, in BC cell-secreted sEVs we detected just 212, 275 and 153 miRNAs in sEV-T47D, sEV-ZR75 and sEV-MDA231, respectively. Again, as total reads mapped to miRNAs are higher in sEV-MCF10A than in the others, we could detect 400 different miRNAs in these sEVs (**Table 8**). Interestingly, we also detected many reads corresponding to the hairpin (immature) sequence of miRNAs in sEVs, which indicate that both, the mature and immature sequences of each miRNAs can be loaded and delivered by sEVs (**Table 8**). In addition, we saw that most of the miRNAs detected in cells were common between the two cell lines, reaching 70.5%. One hundred and one miRNAs were only detected in MDA-MB-231 BC cells and 50 of them were only detected in MCF10A non-tumorigenic cells (**Figure 8a**). sEV-miRs analysis also showed that most of the sEV-miRs were common between the four different sEVs included. Other sEV-miRs were in 2-3 out of 4

sEVs. As we can see in figure 8b, just a small number of the detected sEV-miRs were unique in one sEV (only detected in one sEV). For example, just 5 sEV-miRs were only detected in sEV-MDA231, just 2 sEV-miRs were only detected in sEV-T47D and 22 sEV-miRs were only detected in sEV-ZR75. Particularly in sEV-MCF10A, as we detected 4 times more sEV-miRs than in the other sEVs, we could see that the unique sEV-miRs are also much more, reaching 155. This can also be attributable to the fact that, in contrast to the other cells of origin, which are tumorigenic, this cell line is “normal” (non-tumorigenic) (**Figure 8b**). **Table 9** showed the unique sEV-miRs detected in each of the sEVs analyzed in this work.

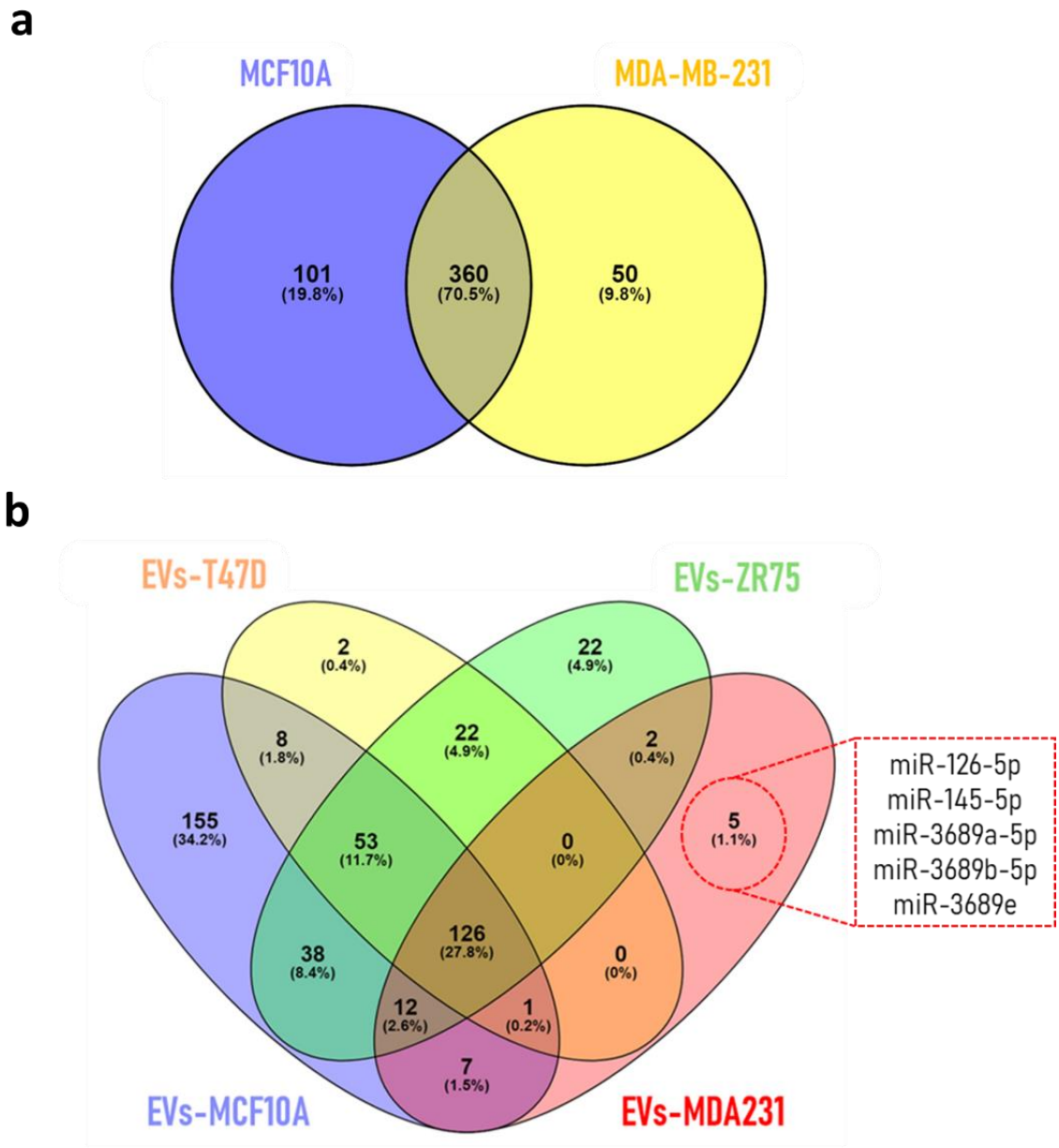

Figure 8: Identification of unique and common miRNAs in BC cell-secreted sEVs (sEV-miRs).

Annotated miRNAs of each sample (cell or sEVs) were separated in lists and organized in Venn diagrams. **(a)** Cellular miRNAs detected in "normal" MCF10A cells (blue) and MDA-MB-231 TNBC cells (yellow). **(b)** sEV-miRs detected in sEVs secreted by different BC cell lines. MCF10A "normal" cells-secreted sEVs (sEV-MCF10A; blue), sEV-T47D (yellow), sEV-ZR75 (green) and sEV-

MDA231 (red). The 5 sEV-miRs uniquely detected in sEV-MDA231 are indicated in the red dashed line box. Numbers inside figures indicate absolute numbers of sEV-miRs detected and percentage of total.

Table 9: Unique sEV-miRs detected in sEV-MCF10A, sEV-T47D, sEV-ZR75 and sEV-MDA231

sEVs sample	sEV-miR
sEV-MCF10A	miR-2682-5p, -1298-5p, -185-3p, -548ao-3p, -3064-5p, -34c-5p, -6786-3p, -3918, -6745, -4755-5p, -1262, -708-3p, -216b-5p, -1226-3p, -335-3p, -6741-5p, -541-5p, -450a-5p, -3118, -1294, -18a-5p, -4665-5p, let-7a-2-3p, -6819-3p, -450b-5p, -4683, -31-5p, -4488, -493-3p, -935, -4743-5p, -299-3p, -3605-3p, -3138, -4677-3p, -4797-3p, -4669, -4684-5p, -6765-5p, -6511a-5p, -139-3p, -1248, -1306-3p, -4429, -6515-5p, -7976, -493-5p, -221-5p, -3173-5p, -4443, -2116-3p, -598-3p, let-7f-2-3p, -6511a-3p, -486-3p, -10401-3p, -487b-3p, -182-3p, -28-5p, -323a-3p, -215-5p, -138-5p, -1237-3p, let-7b-3p, -11400, let-7f-1-3p, -3124-5p, -199b-5p, -504-5p, -191-3p, -3679-5p, -411-3p, -27b-5p, -19a-3p, -6741-3p, -6787-3p, -642a-3p, -1284, -3929, -132-5p, -370-3p, -23a-5p, -4435, -29c-3p, -1910-5p, -19b-3p, -6764-5p, -4745-5p, -6511b-5p, -34a-5p, -335-5p, -10526-3p, -141-3p, -550a-5p, -18a-3p, -3605-5p, -6747-3p, -129-1-3p, -369-5p, -3150a-5p, -338-5p, -135a-5p, -505-5p, -766-5p, -10b-3p, -29b-3p, -4721, -485-5p, -9985, -454-3p, -6089, -641, -382-5p, -4473, -26b-3p, -6866-5p, -3120-5p, -4775, -495-3p, -4516, -942-5p, -1910-3p, -129-2-3p, -204-5p, -1249-3p, -4492, -212-5p, -323b-3p, -1273h-3p, -944, -378f, -6780a-5p, -15a-5p, -369-3p, -365b-3p, -214-3p, -877-3p, -208b-3p, -155-5p, -24-2-5p, -34b-3p, -21-3p, -4661-5p, -345-3p, -2355-3p, -7854-3p, -548u, -142-3p, -5697, -433-3p, -1293, -511-5p, -34c-3p, -365a-3p, -141-5p
sEV-T47D	miR-374a-5p, 3135b
sEV-ZR75	miR-3127-5p, -1323, -1224-5p, -516b-5p, -148b-5p, -483-3p, -3174, -6834-5p, -1255a, -494-3p, -449a, -766-3p, -3127-3p, -203b-3p, -1266-5p, -4741, -483-5p, -195-3p, -6873-3p, -628-3p, -326, -187-5p
sEV-MDA231	miR-126-5p, -145-5p, -3689a-5p, -3689b-5p, -3689e

5.2.3 Different/Several miRNAs are enriched in sEVs compared with parental cells

After the identification of sEV-miRs uniquely detected in each of the BC cells-secreted sEVs, we analyzed the possible enrichment of miRNAs on sEVs versus the parental cell of origin. As mentioned, we only could perform this analysis on MCF10A and MDA-MB-231 cells and sEVs as we lost, because of QC issues, the samples of T47D and ZR75 BC cells RNA. To do that, we compared the normalized read count of each sEV-miR vs their counterpart in the parental cell. miRNAs enriched in sEVs were considered when the ratio sEV-miR norm. read count / cell norm. read count was > 2, i.e. a 2-fold enrichment in sEVs. As we can see in **Table 10**, several miRNAs were identified as enriched in sEVs vs cells, both in sEV-MCF10A and sEV-MDA231. Forty-eight percent of sEV-miRs were enriched in sEVs derived from MCF10A and MDA-MB-231 cells (12 out of 25). For example, miR-122-5p was enriched 11.97 times in sEV-MCF10A (vs MCF10A cells) and 13.45 times in sEV-MDA231 (vs MDA-MB-231 BC cells). On the other hand, 52% (13 out of 25) were enriched either in sEV-MCF10A or in sEV-MDA231, compared with the respective producing cell. This suggest that the enrichment of miRNAs in sEVs to be secreted could be both, a passive or unspecific process (common enriched sEV-miRs), but also it could be an active, selective or specific process, in which some miRNAs are enriched in sEVs depending on the cell type (cell-specific enriched sEVs) (**Table 10**).

Table 10: Enriched miRNAs loaded in sEVs compared with their parental cell of origin

MCF10A cells vs EVs			MDA231 cells vs EVs		
miRNA ID	**log2FC**	**Adjusted p value**	**miRNA ID**	**log2FC**	**Adjusted p value**
-375-3p	14.96	0.00E-00	**-122-5p**	**13.45**	**0.00E-00**
-3168	**12.50**	**0.00E-00**	**-10b-5p**	**10.66**	**0.00E-00**
-122-5p	**11.97**	**0.00E-00**	**-3168**	**9.54**	**0.00E-00**
-6529-5p	**11.06**	**0.00E-00**	**-1246**	**8.89**	**0.00E-00**
-206	10.78	0.00E-00	**-6529-5p**	**8.67**	**4.31E-88**
-412-5p	**10.62**	**0.00E-00**	-105-5p	8.47	1.08E-76
-409-3p	10.59	0.00E-00	**-543**	**7.74**	**2.07E-46**
-204-3p	8.92	2.30E-230	**-199a-5p**	**7.46**	**9.66E-38**
-1468-5p	**8.76**	**6.60E-207**	**-432-5p**	**7.46**	**9.66E-38**
-1908-5p	8.67	5.58E-194	**-412-5p**	**7.29**	**1.40E-33**
-320d	**8.25**	**0.00E-00**	-203a-3p	7.24	1.16E-32
-204-5p	8.19	1.17E-138	-499a-5p	6.75	2.11E-23
-432-5p	**8.13**	**2.99E-133**	-760	6.20	0.00E-00
-10b-5p	**8.08**	**0.00E-00**	-143-3p	6.10	0.00E-00
-1246	**7.89**	**0.00E-00**	-145-5p	5.77	8.69E-12
-323a-3p	7.86	8.48E-110	**-1468-5p**	**5.77**	**8.69E-12**
-937-3p	7.67	2.83E-96	-522-3p	5.77	8.69E-12
-199a-5p	**7.56**	**2.33E-89**	-891a-5p	5.77	8.69E-12
-320c	**7.43**	**0.00E-00**	-320b	5.36	0.00E-00
-370-3p	7.41	2.39E-80	-615-3p	5.29	7.21E-212
-1910-3p	7.38	7.53E-79	**-320c**	**5.11**	**7.09E-319**
-433-3p	7.31	6.07E-75	**-320d**	**4.95**	**1.59E-147**
-543	**7.18**	**0.00E-00**	-328-3p	4.84	6.54E-45
-216b-5p	7.14	7.86E-67	-320a-3p	4.82	0.00E-00
-190b-5p	6.97	2.49E-59	-126-5p	4.36	2.47E-25

sEV-miRs ordered by FC. Bold indicates sEV-miRs enriched in sEV-MCF10A and in sEV-MDA231 compared with the parental cells.

5.2.4 Several sEV-miRs are differentially enriched in sEV-MDA231

After the characterization of the sRNA profile of sEVs secreted by the different BC cells lines and the identification of the miRNAs in their cargo, we aimed to look for sEV-miRs enriched or overrepresented in the different sEVs. As we did not have biological replicates, we used the edgeR software (package), included in the sRNAde web-tool to perform the "differential expression" (DE) analysis. As we were interested in the metastatic potential of MDA-MB-231 BC cells and the possibility of sEV-MDA231 to induce EMT, we took all sEV-miRs detected in each of the sEVs (sEV-MCF10A, sEV-T47D, sEV-ZR75 and sEV-MD231) and use edgeR to identify enriched sEV-miRs present in sEV-MDA231 against all of the other sEVs. This analysis showed 44, 63 and 50 sEV-miRs enriched in sEV-MDA231 vs sEV-MCF10A, sEV-T47D and sEV-ZR75, respectively (**Table 11**). Of those enriched sEV-miRs, 22 of them were commonly enriched in sEV-MDA231, regardless of the sEVs with which they were compared (**Table 12**). Interestingly, Venn diagram shown in figure 9 show 24 sEV-miRs enriched in sEV-MDA231 (**Figure 9**), this is because, oddly, miR-126-5p and miR-145-5p, were also included in the DE analysis although they were only detected in sEV-MDA231 and not in the other sEVs. This was the first step to define the possible "EMT-promoter" sEV-miRs. The next step was to evaluate whether those sEV-miRs only detected and enriched in sEV-MDA231 had an association or were implicated with the process of EMT or other tumorigenic/oncogenic or metastatic process, such as cell migration. To do that, we used miRWalk (http://mirwalk.umm.uni-

heidelberg.de/) and DianaTools, specifically the miRPath v3 tool (https://dianalab.e-ce.uth.gr/html/mirpathv3/index.php?r=mirpath), to look for overrepresented biological processes or pathways favored by the sEV-miRs enriched in sEV-MDA231. KEGG analysis using miRPath (filtering by TarBase v7.0) showed that several oncogenic processes were overrepresented or favored by those 27 sEV-miRs such as fatty acid biosynthesis and metabolism ($p < 1E-325$; p 7.49E-5), ECM-receptor interaction ($p < 1E-325$), Hippo signaling pathway ($p = 8.04E-9$), cell cycle ($p = 2.75E-6$), TGF-β signaling ($p = 1.15E-8$), adherens junctions ($p = 4.72E-12$) and focal adhesion ($p = 3.45E-3$). In terms of overrepresented GO biological processes, the analysis showed that cellular extracellular matrix disassembly and organization, growth factors signaling, mitotic cell cycle, immune processes, neurotrophin TRK receptor signaling, membrane organization and mRNA metabolic process could be favored by those sEV-miRs. In addition, molecular function GO analysis showed overrepresentation of functions like ion binding, RNA binding, cytoskeletal protein binding, transcription factor binding and histone binding; all functions that could regulate tumor progression and metastasis. **Tables 13 and 14** show the more significant pathways (KEGG) and processes (GO) overrepresented by the 27 sEV-miRs enriched in sEV-MDA231. It is noteworthy that if we first use miRWalk to look for possible sEV-miRs targets (predicted and experimentally validated), and then do the GO analysis using Panther, the possible oncogenic overrepresented processes and pathways are increased and include interesting

processes such “miRNA processing”, “response to hypoxia”, “positive regulation of cell migration” (enriched GO_BP; Bonferroni corrected. Experimentally validated targets), “SMAD protein complex assembly”, “DNA damage response, signal transduction by p53”, “negative regulation of cell-matrix adhesion” (enriched GO_BP; FDR corrected. Experimentally validated targets); “RNA binding”, “transcription coactivator binding”, “DNA binding”, “Ubiquitin protein ligase binding”, “chromatin binding”, “protein kinase activity” (GO_MF; FDR corrected. Experimentally validated targets), “p53 pathway”, “Insulin/IGF PKB signaling”, “Ras pathway”, TGF-β signaling pathway”, “PDGF signaling pathway”, “angiogenesis” (GO_Pathways; FDR corrected. Predicted targets) and “signaling by TGF-beta receptor complex in cancer”, “DNA methylation”, “oncogene induced senescence”, “MAP kinase activation”, “FOXO-mediated transcription of cell cycle genes” (GO_Reactome; FDR corrected. Experimentally validated targets). The most relevant results of these analysis are listed in **Table C-F** in Annexes. In summary, the 27 possible “EMT-promoter” sEV-miRs candidates that are enriched or selectively present in sEV-MDA231 could promote and stimulate several oncogenic and pro-metastatic processes and signaling pathways related with the EMT (**Figure 10**). Specifically, the reported role of those 27 sEV-miRs enriched in sEV-MDA231 in the regulation of the EMT is also listed in **Table G** in the annexes. The table show that there is evidence supporting both, an EMT-promoter and EMT-suppressing role for most of the sEV-miRs, which is interesting

because it suggests that their specific role may be cancer-dependent or even sEV-dependent (**Table G** in annexes).

Table 11: Total number of dysregulated sEV-miRs. Enriched and decreased sEV-miRs between each sEVs secreted by the different cell lines are indicated

	sEV-MDA231 vs			sEV-ZR75 vs			sEV-T47D vs		
	Total	**Enriched**	**Decreased**	**Total**	**Enriched**	**Decreased**	**Total**	**Enriched**	**Decreased**
sEV-MCF10A	337	44	293	370	128	242	355	83	272
sEV-T47D	194	63	131	161	110	51			
sEV-ZR75	226	50	176						

Table 12: List of the twenty-two sEV-miRs identified as enriched in sEV-MDA231 compared with every other BC cells-secreted sEVs analyzed

	Fold Change		
Mature sEV-miR	**MDA231 vs ZR75**	**MDA231 vs T47D**	**MDA231 vs MCF10A**
miR-1-3p	118,2	1335,7	271,9
miR-10a-3p	3,2	28,6	82,1
miR-100-5p	381,9	28,3	2,7
miR-122-5p	41,5	115,0	6,2
miR-125b-1-3p	1248,3	931,1	3,2
miR-133a-3p	55,7	41,7	19,0
miR-143-3p	20,3	7,0	10,9
miR-146a-5p	57,5	51,6	148,8
miR-199a-3p	5,7	2,6	2,8
miR-199a-5p	4,0	3,7	4,4
miR-199b-3p	4,9	2,6	2,6
miR-218-5p	29,2	22,0	2,7
miR-223-3p	3,7	23,4	66,7
miR-432-5p	9,7	48,3	3,0
miR-499a-5p	39,8	3,2	3,2
miR-503-5p	207,2	154,7	3,6
miR-522-3p	2,6	15,5	10,8
miR-760	3,1	48,6	2,6
miR-891a-5p	20,4	15,5	9,6

miR-1307-5p	3,2	9,3	3,2
let-7d-5p	2,5	2,3	4,4
let-7i-5p	4,6	2,3	2,7

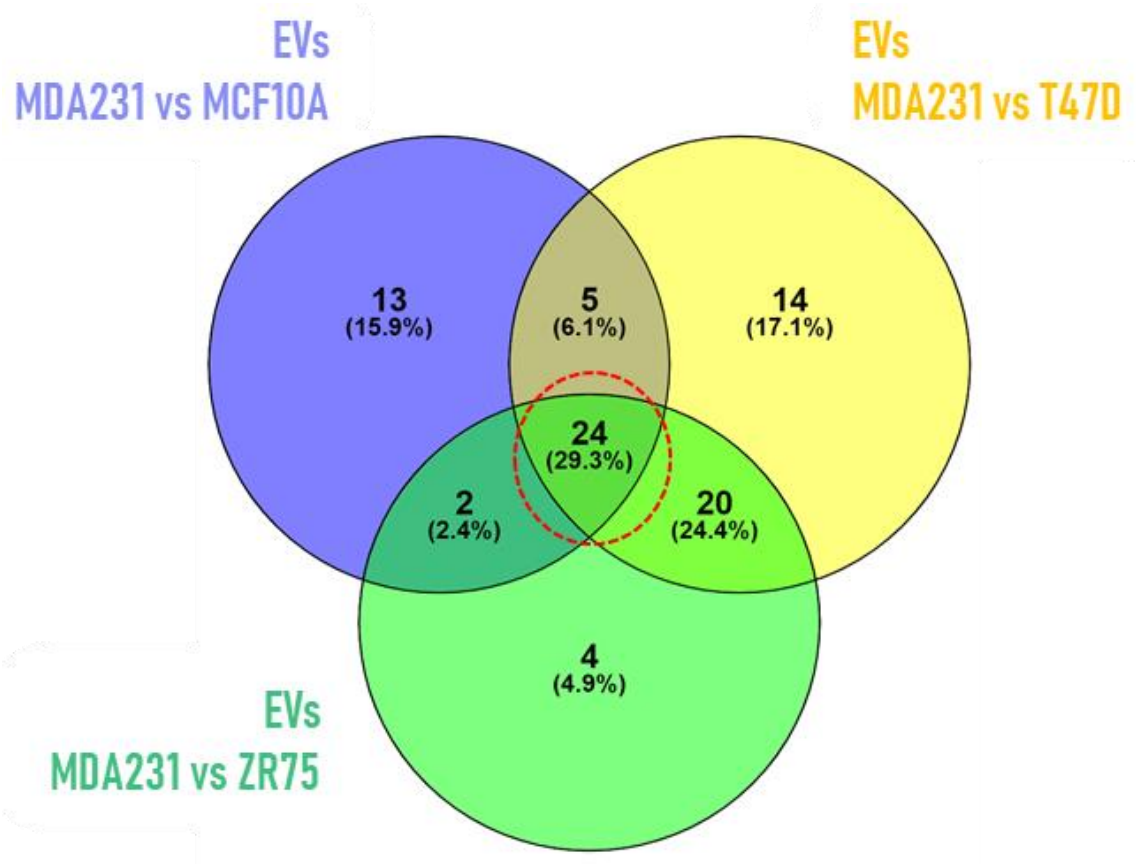

Figure 9: Identification of sEV-miRs differentially enriched in sEV-MDA231.

Annotated enriched miRNAs of each sEVs sample were separated in lists and organized in a Venn diagram. sEV-miRs enriched in sEV-MDA231 compared with every other BC cells-secreted sEVs are compared (blue: sEV-MDA231 vs sEV-MCF10A; yellow: sEV-MDA231 vs sEV-T47D; green: sEV-MDA231 vs sEV-ZR75). Twenty-four sEV-miRs were always differentially enriched in sEV-MDA231 and are indicated in the red dashed line circle. Numbers inside figures indicate absolute numbers of sEV-miRs detected and percentage of total.

Table 13: KEGG analysis of the 27 sEV-miRs enriched or selectively present in sEV-MDA231

KEGG pathway	Adj. p-value	#genes	#sEV-miRs
Fatty acid biosynthesis	p < 1E-325	2	5
ECM-receptor interaction	p < 1E-325	31	7
Proteoglycans in cancer	p < 1E-325	126	11
Pathways in cancer	1.53E-13	182	10
Fatty acid metabolism	1.71E-13	6	5
Adherens junction	4.72E-12	48	8
Viral carcinogenesis	1.91E-11	83	7
Hippo signaling pathway	8.04E-9	75	7
TGF-beta signaling pathway	1.15E-8	46	10
Hepatitis	3.36E-7	70	9
Cell cycle	2.75E-6	65	6
Colorectal cancer	7.06E-5	31	9
Chronic myeloid leukemia	7.71E-5	43	5
Glioma	1.51E-4	36	8
P53 signaling pathway	2.67E-4	36	5
Transcriptional misregulation in cancer	6.31E-4	59	4
Focal adhesion	3.45E-3	69	4
FoxO signaling pathway	4.83E-3	63	5
Lysine degradation	5.30E-3	18	5
Thyroid hormone signaling pathway	3.03E-2	58	6

Table 14: GO analysis of the 27 sEV-miRs enriched or selectively present in sEV-MDA231

GO biological process	Adj. p-value	#genes	#sEV-miRs
Extracellular matrix disassembly	p < 1E-325	49	7
Transcription initiation from RNA pol II promoter	p < 1E-325	92	8
Fibroblast growth factor receptor signaling pathway	p < 1E-325	80	8
RNA metabolic process	p < 1E-325	117	9
Extracellular matrix organization	p < 1E-325	135	9
Epidermal growth factor receptor signaling pathway	p < 1E-325	100	10
Cell death	p < 1E-325	362	10
Protein complex assembly	p < 1E-325	282	11

mRNA metabolic process	p < 1E-325	115	11
Platelet activation	p < 1E-325	86	11
Mitotic cell cycle	p < 1E-325	228	12
Immune system process	p < 1E-325	493	12
DNA metabolic process	p < 1E-325	317	12
Blood coagulation	p < 1E-325	193	13
Cellular component assembly	p < 1E-325	514	13
Macromolecular complex assembly	p < 1E-325	366	13
Fc-epsilon receptor signaling pathway	p < 1E-325	89	14
Cellular protein metabolic process	p < 1E-325	250	14
Small molecule metabolic process	p < 1E-325	919	14
Neurotrophin TRK receptor signaling pathway	p < 1E-325	146	15
GO molecular function	**Adj. p-value**	**#genes**	**#sEV-miRs**
Cytoskeletal protein binding	p < 1E-325	283	12
Nucleic acid binding transcription factor activity	p < 1E-325	392	13
Protein binding transcription factor activity	p < 1E-325	255	14
RNA binding	p < 1E-325	798	17
Ion binding	p < 1E-325	2282	21
Poly(A) RNA binding	p < 1E-325	644	17

a

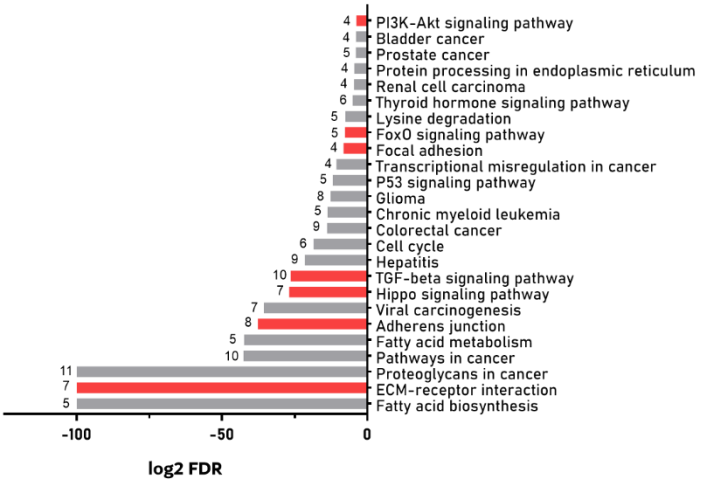

b

GO_BP Analysis

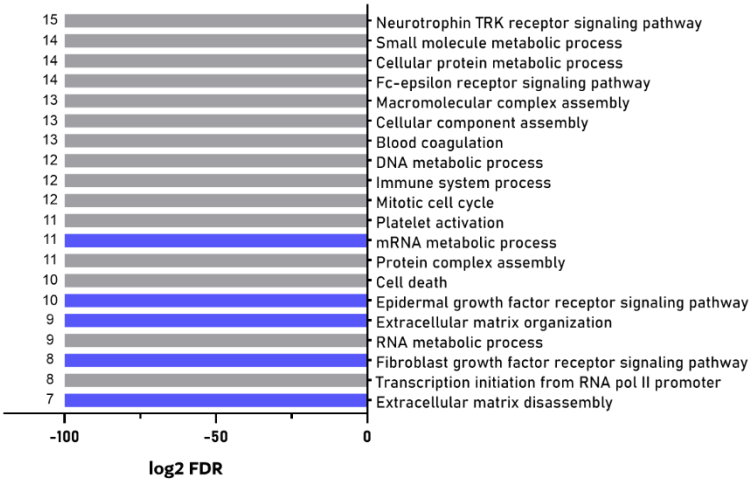

c

GO_MF Analysis

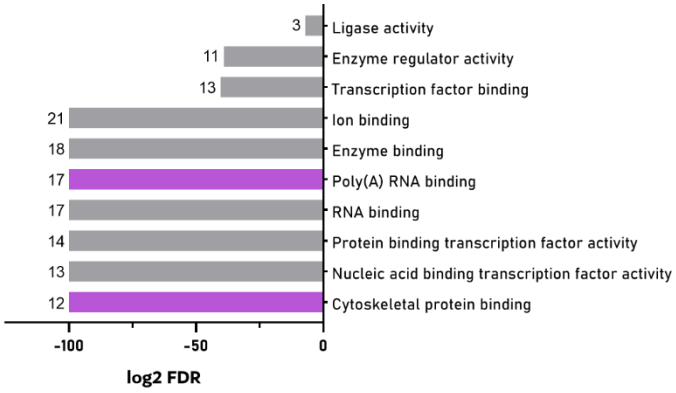

Figure 10: GO and pathway (KEGG) analysis summary of enriched sEV-miRs present in sEV-MDA231.

The 27 "EMT-promoter" candidate sEV-miRs enriched in sEV-MDA231 were used to perform KEGG **(a)** and GO analyses **(b,c)** using the miRPath v3 webtool. Parameters were set as default and false discovery rate (FDR) correction was used to evaluate statistical significance (adjusted p value < 0.05). The top 25 **(a)**, 20 **(b)** and 10 **(c)** overrepresented pathways, processes and functions are shown in each graph. Numbers next to each bar indicates the number of sEV-miRs involved in each process.

5.2.5 Validation of candidate "EMT-promoter" sEV-miRs using miQPCR

Finally, to validate the enrichment of those 27 sEV-miRs in sEV-MDA231 after the analysis of sRNA-seq data, we used a particular format of RT-qPCR, called miQPCR, developed by Benes and coworkers (146). miQPCR primers and oligos sequences can be found in the original article and in **Table A** in Annexes. As there are no validated housekeeping sRNAs regarding to sEVs, we first needed to found the best sEV-miR (or combination of sEV-miRs) to normalize our results. Eight miRNAs previously used as normalizers in the literature (110,114,151–156) were tested as possible normalizers of our data. The possible normalizer miRNAs tested were miR-16-5p, miR-21-5p, miR-25-3p, miR-125a-5p, miR-148a-3p, miR-423-3p, miR-451a and miR-484. We used the NormFinder add in of Microsoft Excel to analyze the individual Ct of each miRNA and found the best normalizer/s according to their expression stability (variability) in a given sample set and given experimental design (147). We saw that, among all the possible miRNAs tested

as normalizers, miR-16-5p, miR-21-5p, miR-148a-3p and miR-484 were the ones with the least variability (**Table H** in Annexes). Among them, the combination of miR-16-5p and miR-148a-3p was the best normalization combination. Therefore, this combination was used as normalizer for subsequent analyses. With the best normalizers defined, we sought to validate the enriched sEV-miRs detected in sEV-MDA231 after the sRNA-seq analysis. Using the miQPCR assay, we standardize the assay using an amount of cDNA corresponding to the same number of particles, as quantified by NTA (1.0×10^5 total particles). According to the sRNA-seq analysis, among the 27 sEV-miRs enriched in sEV-MDA231, we were able to validate the detection of 8 sEV-miRs. Of them, six out of eight validated sEV-miRs were detected as enriched in sEV-MDA231, thus agreeing with the sRNA-seq (**Figure 11**). The 6 validated enriched sEV-miRs were miR-100-5p (17.8-fold vs sEV-MCF10A), miR-122-5p (36.7-fold vs sEV-MCF10A), miR-146a-5p (9748.3-fold vs sEV-MCF10A) (**Figure 11a-c**), and despite not being statistically significant against sEV-ZR75, let-7d-5p (12-fold vs sEV-MCF10A), miR-223-5p (4.9-fold vs sEV-MCF10A), and miR-760 (12.4-fold vs sEV-MCF10A) (**Figure 11d-f**). Interestingly, we also saw in the process of enrichment validation that, in contrast of the sRNA-seq data, let-7i-5p behaved as a suitable endogenous control (**Figure S2a** in Annexes). Thus, we also normalize miQPCR data against let-7i-5p expression to have a comparison against defined normalizers and we saw similar results (**Figure S2b,g**).

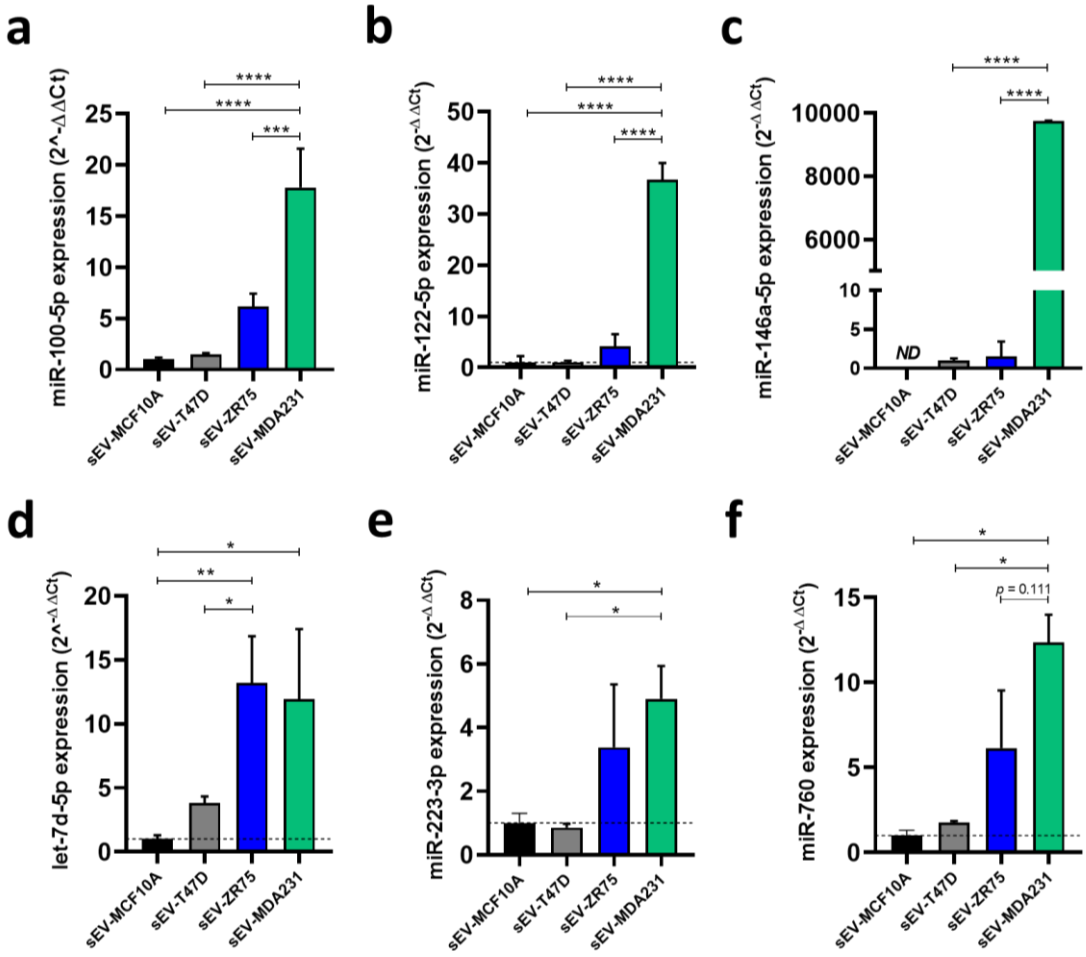

Figure 11: Validation of the presence and levels of "EMT-promoter" sEV-miRs in sEV-MDA231 through miQPCR.

The twenty-seven candidate sEV-miRs enriched in sEV-MDA231 through the sRNA-seq analyses were experimentally tested by miQPCR. Eight of them were correctly detected and six were effectively validated as enriched in sEV-MDA231. **(a)** miR-100-5p; **(b)** miR-122-5p; **(c)** miR 146a-5p; **(d)** let-7d-5p; **(e)** miR-223-3p and **(f)** miR-760. Graphs shows mean ± SD. Each miRNA expression was normalized against RNU6b. All data is representative of 3 independent experiments. (*) $p < 0.05$; (**) $p < 0.01$; (***) $p < 0.001$; (****) $p < 0.0001$.

Interestingly, pathway analysis (KEGG) (**Figure 12a**) and GO (Biological processes) (**Figure 12b**) showed that these 6 sEV-miRs are implicated in several oncogenic processes related with cell migration and EMT, such as TGF-β signaling pathway, adherens junction, FoxO signaling pathway, ECM-interaction, regulation of locomotion and cell motility, among others (**Figure 12**). These 6 validated sEV-miRs were used in the next co-transfection experiments.

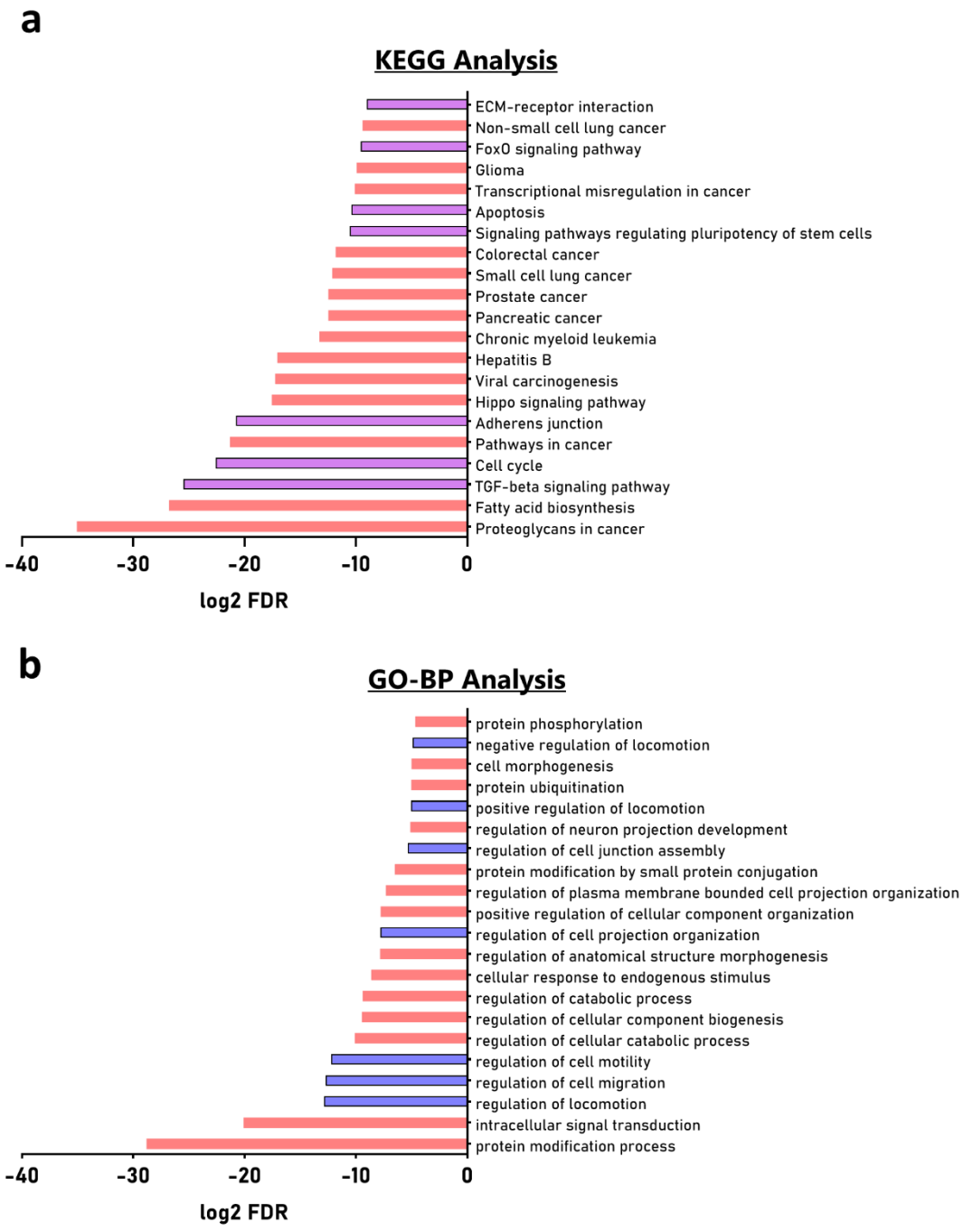

Figure 12: Pathway (KEGG) and GO analysis summary of the six experimentally validated sEV-miRs present and enriched in sEV-MDA231.

The six miRNAs were listed in the web server DianaTools to use mirPath tool (https://dianalab.e-ce.uth.gr/html/mirpathv3/index.php?r=mirpath). **(a)** KEGG (up) and **(b)** GO Biological processes (down) analyses were performed with default settings using TarBase v7.0 database as interaction database. P-value was set at 0.05 and adjusted p-value was calculated with FDR correction. Bars in purple (KEGG) and blue (GO-BP) indicate pathways and processes closely related with EMT.

In summary, the smallRNA and miRNA profile of different BC cells-secreted sEVs were characterized. Interestingly, tRNA fragments, and not miRNAs are the most abundant sRNA species in BC sEVs. On the other hand, after sRNA-seq, several sEV-miRs were detected as enriched in metastatic sEV-MDA231 versus other BC cells-secreted sEVs. They could participate in several oncogenic processes related with the EMT, most notably cell migration, locomotion, and the TGF-β pathway.

5.3 Specific aim 3 results

To evaluate the role of candidate sEV-miRs overrepresented in metastatic sEV-MDA231 on the expression of EMT molecular markers in non-metastatic BC cells.

5.3.1 Evaluation of EMT-related genes in MCF10A and T47D cells after co-transfection of validated "EMT-promoter" sEV-miRs

Validated candidate "EMT-promoter" sEV-miRs were co-transfected in MCF10A mammary epithelial non-tumorigenic and T47D non-metastatic BC cells according to **Table 15** using Lipofectamine 2000 reagent. According to sRNA-seq data of

sEV-MDA231, i.e. normalized read count, we aimed to transfect each sEV-miR proportionally. So, **Table 15** show the stoichiometry of the co-transfection experiment.

Table 15: Stoichiometry and final concentration of each sEV-miR for the co-transfection assays

sEV-miR (MDA231)	Read count	RPM adj. (total)	Ratio (vs RPM)	Volume (WS 10 µM)	Final Conc (nM)	Ratio
miR-100-5p	31758	5579,14	1	2.5 uL	12.5	250
miR-122-5p	14949	2629,92	0.471	1.2 uL	6.0	120
miR-146a-5p	2329	406,13	0.073	1.8 uL (1 uM)	0.9	18
miR-223-3p	568	99,93	0.018	4.5 (0.1 uM)	0.225	4,5
miR-760	317	55,77	0.010	2.5 (0.1 uM)	0.125	2,5
let-7d-5p	116	20,41	0.004	1.0 (0.1 uM)	0.05	1

First, we aimed to evaluate co-transfection efficiency using an anti-sense oligonucleotide (ASO) conjugated with Alexa Fluor 594 fluorophore as a witness of transfection. We evaluated the transfection of the ASO alone, or in combination with one sEV-miR mimic as a test (let-7d-5p). With this strategy, we saw that transfection efficiency was near 100%, since almost all cells present AF594 fluorescence 24 and 48 h post-transfection (MCF10A cells) (**Figure 13a**). Moreover, miRNA overexpression was maintained at least for 48 h (**Figure 13b**).

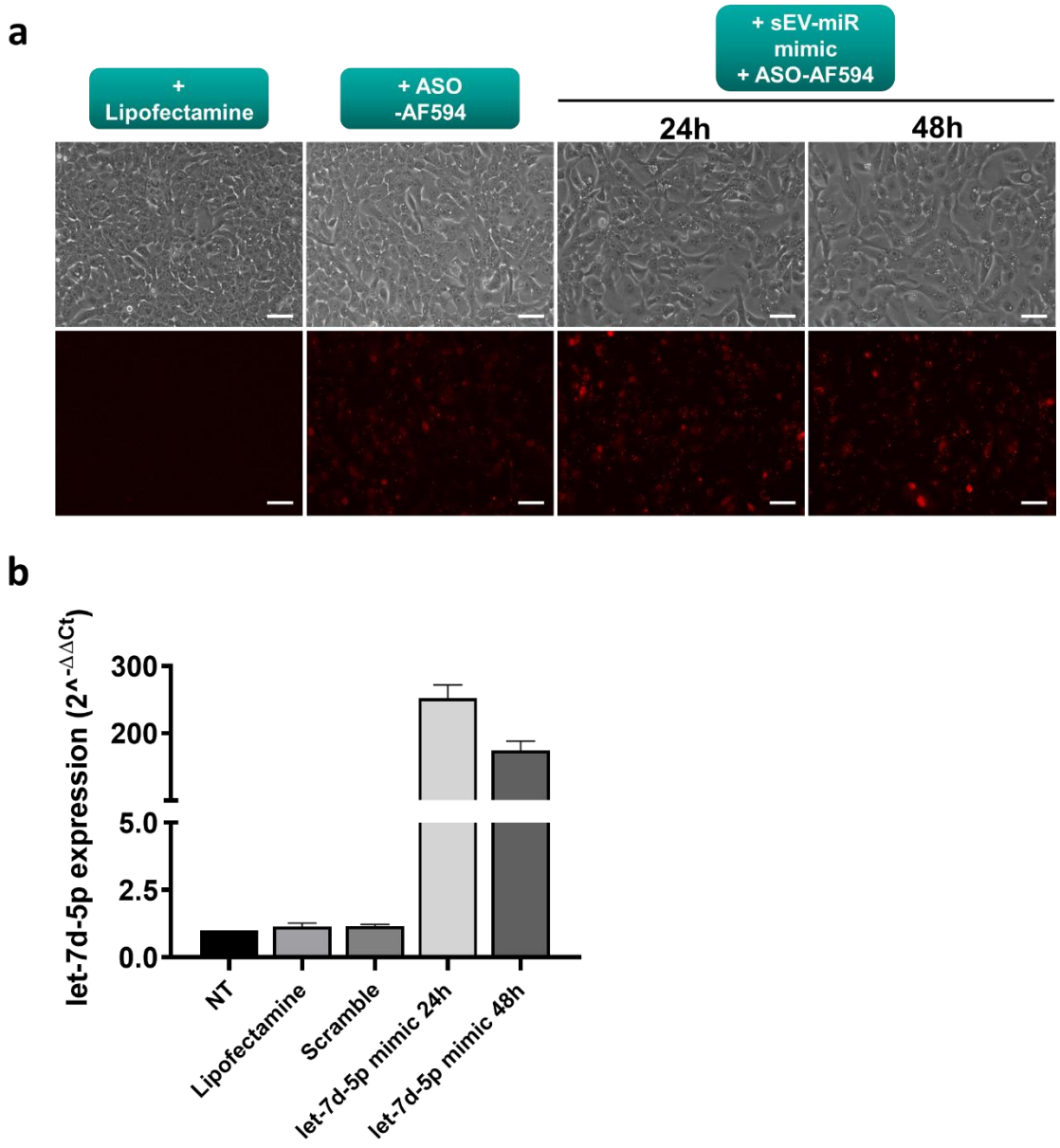

Figure 13: Evaluation of miRNA mimic transfection efficiency in MCF10A cells.

To evaluate mimic transfection efficiency, let-7d-5p mimic was co-transfected with a fluorescently-conjugated antisense oligonucleotide (ASO-AF594), and efficiency was assessed by red fluorescence due to ASO expression 24 and 48 h post-transfection. **(a)** Fluorescence and images were recorded in a Nikon Eclipse Ti epifluorescence microscope and analyzed with the NIS-elements AR v4.30.01 software. **(b)** miQPCR analysis to valuate let-7d-5p expression after co-

transfection with ASO-AF594. Let-7d-5p expression was normalized against RNU6b. Images shown are 20X magnified and size bar represents 30 µm.

Considering that almost all the cells were transfected with our setting, the next step was the co-transfection of the six validated sEV-miRs in MCF10A and T47D cells. The setting of the co-transfection is shown in **Table 15**, as previously mentioned. In parallel, both cell lines were incubated with sEV-MDA231 for 24 or 48 h. Five out of six co-transfected sEV-miRs mimics were overexpressed in both cell lines after mimic co-transfection; miR-100-5p, miR-122-5p, miR-146a-5p, miR-223-5p and miR-760. The incubation of MCF10A mammary epithelial cells and T47D BC cells with sEV-MDA231 also increase the levels of those sEV-miRs. However, the co-transfection of sEV-miRs mimics results in even higher levels of these sEV-miRs (**Figure 14-15**). Transfection of let-7d-5p mimic result in just a slight increase of its expression in MCF10A cells and no increase in transfected T47D BC cells. This was expected as the amount of let-7d-5p mimic transfected was very small, (final concentration in the pmol order) and the basal level of this miRNA was higher in T47D than in MCF10A cells. With these results, we showed that co-transfection of “EMT-promoter” sEV-miRs mimics results in an overexpression of those miRs in recipient cells. This overexpression was even greater than that achieved after incubation of these cells with sEV-MDA231 (**Figures 14-15**).

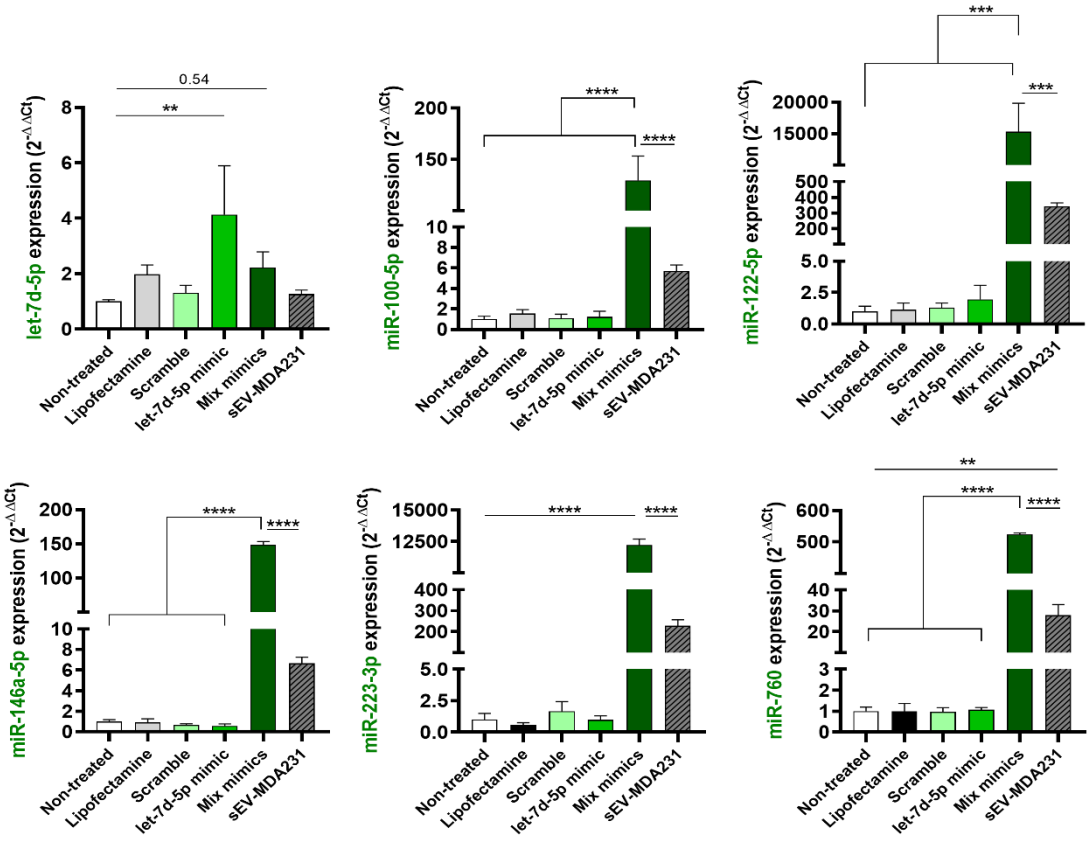

Figure 14: Evaluation of sEV-miRs overexpression after co-transfection of "EMT-promoter" sEV-miRs mimics and treatment with sEV-MDA231 in MCF10A cells.

The six "EMT-promoter" sEV-miRs were co-transfected in MCF10A cells using lipofectamine 2000 and their overexpression was evaluated 24 h later. Treatment of cells with sEV-MDA231 was used as control/comparison. Graphs show mean ± SEM. All data is representative of 3 independent experiments. (**) $p < 0.01$; (***) $p < 0.001$; (****) $p < 0.0001$.

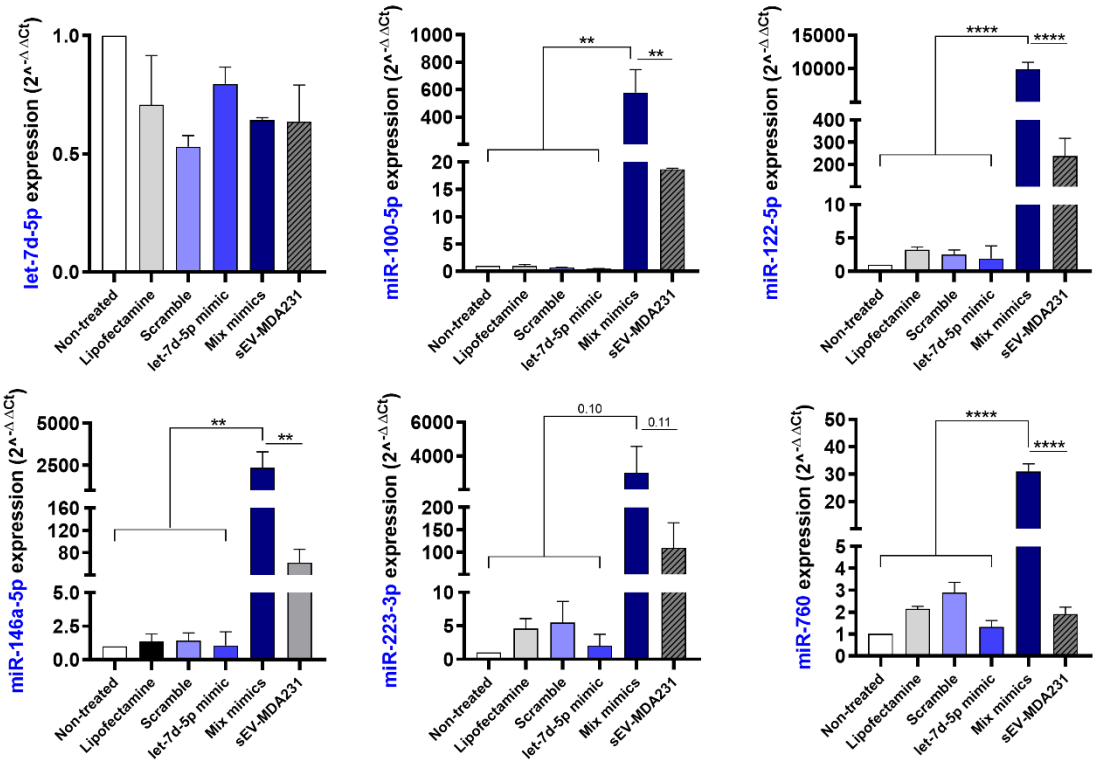

Figure 15: Evaluation of sEV-miRs overexpression after co-transfection of "EMT-promoter" sEV-miRs mimics and treatment with sEV-MDA231 in T47D BC cells.

The six "EMT-promoter" sEV-miRs were co-transfected in MCF10A cells using lipofectamine 2000 and their overexpression was evaluated 24 h later. Treatment of cells with sEV-MDA231 was used as control/comparison. Graphs show mean ± SEM. All data is representative of 3 independent experiments. (**) $p < 0.01$; (****) $p < 0.0001$.

5.3.2 Analysis of EMT-related markers after co-transfection of MCF10A and T47D BC cells with "EMT-promoter" sEV-miRs mimics

After the confirmation of overexpression of the co-transfected "EMT-promoter" sEV-miRs, we aimed to analyze gene expression and protein levels of some characteristic EMT-related markers. mRNA levels of the following EMT-related

markers were measured in sEV-miRs mimics co-transfected or sEV-MDA231-treated MCF10A and T47D cells: E-Cadherin (*CDH1*), N-Cadherin (*CDH2*), Vimentin (*VIM*), Zeb1 (*ZEB1*), Twist1 (*TWIST1*), Snail (*SNAI1*), Fibronectin (*FN*), Oct4 (*OCT4*), Sox2 (*SOX2*) and Nanog (*NANOG*). In MCF10A cells, sEV-miRs mimics co-transfection slightly increase the expression of *CDH1*, *CDH2*, *FN*, VIM, and *NANOG* (**Figure 16a-d – Figure 17a**), analyzed 24 h after transfection. On the other hand, the expression of the other stem-related transcription factors *SOX2* and *OCT4* was the same in all conditions (**Figure 17b,c**). Interestingly, the expression of the EMT transcription factors (EMT-TFs) *TWIST1, ZEB1* and *SNAI1* were also not different than that of untreated cells (**Figure 17d-f**), despite the apparent increase (yet not significant) in *SNAI1* expression after co-transfection of the sEV-miRs mimic mix (**Figure 17f**). These results suggest that the co-transfection of these 6 “EMT-promoter” sEV-miRs promote/stimulate some kind of “partial EMT”, increasing the levels of some characteristic EMT-markers, but not that of the EMT-TFs.

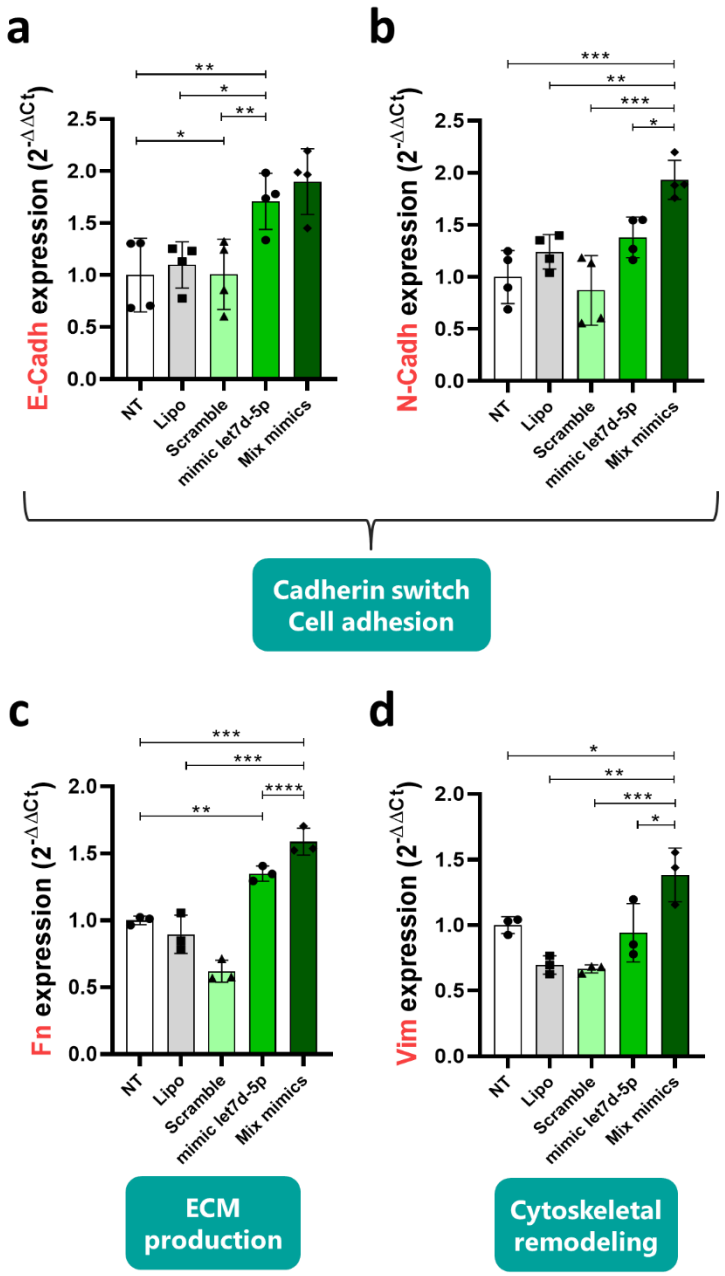

Figure 16: Evaluation of the expression of EMT-markers after the co-transfection of "EMT-promoter" sEV-miRs mimics in MCF10A cells.

The six "EMT-promoter" sEV-miRs were co-transfected in MCF10A cells using lipofectamine 2000 and their effect on EMT-markers expression was evaluated 24 h later. **(a)** E-Cadherin (*CDH1*), **(b)** N-Cadherin (*CDH2*), **(c)** Fibronectin (*Fn*) and **(d)** Vimentin (*Vim*) expression were quantified.

Graph shows mean ± SD. All data is representative of 3-4 independent experiments. (*) $p < 0.05$; (**) $p < 0.01$; (***) $p < 0.001$; (****) $p < 0.0001$.

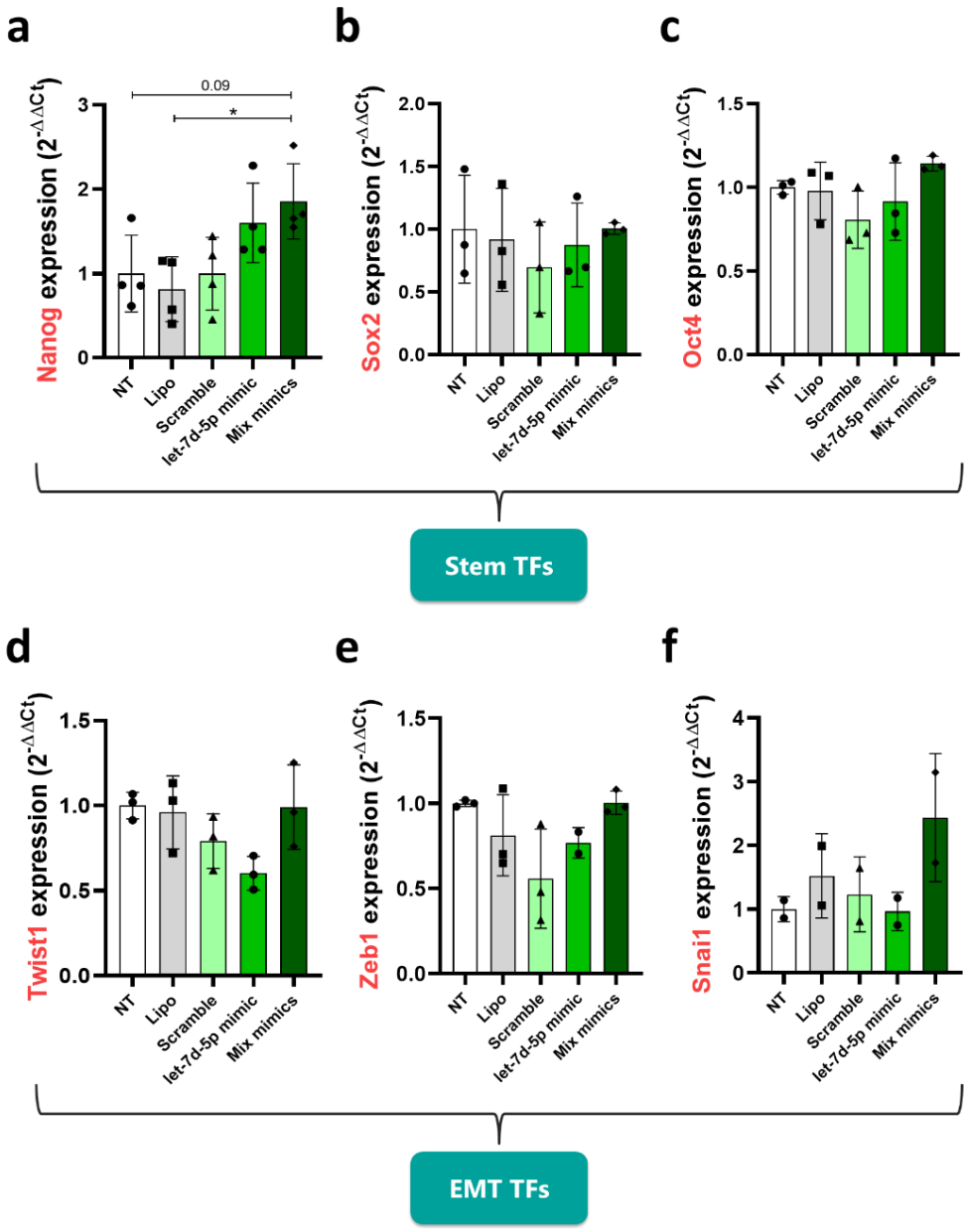

Figure 17: Evaluation of the expression of stemness and EMT-TFs after the co-transfection of "EMT-promoter" sEV-miRs mimics in MCF10A cells.

The six “EMT-promoter” sEV-miRs were co-transfected in MCF10A cells using lipofectamine 2000 and their effect on stemness- **(a-c)** and EMT-related transcription factors (TFs) **(d-f)** expression was evaluated 24 h later. Graphs show mean ± SD. All data is representative of 2-3 independent experiments. (*) $p < 0.05$.

In the case of T47D BC cells, co-transfection of the “EMT-promoter” sEV-miRs caused contradictory results. On one hand, let-7d-5p mimic transfection, co-transfection of sEV-miRs mimics cocktail and sEV-MDA231 treatment increased the expression of *CDH1* (E-Cadh) and *Fn* (Fibronectin). On the other hand, they did not change *Vim* (Vimentin) expression (**Figure 18**). *CDH2* (N-Cadherin) could not be detected. In terms of stem-TFs, let-7d-5p mimic transfection, co-transfection of sEV-miRs mimics cocktail and sEV-MDA231 treatment did not change the expression of *Nanog* or *Six2*, but they seemed to decreased the expression of *Oct4*. However, transfection of the scramble miRNA caused similar results (**Figure 19a-c**), thus, this result needs to be taken with caution. Interestingly, co-transfection of the “EMT-promoter” sEV-miRs significantly increased the expression of *Snai1* (Snail) EMT-TF (Figure 19d). However, they did not change the expression of the other *Zeb1* or *Twist1* (**Figure 19e,f**). Despite the fact that some genes tested changed their expression in response to the mimics transfected, these results could suggest that the EMT itself is not promoted in these BC cells after the co-transfection of those miRNAs.

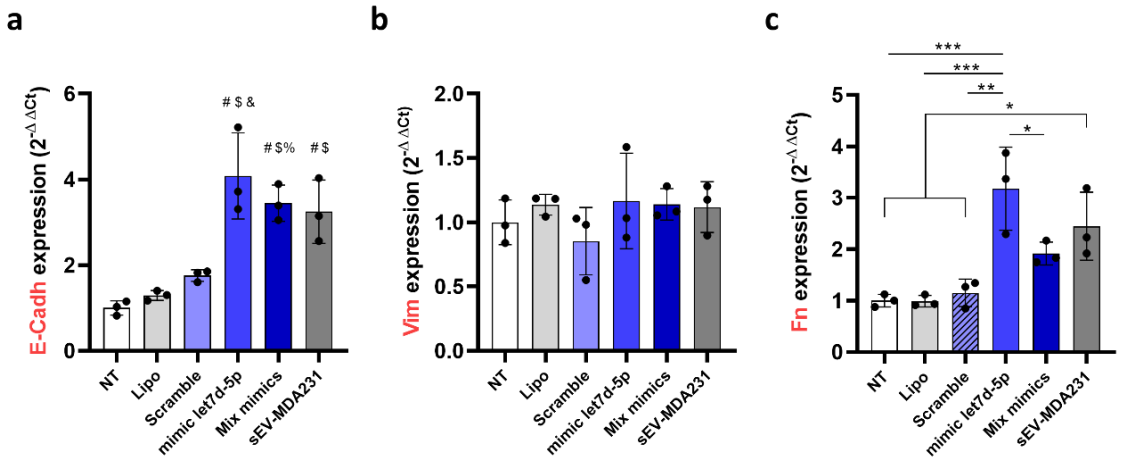

Figure 18: Evaluation of the expression of EMT-markers after the co-transfection of "EMT-promoter" sEV-miRs mimics in T47D BC cells.

The six "EMT-promoter" sEV-miRs were co-transfected in T47D cells using lipofectamine 2000 and their effect on EMT-markers expression was evaluated 24 h later. Treatment of cells with sEV-MDA231 was used as control/comparison. **(a)** E-Cadherin (*CDH1*), **(b)** Vimentin (*Vim*) and **(c)** Fibronectin (*Fn*) expression were quantified Graph shows mean ± SD. All data is representative of 3 independent experiments. (*) $p < 0.05$; (**) $p < 0.01$; (***) $p < 0.001$. (#) $p < 0.01$ vs NT; ($) $p < 0.01$ vs Lipo; (&) $p < 0.01$ vs Scramble; (%) $p < 0.05$ vs Scramble.

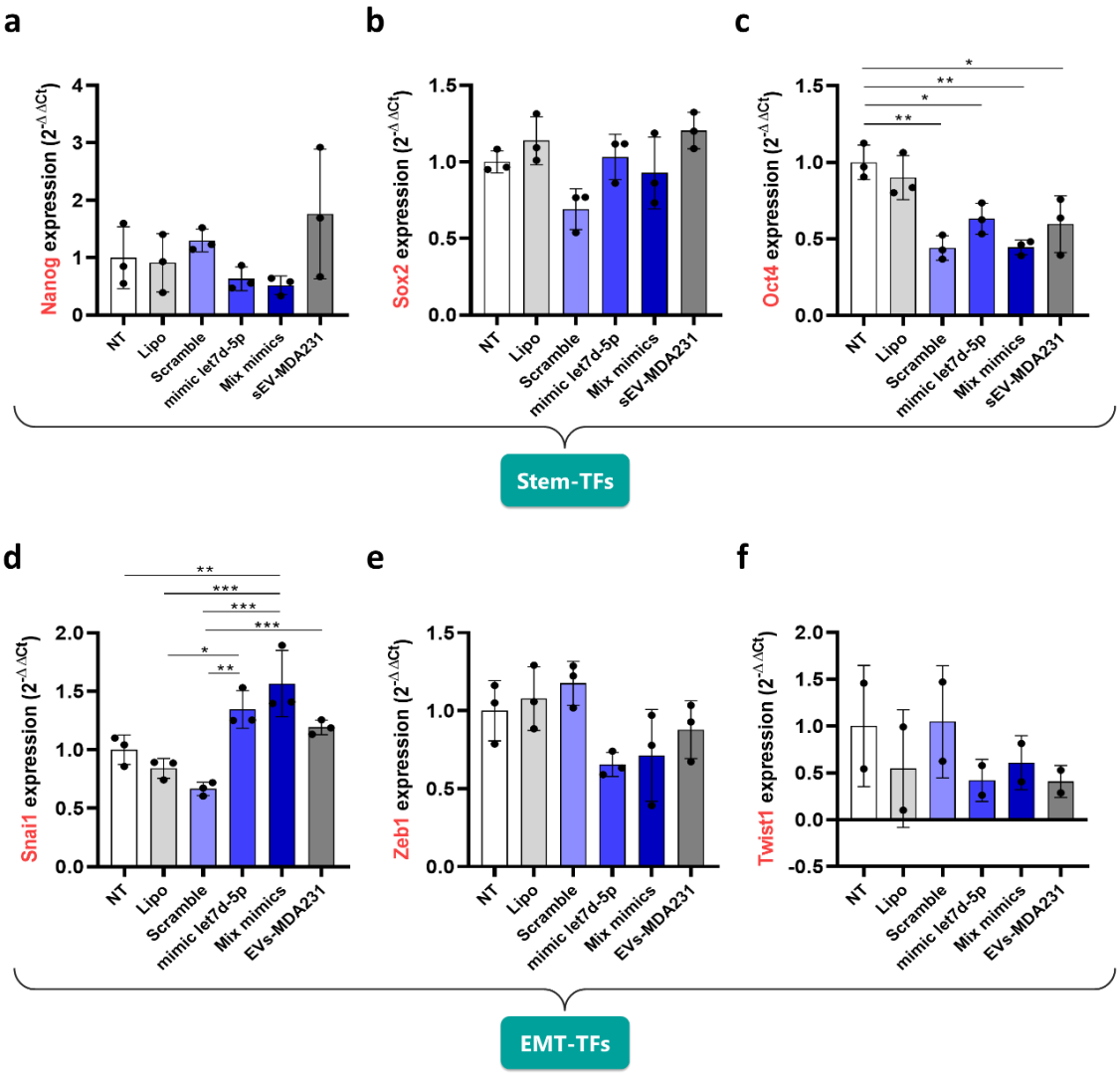

Figure 19: Evaluation of the expression of stemness and EMT-TFs after the co-transfection of "EMT-promoter" sEV-miRs mimics in T47D BC cells.

The six "EMT-promoter" sEV-miRs were co-transfected in T47D cells using lipofectamine 2000 and their effect on stemness- **(a-c)** and EMT-related **(d-f)** transcription factors (TFs) expression was evaluated 24 h later. Treatment of cells with sEV-MDA231 was used as control/comparison. Graphs show mean ± SD. All data is representative of 2-3 independent experiments. (*) $p < 0.05$; (**) $p < 0.01$; (***) $p < 0.001$.

In a similar way, we tried to evaluate protein levels of some of the EMT-related genes in co-transfected MCF10A and T47D cells. Protein samples were obtained 24 and 48 h after co-transfection or after incubation with sEV-MDA231. Despite de fact that gene expression was just slightly affected, both, co-transfection of "EMT-promoter" sEV-miRs mimics or sEV-MDA231 treatment increase the presence of some EMT characteristic proteins in MCF10A non-tumorigenic mammary epithelial cells 24 h post-treatment. First, E-Cadherin (~130 kDa; epithelial marker) levels seemed to increase 24 h after transfection of let-7d-5p mimic alone and after co-transfection of "EMT-promoter" sEV-miRs mimics cocktail. Also, incubation of these cells with sEV-MDA231 for 24 and 48 h caused a ~5-fold increase in the expression of this protein, however, it was not statistically significant (**Figure 20a,b**). N-Cadherin (~130 kDa), a more mesenchymal marker seemed to slightly (but not significant) increase 48 h post-transfection with the combination of sEV-miRs mimics. Interestingly, sEV-MDA231 caused a significant effect 48 h post-treatment (**Figure 20a,c**). On the other hand, Vimentin (~55 kDa) protein levels were increased 24 h post-transfection (and at a lesser extent 48 h post-transfection) with either, let-7d-5p mimic alone, and with the combination of sEV-miRs mimics. Incubation with sEV-MDA231 for 24 and 48 h also increased Vimentin protein levels (~3 and ~5-fold increase). Noteworthy, Vimentin levels stayed high after 48 h post-incubation with sEV-MDA231, however, none of those changes were statistically significant (**Figure 20a,d**). In the case of EMT-TFs, Snail/Slug and Twist1 levels seemed to be higher in co-

transfected and sEV-MDA231-treated MCF10A cells 24 h after either of the interventions (**Figure 20e,f**). Transfection with let-7d-5p mimic alone achieved the higher increase in Twist1 at 24 h ($p < 0.01$). Co-transfection of sEV-miR mimics cocktail also increased Twist1 protein levels, but at a lesser extent (yet not significant). Interestingly, this tendency was maintained 48 h after co-transfection. Treatment with sEV-MDA231 also seemed to increase Twist1, but only at 24 h post-treatment (**Figure 20e**). In the case of Snail/Slug, a tendency to increase was obtained 24 h after each treatment, however, protein levels were normalized at 48 h. This could suggest that sEV-miRs mimics co-transfection have a short-time effect over EMT-characteristic proteins levels, and that sEV-MDA231 treatment have a longer effect than the co-transfection. However, these results need to be taken with caution as some of these consider just two repetitions of the experiment. Besides, other EMT-related proteins/markers (such as those evaluated through qPCR) should be evaluated to draw conclusions that are more reliable.

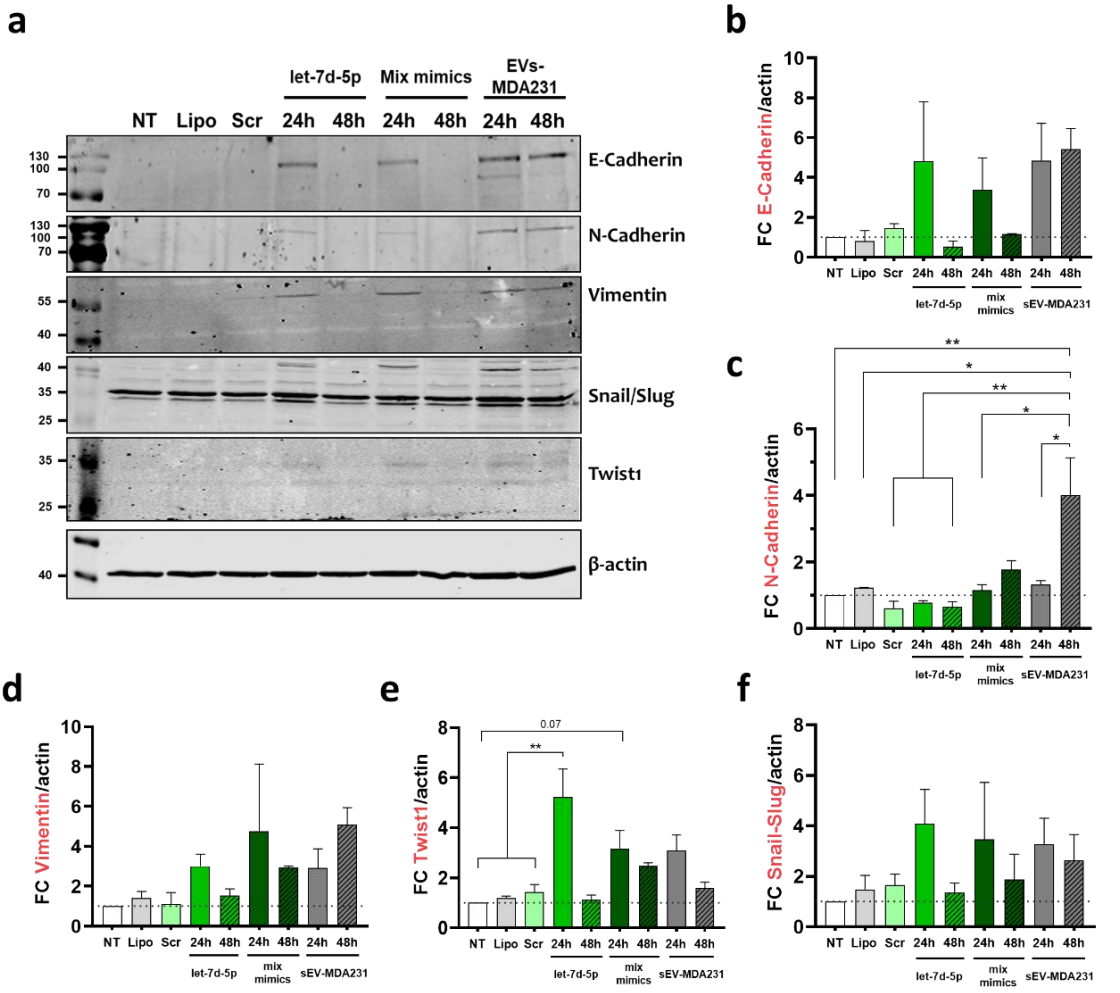

Figure 20: Co-transfection of "EMT-promoter" sEV-miRs mimics in MCF10A cells. EMT-proteins evaluation by Western blot.

The six "EMT-promoter" sEV-miRs were co-transfected in MCF10A cells using lipofectamine 2000 and their effect on EMT-markers protein levels were evaluated 24 and 48 h later. **(a)** Representative blot of EMT proteins. **(b-f)** Quantification of each EMT-related protein. E-Cadherin **(b)**, N-Cadherin **(c)**, Vimentin **(d)**, Twist1 **(e)** and Snail/Slug **(f)**. Treatment of cells with sEV-MDA231 was used as control/comparison. β-actin was used as housekeeping protein to normalize the data. Horizontal dashed line at y=1 indicates NT normalization. Graphs show mean ± SEM. All data is representative of 2-3 independent experiments. (*) $p < 0.05$; (**) $p < 0.01$.

On the other hand, T47D cells seems to be less responsive after any of the treatments given (either transfection of let-7d 5p mimic alone, co-transfection of sEV-miRs mimics cocktail or incubation with sEV-MDA231 (**Figure 21a**). Only let-7d-5p mimic transfection seemed to cause a decrease in E-Cadherin protein 48 h post-transfection (**Figure 21a,b**); no other changes were achieved compared with the non-treated cells. N-Cadherin protein levels seems to decrease 48 h after transfection with let-7d-5p mimic and 24 h after co-transfection with sEV-miRs mimics cocktail or treatment with sEV-MDA231, however, those apparent changes are not statistically significant (**Figure 21a,c**). On the other hand, Vimentin levels seemed to increase only after the co-transfection with the sEV-miRs mimics cocktail and with the treatment with sEV-MDA231, both at 24 and 48 h. However, this result needs to be taken with caution because scramble miRNA transfection also caused an increase of this protein (**Figure 21a,d**). In the case of EMT-TFs, only Twist1 seemed to increase its expression after incubation with sEV-MDA231 for 48 h, although this effect was not statistically significant (**Figure 21a,e**). Other treatments have protein levels similar to untreated cells.

In summary, co-transfection of “EMT-promoter” sEV-miRs mimics promote the expression of several EMT proteins in MCF10A “normal” non-tumorigenic mammary epithelial cells but just in short times (24 h after transfection). Treatment of MCF10A cells with one dose of sEV-MDA231 increase and maintain their overexpression for at least 48 h. On the contrary, it seems that neither the co-

transfection of “EMT-promoter” sEV-miRs mimics, nor the incubation with sEV-MDA231 promote the expression of EMT-characteristic protein markers in T47D non-metastatic BC cells (Figure 20-21).

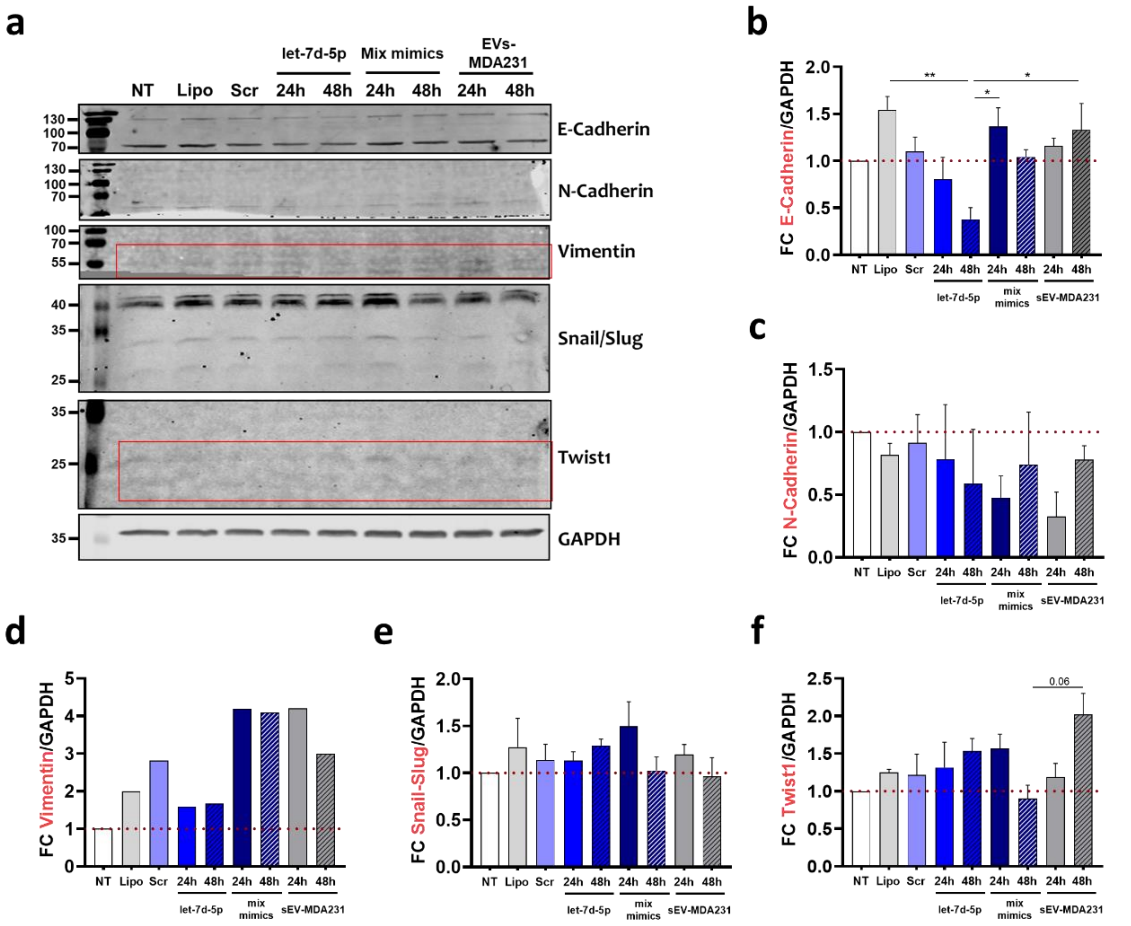

Figure 21: Co-transfection of “EMT-promoter” sEV-miRs mimics in T47D BC cells. EMT-proteins evaluation by Western blot.

The six “EMT-promoter” sEV-miRs were co-transfected in T47D cells using lipofectamine 2000 and their effect on EMT-markers protein levels were evaluated 24 and 48 h later. **(a)** Representative blot of EMT proteins. **(b-f)** Quantification of each EMT-related protein. E-Cadherin **(b)**, N-Cadherin **(c)**, Vimentin **(d)**, Snail/Slug **(e)** and Twist1 **(f)**. Treatment of cells with sEV-

MDA231 was used as control/comparison. GAPDH was used as housekeeping protein to normalize the data. Horizontal dashed line at y=1 indicates NT normalization. Graphs show mean ± SEM. All data is representative of 2-3 independent experiments. (*) $p < 0.05$; (**) $p < 0.01$.

5.3.3 Evaluation of the expression of direct mRNA targets of co-transfected "EMT-promoter" sEV-miRs mimics

To have a deeper notion on the effect of sEV-miRs mimics and sEV-MDA231 on transfected cells/recipient cells, we evaluated the expression of several predicted mRNA targets of co-transfected sEV-miRs. Predicted targets for the co-transfected sEV-miRs were obtained using KEGG (negative regulation of EMT), GO (GO 0010719; negative regulation of EMT) (https://www.informatics.jax.org/vocab/gene_ontology/GO:0010719) and then miRWalk associate sEV-miRs with the genes involved in negative regulation of EMT. The idea behind was that if a sEV-miR inhibit the expression of an EMT inhibitor, then the EMT process would be promoted. **Table 16** shows a list of predicted targets (using miRWalk) of the co-transfected sEV-miRs which negatively regulates the EMT. It also shows which sEV-miRs could potentially target the expression of that gene.

Table 16: Predicted mRNA targets for the six "EMT-promoter" sEV-miRs enriched in sEV-MDA231

Predicted target	N° of sEV-miRs
KCTD16	6 (miR-100-5p, -122-5p, -146a-5p, -223-3p, -760, let-7d-5p

IL17RD	4 (miR-100-5p, -122-5p, -146a-5p, -223-3p)
PCDH9	4 (miR-100-5p, -122-5p, -223-3p, -760)
TXN2	4 (miR-146a-5p, -223-3p, -760, let-7d-5p)
DAB2IP	3 (miR-100-5p, -760, let-7d-5p)
PTEN	2 (miR-100-5p, let-7d-5p)
SPRY1	2 (miR-146a-5p, -760)
SPRED1	2 (miR-122-5p, let-7d-5p)
SFRP1	2 (miR-122-5p, let-7d-5p)

Firstly, in MCF10A normal mammary epithelial cells, *KCTD16* expression tended to be downregulated 24 h after transfection with let-7d-5p mimic alone, after co-transfection with the whole sEV-miRs cocktail and after incubation with sEV-MDA231 (more than 50% versus the NT condition, but not statistically significant). Those changes were normalized 48 h after let-7d-5p transfection and sEV-miRs mimics co-transfection, but not after treatment with sEV-MDA231 (**Figure 22a**). *PTEN* expression, which is a well-known tumor suppressor does not change after treatments, compared with the NT condition, however let-7d-5p mimic transfection and sEV-MDA231 treatment for 24 h seems to downregulate its expression when compared with the lipofectamine condition (**Figure 22b**). Similar changes were observed with *IL17RD* expression. There were no changes as compared versus the NT cells. However, *IL17RD* expression was downregulated 24 h after transfection with let-7d-5p mimic alone, after co-transfection with the whole sEV-miRs cocktail and after incubation with sEV-MDA231 compared with lipofectamine and miRNA scramble transfection conditions; changes that were normalized 48 h after each of the treatments (**Figure 22c**). On the other hand, the

only gene which expression was downregulated versus the NT cells was *DAB2IP*. The expression of DAB2IP, which is a member of the Ras GTPase-activating protein family, regulating cell proliferation, survival, apoptosis and metastasis (157), was decreased almost by half 24 h after transfection with let-7d-5p mimic alone, after co-transfection with the whole sEV-miRs cocktail and after incubation with sEV-MDA231. Of note, complete mix of sEV-miRs almost maintained *DAB2IP* downregulation for 48 h, in contrast to let-7d-5p alone or treatment with sEV-MDA231. It also should be noted that both, lipofectamine treatment alone and scramble miRNA transfection seemed to cause a small decrease in *DAB2IP* expression (**Figure 22d**). In the cases of other genes (*TXN2* and *SPRY1*), all interventions caused a slight decrease in gene expression, however, they were not statistically significant and were normalized at 48 h post-treatments (**Figure 22e,f**). Strikingly, despite the fact that two sEV-miRs could target *SFRP1* mRNA (**Table 16**), co-transfection of the 6 sEV-miRs mimics caused a 2-fold increase of gene expression 48 h post-transfection (**Figure 22g**). Finally, there were no changes in *PCDH9* and *SPRED1* expression with any of the stimuli (**Figure 22h,i**).

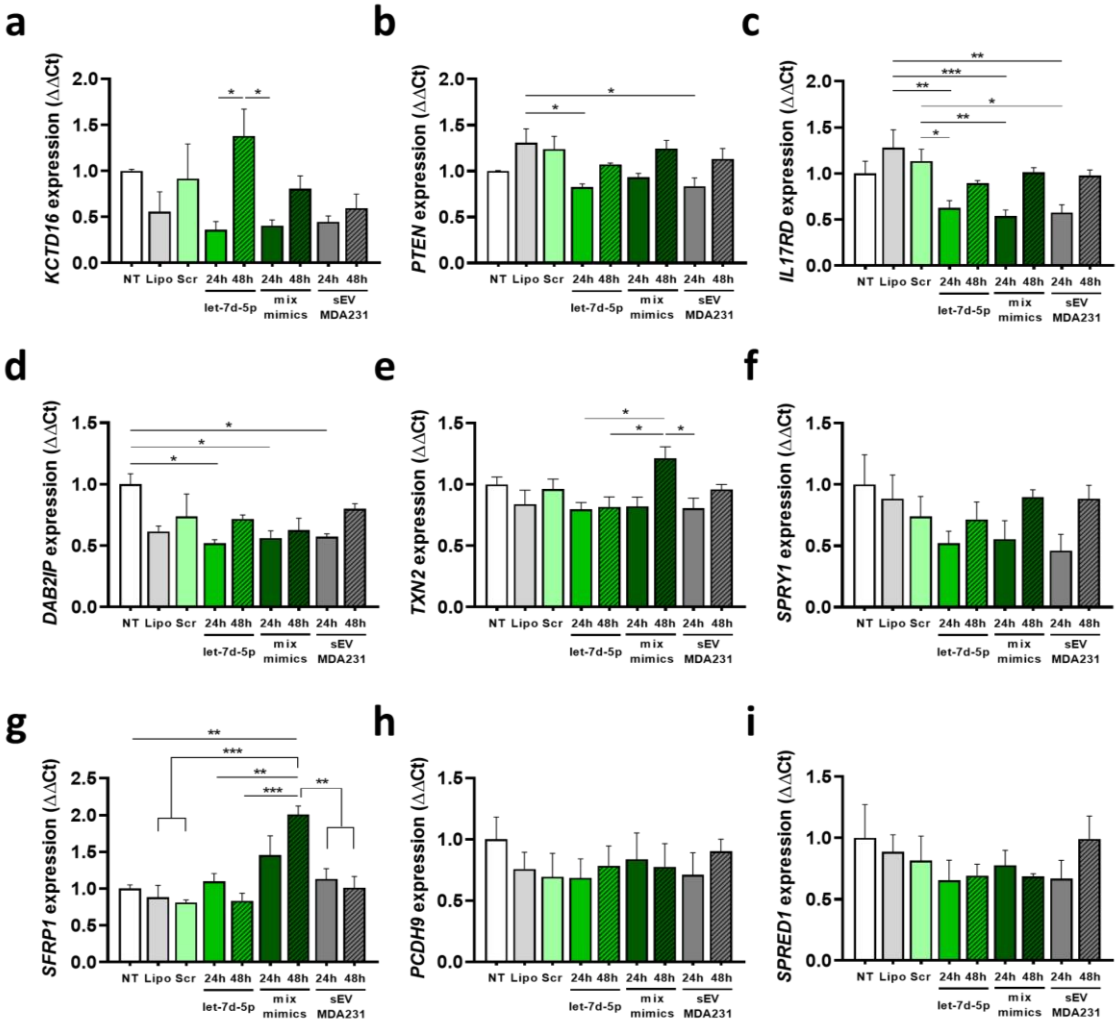

Figure 22: Effect of "EMT-promoter" sEV-miRs mimic co-transfection on the expression of predicted mRNA targets in MCF10A cells.

The six "EMT-promoter" sEV-miRs were co-transfected in MCF10A cells using lipofectamine 2000 and their effect on the expression of some mRNA predicted targets were evaluated 24 and 48 h later. *KCTD16* **(a)**, *PTEN* **(b)**, *IL17RD* **(c)**, *DAB2IP* **(d)**, *TXN2* **(e)**, *SPRY1* **(f)**, *SFRP1* **(g)**, *PCDH9* **(h)** and *SPRED1* **(i)** expression was quantified using the ΔΔCt method. Treatment of cells with sEV-MDA231 was used as control/comparison. GAPDH was used as housekeeping gene to normalize the data. Graph shows mean ± SEM. All data is representative of at least 3 independent experiments. (*) $p < 0.05$; (**) $p < 0.01$; (***) $p < 0.001$.

On the other hand, transfection of let-7d-5p mimic or sEV-miRs mimic cocktail seemed to have an opposite effect in T47D BC cells 24 h post-transfection. For instance, *PTEN* and *SPRY1* expression was increased after transfection with either let-7d-5p mimic alone or the combination of sEV-miRs mimics (**Figure 23a,d**). Transfection with let-7d-5p mimic also increased the expression of *DAB2IP*, but co-transfection of the sEV-miRs mimics cocktail did not (**Figure 23c**). Finally, both let-7d-5p mimic alone and the combination of sEV-miRs mimics caused a tendency to increase the expression of *IL17RD* and *PCDH9*, however the results were not statistically significant (**Figure 23b,e**). In summary, the six "EMT-promoter" sEV-miRs enriched in sEV-MDA231 cause a downregulation of some tumor suppressor predicted mRNA targets in MCF10A cells. On the contrary and interestingly, they cause an upregulation of some of those targets in T47D BC cells.

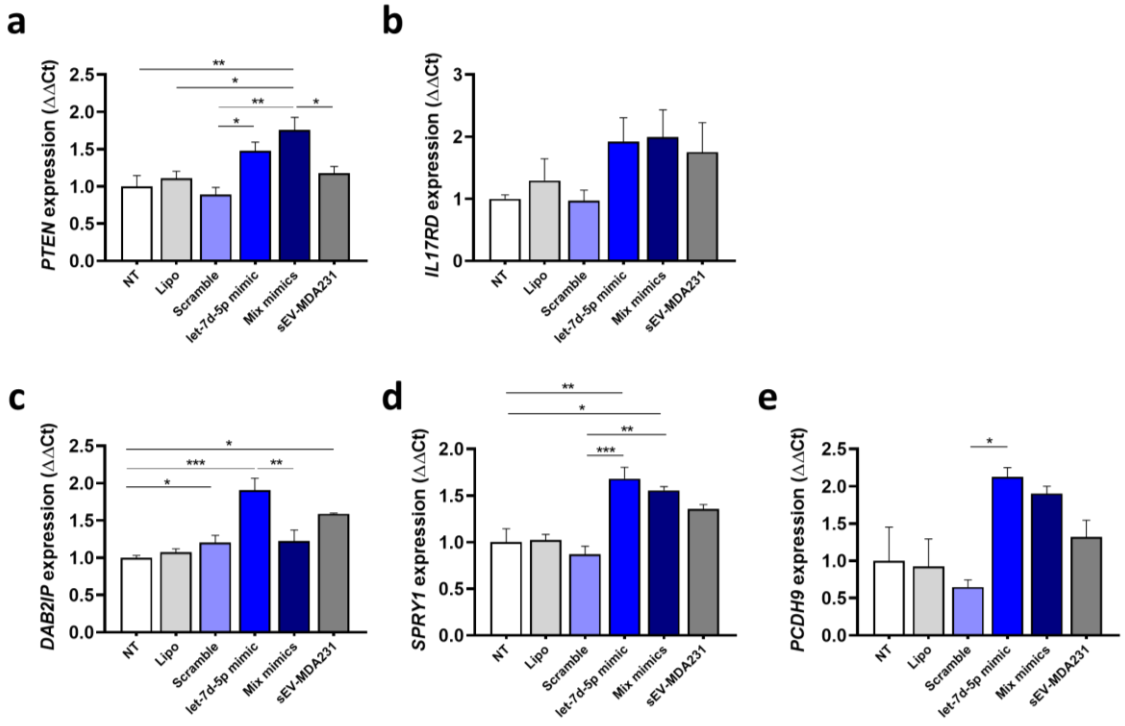

Figure 23: Effect of "EMT-promoter" sEV-miRs mimic co-transfection on the expression of predicted mRNA targets T47D cells.

The six "EMT-promoter" sEV-miRs were co-transfected in T47D cells using lipofectamine 2000 and their effect on the expression of some mRNA predicted targets were evaluated 24 h later. *PTEN* **(a)**, *IL17RD* **(b)**, *DAB2IP* **(c)**, *SPRY1* **(d)**, and *PCDH9* **(e)** expression was quantified using the ΔΔCt method. Treatment of cells with sEV-MDA231 was used as control/comparison. GAPDH was used as housekeeping gene to normalize the data. Graphs show mean ± SEM. All data is representative of at least 3 independent experiments. (*) $p < 0.05$; (**) $p < 0.01$; (***) $p < 0.001$.

5.4 Specific aim 4 results

To evaluate the role of candidate sEV-miRs overrepresented/enriched in metastatic sEV-MDA231 on the migration capacity of non-tumorigenic and non-metastatic BC cells (as a surrogate of the EMT).

5.4.1 "EMT-promoter" sEV-miR mimics promote the 3D migration capacity of "normal" mammary epithelial MCF10A cells and tumorigenic non-metastatic T47D BC cells

Finally, to evaluate the functional consequence of the co-transfection of the "EMT-promoter" sEV-miRs mimics cocktail, we performed a transwell migration assay in co-transfected or sEV-MDA231-treated MCF10A cells and in T47D BC cells. We co-transfected the cells for 24 h, treated with 5 µg sEV-MDA231/cell (1st dose) or left untreated. Then, we detached the cells and seeded 2.5 x 10^4 in the upper well of a Boyden chamber. Previously non-transfected MCF10A/T47D cells were then incubated with another 5 µg of sEV-MDA231 (2nd dose) and the migration assay was performed for 16 h (**Figure 24a**). As we previously showed, the treatment with sEV-MDA231 increased the migratory capacity of MCF10A cells. Interestingly, the co-transfection of the "EMT-promoter" sEV-miRs mimics cocktail 24 h before the assay itself increased their migratory potential even more (**Figure 24b**), suggesting that, even slight increases in some EMT-related markers could be associated with the increased migration of these cells. Similar results were obtained in transfected or sEV-MDA231-treated T47D BC cells. Co-transfection of the cocktail of sEV-miRs mimics and treatment with 2 doses of sEV-MDA231 generates a 2.2-fold increase in their migratory capacity (**Figure 24c**).

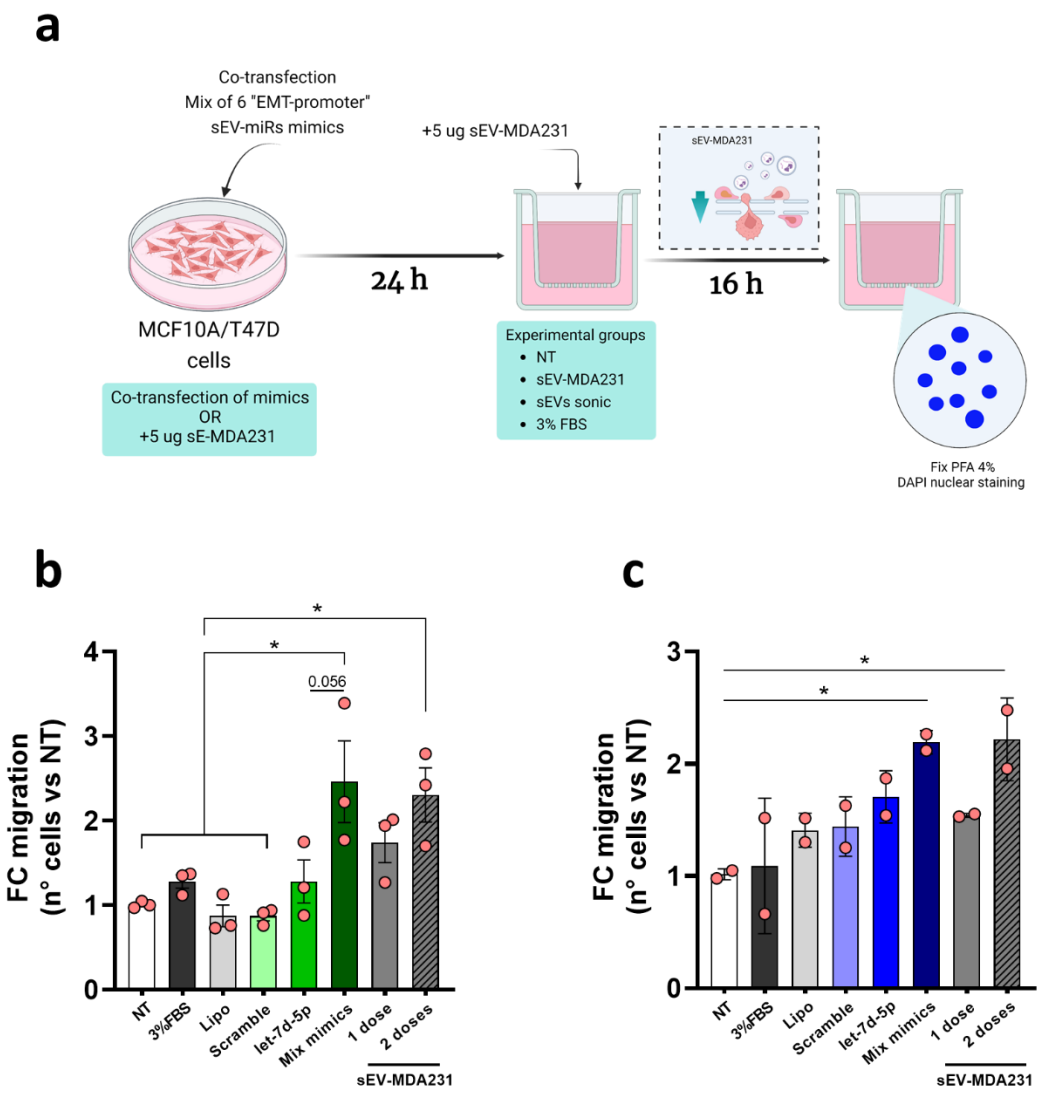

Figure 24: Evaluation of MCF10A and T47D cell migration after co-transfection with "EMT-promoter" sEV-miRs.

The six "EMT-promoter" sEV-miRs were co-transfected in MCF10A or T47D cells using lipofectamine 2000 and their effect on their migration capacity was evaluated by a transwell migration assay. **(a)** Schematics of the assay. Cells were previously transfected with the mix of sEV-miRs mimics or treated with one dose of sEV-MDA231. Twenty-four hours later, cells were detached and seeded on PET-membrane Boyden transwell chambers. At this point, sEV-

MDA231-treated cells were treated with a second dose of sEV-MDA231. After 16 h, the membrane inserts were collected, fixed and DAPI-stained to quantify migratory cells. **(b)** Quantification of co-transfected MCF10A cells migration. (c) Quantification of co-transfected T47D cells migration. Cells into the reverse side of the membrane were counted in at least 10 fields on an inverted fluorescence microscope and then quantified. Graphs show mean ± SD. All data is representative of at least 2-3 independent experiments (different transfections). (*) $p < 0.05$.

6. DISCUSSION AND CONCLUSIONS

6.1 sEV-MDA231 promotes pro-metastatic capacities of recipient cells and greatly enhance the metastatic behavior of MDA-MB-231 TNBC cells *in vivo*

Tumor-secreted sEVs are well-known players in intercellular communication in the tumor microenvironment, promoting tumor growth, migration, invasion, survival and angiogenesis, and in distant tissues, preparing the metastatic niche and promoting metastasis (16,22,129,158,159). MDA-MB-231 TNBC cells are commonly used as a model metastatic TNBC cell line. In addition, the role of their secreted sEVs (sEV-MDA231) has been widely studied regarding the promotion of tumorigenic and pro-metastatic capacities when incorporated in a recipient cell (37,38,160–162). In this thesis, we showed that sEV-MDA231 promotes different oncogenic capacities in different BC recipient cells characterized to be less aggressive than MDA-MB-231 BC cells (**Figures 1-5**). First, we isolated sEV-MDA231 TNBC cells using ultracentrifugation and characterized them by NTA, TEM and WB (**Figure 1**). sEV-MDA231 have a narrow size distribution with a

mode size of ~112 nm evaluated by NTA. They also presented characteristic cup-shaped structures evaluated by TEM (**Figure 1a**), which evaluates the integrity of the isolated sEVs and the presence of EV protein markers such as CD63, TSG101 and Flotillin-1 (**Figure 1b**). We aimed to evaluate the effect of sEV-MDA231 on cell migration using several BC cell lines with different degrees of aggressiveness and representing different BC subtypes as recipient cells. We used tumorigenic, non-metastatic MCF7 adenocarcinoma BC cells (luminal A-like; ER+/PR+/HER2-), tumorigenic, non-metastatic T47D ductal carcinoma BC cells (luminal A-like; ER+/PR+/HER2-) and tumorigenic, non-metastatic ZR75 ductal carcinoma (luminal B-like; ER+/PR-/HER2-). We also used the same sEV-producer cell line, metastatic TNBC MDA-MB-231 (basal-like; ER-/PR-/HER2-) and normal non-tumorigenic mammary epithelial MCF10A cells as control. On the other hand, the limited basal migration of MCF10A cells (**Figure 2a**) could explain, in part, why the treatment with sEV-MDA231 did not increase their migration capacity (not shown). On the other hand, the treatment with sEV-MDA231 increased the basal migratory capacity of MCF7, T47D and ZR75 BC cells, but not that of metastatic MDA-MB-231 (also just a tendency to increase) (**Figure 2b-e**). These variable results could be attributable to the intrinsic cell variability, i.e. differences in the response depending on BC cell subtype, basal migratory machinery capacity or sEV uptake, which was not directly evaluated in this study. It can also be possible that differences in sEV-MDA231 batch preparation could exists/occur, because we used different batches of sEV-MDA231 along this study. It is also important to

mention that responding cells just increase their basal migration by ~2-3 fold, according with other results by our research group (37,38) (Durán-Jara, E. et al., 2023. In revision).

Then, we aimed to evaluate the clonogenic potential (or colony formation potential) of BC recipient cells stimulated by sEV-MDA231. This assay, also known as anchorage-independent growth assay (because it is performed using a semi-solid scaffold), evaluates the capacity of cells to survive without a solid surface to adhere, therefore extrapolating the results with their capacity to growth and survive in the in circulation (163–165). Similar to what we saw in the evaluation of cell migration, sEV-MDA231 did not improve anchorage-independent growth of normal breast epithelial MCF10A cells (**Figure 3a**). sEV-MDA231 treatment only stimulates the anchorage-independent growth of some BC recipient cells. Interestingly, these responding BC cells correspond to ductal carcinomas (**Figure 3b-c**). Neither MCF7 nor MDA-MB-231 BC cells increased their colony formation potential after treatment with sEV-MDA231 (**Figure 3d-e**).

In the same line, we evaluated the effect of sEV-MDA231 on the tumoroid formation capacity of recipient BC cells. Tumoroids are 3D structures composed of an enriched population of cancer stem cells (CSCs), thus this assay evaluates directly the effect of sEV-MDA231 over those tumor cells and their metastatic capacity in a 3D environment, and no in 2D as a monolayer (166,167). Opposite

that what we obtained in the other assays, sEV-MDA231 given in one dose did increase the tumoroid formation capacity of MCF10A normal mammary epithelial cells almost by 4.5-fold (**Figure 4a**). On the other hand, they just slightly increased this potential in tumorigenic MCF7 and metastatic MDA-MB-231 BC cells (**Figure 4b-c**; ~2-fold increase, not significant), which suggest that more sEV-MDA231 are needed to improve this capacity in tumor cells than in non-tumor cells. We could not evaluate tumoroid formation potential in T47D and ZR75 ductal carcinoma cells because, in our hands, they were not able to form tumoroids/spheroids structures. Of note, we were not able to evaluate the differential incorporation or uptake of the metastatic sEV-MDA231 into each BC recipient cell. In this context, differences in the uptake of those metastatic sEVs by each recipient cell may contribute to the differences in the results observed between different cell lines (12). So, our results need to be taken with caution and the incorporation of sEV-MDA231 into each of the BC recipient cells tested need to be performed in order to draw better conclusions.

It is important to mention that in these *in vitro* assays evaluating the promotion of pro-metastatic capacities mediated by the metastatic sEV-MDA231 we used the same sEVs but previously sonicated. This control gave us information about the need of the entire undisrupted sEVs to mediate those pro-metastatic changes. In this case, we saw that sonicated sEV-MDA231 did not promote the pro-metastatic changes that the undisrupted sEVs did generate (**Figure 2 and 4**). Thus, the

changes promoted by the metastatic sEV-MDA231 on non-metastatic recipient cells are mediated by the complete undisrupted sEVs (12). Of note, despite the fact that mild sonication is used to disrupt sEVs (168), or even to improve miRNA or siRNA loading into sEVs (169–171), it seems that can disrupt proteins or miRNAs, thus we cannot rule out that the loss of effect observed with sonicated sEV-MDA231 was due to the partial disruption of miRNAs or proteins inside their cargo (172,173).

Finally, we evaluated the effect of the sEV-MDA231 *in vivo*, in a peritoneal carcinomatosis murine model. As shown, peritoneal co-injection of MDA-MB-231 TNBC cells plus sEV-MDA231 greatly and clearly increase the metastatic capacity of the injected tumor cells, promoting the formation of malignant ascites and peritoneal/mesenteric metastatic foci (**Figure 5**). This notable difference between the *in vivo* and *in vitro* effects could be explained by the intercellular communication within a living organism, in which several cell types coexist and influence each other. It could be possible that sEV-MDA231 have a more important effect in cell types other than tumor cells (even when they were the same sEVs producer cells), for instance, fibroblasts or endothelial cells (174–177). sEV-MDA231 could be incorporated by these cells and mediate functional and gene expression changes that finally promotes metastasis formation.

In summary, these results suggest that sEVs secreted by a highly aggressive and metastatic TNBC cell line (sEV-MDA231) can promote tumorigenic and pro-metastatic capacities of less aggressive (tumorigenic, non-metastatic) recipient BC cell lines *in vitro*, such as migration, tumoroid formation and clonogenic potential. Moreover, sEV-MDA231 can even increase some of these capacities in an immortalized, normal mammary epithelial cell line (migration and spheroid formation) highlighting their tumorigenic and pro-metastatic effect. Notably, sEV-MDA231 can greatly promote malignant ascites and metastatic tumor nodules formation *in vivo*.

6.2 Characterization of the sRNA profile of sEV-MDA231 show the enrichment of several oncomiRs, participating in processes related with cell migration and EMT

To better understand the molecules in sEV-MDA231 responsible (or mediating) these functional changes, we aimed/focused to/on characterize the miRNA profile of those sEVs (sEV-miRs). miRNAs are an important component of sEVs, and several studies have demonstrated functional roles of sEV-miRs promoting oncogenic and pro-metastatic changes in recipient cells (111,113,115,132,178). Thus, we isolated and characterized sEVs secreted by different BC cell lines (characterized by different aggressiveness) (**Figure 6**) and performed RNA sequencing of the small RNA fraction (small RNA-seq) present in those sEVs, with emphasis in the subsequent analysis of sEV-miRs. The aim of using sEVs

secreted by several and biologically different BC cell lines was that these cell lines represents different BC subtypes (179), express different miRNA molecular signatures (180), and also have different aggressiveness profiles, both *in vitro* and *in vivo*. The QC filtering of each sample left between 11-20M reads to perform subsequent bioinformatic analyses (**Table 7**). For miRNA-seq analysis, it is well-recommended that at least 5M reads should be include to perform alignment and mapping (www.illumina.com; www.novogene.com), so, our samples fulfill that requisite. Unfortunately, due to QC issues, two cellular RNA samples were lost previous to the small RNA-seq and could not be included in this work (T47D_cells and ZR75_cells). Cellular miRNAs corresponded to 40-60% of all sRNAs in MCF10A and MDA-MB-231 cells, which make them the most abundant cellular sRNAs. Importantly, almost a ~20% of cellular reads could not be assigned at the moment of the analysis, which could be attributable to an outdated webpage and database used (GRCh38_p10 genome version) (**Figure 7a**). On the other hand, sEV-miRs are far less abundant compared with cellular miRNAs, corresponding to 1-3% of total sRNAs reads). Notably, sEV-miRs correspond to almost 20% of sRNAs in sEV-MCF10A, which are “normal”, non-tumorigenic mammary epithelial cells. This is interesting as it is described that tumor cells have a dysfunctional miRNA and EVs biogenesis machinery, which can partially explain in why a non-tumor cell line can secrete more sEV-miRs (13,57,180–184). Interestingly/Strikingly, we found that the main sRNA component in BC cell-secreted sEVs were tRNA fragments (**Figure 7b**). A few recent studies have

shown this behavior, and demonstrated that tRNAs are a main component of sEVs, being one, even the most abundant sRNA specie (185–188). Also, at the time of analysis, an important proportion of sRNA reads were unable to be aligned, resulting in unassigned reads. These sRNAs could correspond to piwiRNAs and other sRNA species that were not included in the web-tool database. Other sRNAs detected and correctly aligned corresponded to snRNA, snoRNAs, vRNAs and other less abundant sRNA species (**Figure 7b**).

As we show in **Table 8**, we were able to detect more than 400 mature miRNAs in MCF10A and MDA-MB-231 cells, of which 360 were common between cells, 50 were MDA-MB-231 expressed-only, and 101 were MCF10A expressed only (**Figure 8a**). Among those MDA-MB-231 uniquely-expressed miRNAs, there are several miRNAs widely associated with oncogenic (oncomiRs) and metastatic (metastamiRs) processes (189,190). On the other hand, we detected between 153-400 sEV-miRs, of which 126 were common between the four different sEVs analyzed. Interestingly, five sEV-miRs were only detected in sEV-MDA231: miR-145-5p, miR-126-5p, miR-3689a-5p, miR-3689b-5p, miR-3689e (**Figure 8b – Table 9**). Some of these sEV-miRs such as miR-145-5p and miR-126-5p have been widely studied. Interestingly, most of the studies have shown antitumor (tumor-suppressor) roles for these miRs (191–195). This is very interesting because it would suggest that a metastatic and highly aggressive TNBC cell line such as MDA-MB-231 actively secrete miRNAs in sEVs that could be detrimental

for tumor cell biology. On the other hand, there are no studies regarding miR-3689, and it was just detected in high-throughput studies (196,197). However, those 5 sEV-miRs were very rare; they are less abundant, with a small number of reads detected. Thus, this finding must be carefully taken into consideration.

Next, we asked whether there was specific enrichment of some miRs in the secreted sEVs. As we saw in **Table 10** several sEV-miRs were enriched in sEVs, both in sEV-MCF10A (vs MCF10A cells) and sEV-MDA231 (vs MDA-MB-231 cells). As we mentioned, tumor cells-secreted sEVs can actively participate in intercellular communication and can deliver their cargo, including sEV-miRs into a recipient cell. Interestingly, this loading, transport and delivery may be relevant in two different contexts; i) cells can use secreted sEVs as disposal structures to eliminate detrimental molecules, including miRNAs (120,198–202), and ii) cells can use secreted sEVs to transport oncogenic molecules that could transform neighbor cells and promote the tumorigenic and metastatic processes (17–19,25,178,203,204). We saw that almost half of the enriched sEV-miRs are shared between MCF10A normal mammary and MDA-MB-231 TNBC cells, which could suggest some kind of non-specificity in the loading of those sEV-miRs (bold in **Table 10**). On the other hand, the other half of sEV-miRs are specifically loaded in sEV-MCF10A or sEV-MDA231. In the case of sEV-MDA231, 13 out of 25 sEV-miRs are enriched most than 2-fold in sEVs compared with the producing cells. Those sEV-miRs are involved in several oncogenic processes such as ECM-

interaction, fatty acid biosynthesis, adherens junction, Hippo and TGF-β signaling, blood coagulation and mitotic cell cycle (mrPath v3 – DianaTools. Not shown), which suggest that MDA-MB-231 cells can specifically encapsulate these miRs to promote oncogenic and pro-metastatic processes in recipient cells. On the other hand, we analyzed and compared the sEV-miRs profile from different cell lines in search of possible candidate sEV-miRs, promoters of pro-tumorigenic and pro-metastatic processes such as cell migration and EMT. We used the sRNAde web-tool (part of the sRNAbench tools), which allowed us to use edgeR as software to analyze differential expression without the need for replicates (139,205).

As mentioned before, we were interested in the metastatic potential of MDA-MB-231 BC cells and, as MDA-MB-231 are poorly differentiated and have a more mesenchymal phenotype (206–208), in the possibility of sEV-MDA231 to induce EMT. Thus, we took all sEV-miRs detected in each of the sEVs (sEV-MCF10A, sEV-T47D, sEV-ZR75 and sEV-MD231) and use edgeR to identify enriched sEV-miRs present in sEV-MDA231 against all of the other sEVs. As shown in **Figure 9** and **Table 12**, we found 24 sEV-miRs enriched specifically in sEV-MDA231, which added to the 3 other specifically-contained sEV-miRs (miR-3689a-5p, miR-3689b-5p, miR-3689e), gives us a total of 27 sEV-miRs enriched sEV-MDA231. Notably, GO and KEGG analysis of those sEV-miRs (themselves and their predicted targets) showed that they are involved in several oncogenic processes, including some closely related with cell migration and EMT promotion (**Tables 13-**

14 and Figure 10). We further validated the enrichment of 6 of those sEV-miRs in sEV-MDA231 by miQPCR (**Figure 11**), which went from a ~5-fold enrichment for miR-223-3p to an almost 10,000-fold enrichment for miR-146a-5p (versus sEV-MCF10A). Notably as mentioned, pathway analysis (KEGG) and GO (biological processes) showed that these 6 sEV-miRs are implicated in several oncogenic processes related with cell migration and EMT, such as TGF-β signaling pathway, adherens junction, FoxO signaling pathway, ECM-interaction, regulation of locomotion and cell motility, among others (**Figure 12**). Thus, these 6 validated sEV-miRs were used as candidate "EMT-promoter" sEV-miRs in co-transfection experiments to further evaluate their role in the promotion EMT molecular markers and cell migration as a surrogate and initial functional parameter (marker) of the EMT process *per se*.

6.3 The "EMT-promoter" sEV-miRs slightly promotes the expression of some EMT-markers in MCF10A "normal" mammary epithelial cells but not in T47D tumorigenic BC cells

After the validation of the enrichment of the 6 sEV-miRs in sEV-MDA231, we aimed to evaluate their role in the promotion of cell migration and the EMT process. To do that, we co-transfected sEV-miRs mimics (mature sequence) in MCF10A "normal" mammary epithelial and T47D tumorigenic and non-metastatic BC cells. We also treated these cells with sEV-MDA231 to compare the effect of the complete cargo of the sEVs, including the role of the protein cargo. **Table 15**

show the stoichiometry of the co-transfection experiment. As we do not have the absolute abundance of each sEV-miR, to get closer to the abundance of each sEV-miR in sEV-MDA231, we needed to the use the read count of the small RNA-seq assay as an approximation. So, we used different amounts of each miRNA mimic relative to the abundance of that miRNA in sEV-MDA231 according to the small RNA-seq data. In a quick test, we used a fluorescently-conjugated ASO, together with a sEV-miR mimic to demonstrate that we were able to efficiently transfect our target cell lines. We saw that almost 100% of MCF10A cells were fluorescently-labeled, indicating that they were transfected with the ASO and the mimic. Overexpression of the mimic transfected (let-7d-5p) was also achieved and demonstrated by miQPCR (**Figure 13**). After that, we co-transfected all 6 sEV-miRs mimics in MCF10A or T47D cells and we saw an overexpression of almost all sEV-miRs, the only exception was let-7d-5p, which was expected as the amount used was very low (**Table 15**; 0.05 nM; **Figures 14-15**). We also incubated the cells with sEV-MDA231; the treatment with these sEVs did clearly increase the expression of 4 out of 6 “EMT-promoter” sEV-miRs, however, it was less than that reached by mimic co-transfection (**Figures 14-15**). This was expected as we didn’t know the absolute concentration of each sEV-miR in sEV-MDA231 and the overexpression also depends on basal levels of each miRNA in each cell line.

Subsequently, we saw that sEV-miRs mimics co-transfection increased mRNA and protein levels of some of the EMT-related markers evaluated, while others remain unaltered in MCF10A “normal” mammary epithelial cells (**Figures 16,17,20**), which can be indicative of some sort of partial or hybrid EMT (76,80,209). “EMT-promoter” sEV-miRs increased the expression of *CDH1* (E-Cadherin), *CDH2* (N-Cadherin), *Fn* (Fibronectin), and *Vim* (Vimentin), molecules that can be considered as “effectors” (**Figure 16**). On the other hand, mimics co-transfection did not increase the expression of either, the Stemness-TFs evaluated, nor the EMT-TFs (**Figure 17**), except for a tendency of an increase of *Nanog* expression. This is interesting and relevant because at least one EMT-TF should be increased for this process to be considered as an EMT (76,80). In line with qPCR, WB analysis showed a small but not significant overexpression of EMT protein levels such as N-Cadherin, Vimentin, Twist and Snail/Slug in MCF10A cells (**Figure 20**). Analysis of EMT-associated markers in co-transfected T47D BC cells showed similar and more confusing results. While *Fn* expression was increased after co-transfection, it was also accompanied by *CDH1* overexpression (also seen in MCF10A cells). No changes were seen in *Vim* (**Figure 18**), *CDH2* (not shown), Stem-TFs or EMT-TFs (**Figure 19**), with the exception of a small increase in *Snai1* expression. Protein levels of EMT-markers almost did not change (**Figure 21**).

miRNAs are master regulators of gene expression, which functions as tumor suppressors or oncomiRs depending of several aspects (56,65,210–214). A single miRNA can target several mRNAs. Similarly, one mRNA can be targeted by several miRNAs. This versatility or promiscuity regarding miRNAs function could, in part, explain our results. As the 6 candidate “EMT-promoter” sEV-miRs have both anti-tumor and oncogenic functions reported (**Table G** in annexes), it is possible that they could be competing intracellularly to regulate both processes at the same time. For instance, most studies have demonstrated that let-7d-5p have a tumor-suppressing role (215–218). However, in some contexts it also acts as an oncomiR (217–219). Our results showed that some of the changes evidenced by the co-transfection of all 6 sEV-miRs could also be obtained by the transfection of let-7d-5p mimic alone. This is relevant because it shows the complexity of functions this miRNA has, but most importantly, it remarks the need to evaluate each miRNA separately, to better dissect the contribution of each one in the regulation of the EMT.

Finally, focused on negative regulators of the EMT according with the GO and KEGG databases, we aimed to evaluate the effect of the cocktail of 6 sEV-miRs and sEV-MDA231 on the expression of some genes that are predicted targets of those miRNAs. In MCF10A non-tumorigenic cells, we saw a downregulation of most of the genes tested, however significant difference versus the NT condition was achieved just in *DAB2IP* expression (**Figure 22**). Both, let-7d-5p transfection

alone and the co-transfection of the mix of mimics results in a ~50% downregulation of several mRNA targets at 24 h (*KCTD16, PTEN, IL17RD, SPRY1, DAB2IP*) but not at 48 h post-transfection. Treatment with sEV-MDA231 showed similar temporal results. This show an early effect of the miRNA transfection, which could be even higher at earlier times; this needs further evaluation. It is also possible that the combination/accumulation of effects could have a greater effect when compared with each gene separately. Future analysis are also needed to assess/demonstrate the direct interaction between each miRNA and their predicted mRNA targets. On the contrary, opposite to what we saw in MCF10A cells, the co-transfection of the 6 sEV-miRs mimics did not downregulated the expression of the predicted mRNA targets in T47D BC cells. Moreover, it seemed to cause the opposite effect; the co-transfection of the mix of sEV-miRs mimics caused a ~2-fold overexpression of some of the predicted mRNA targets (**Figure 23**).

In summary, the 6 “EMT-promoter” sEV-miRs slightly regulated gene and protein levels of some EMT-related markers. They also downregulated the expression of some predicted targets that inhibit the EMT process in MCF10A “normal” mammary epithelial cells, which subsequently may result in the promotion of the EMT. Transfection of let-7d-5p mimic alone have similar effects. This strongly suggest that a separate evaluation need to be done for each transfected miRNA to have better, more reliable and cleaner results regarding their participation in

the modulation of the EMT. On the other hand, it seems that neither the co-transfection of the “EMT-promoter” sEV-miRs, nor the treatment with sEV-MDA231 have clear effects regulating the expression of EMT-markers in T47D BC cells in our experimental setup.

6.4 The “EMT-promoter” sEV-miRs increase the migration capacity of MCF10A and T47D cells

The EMT is a complex, dynamic and non-categorical process in which a cell (mainly epithelial) lose basal-apical polarity, gain mesenchymal properties or characteristics, and/or lose epithelial markers (76–78,80). As a consequence, functionally those cells suffering or entering the EMT increase their motility and migratory capacity, enhance their invasive potential, among other characteristics (76,80,220,221). Thus, as a functional consequence of the co-transfection of the “EMT-promoter” sEV-miRs mimics cocktail, we evaluated the migration capacity of co-transfected or sEV-MDA231-treated MCF10A and T47D BC cells as a characteristic and surrogate marker of the EMT. In line with what we saw in aim 1 and 3, the treatment with sEV-MDA231 increased the migratory capacity of MCF10A cells. Moreover, the co-transfection of the “EMT-promoter” sEV-miRs mimics cocktail 24 h before the assay itself increased their migratory potential even more (**Figure 24b**), suggesting that, even slight increases in some EMT-related markers could be associated with the increased migration of these cells. It also suggests that other signaling pathways may be involved in the increase of

migration in co-transfected/treated MCF10A cells, such as focal adhesion kinase (FAK/pFAK) (222), small GTPases (Rac1/Cdc42) (223,224) or Wnt signaling pathways (225,226). Further analysis evaluating these pathways are needed to better understand their role promoting cell migration in our experiments. On the other hand, the combination of all 6 sEV-miRs mimics as well as the treatment with sEV-MDA231 increased the migration capacity of T47D BC cells in our setting by almost 2.2-fold (**Figure 24c**). However, as lipofectamine and miRNA scramble transfection also slightly increase T47D cells migration, the results are only statistically significant against the non-treated cells and conclusions needs to be taken with caution.

Nowadays, several studies have allowed us to understand that the EMT is not black and white; there are several hybrid or partial states of EMT, in which cells not necessarily abrogate the expression of epithelial makers, or where not all EMT-TFs need to be overexpressed or active (80,92). A recent and interesting report using MDA-MB-231 TNBC cells have shown that there is a hybrid EMT in migratory and invasive tumor cells. The authors also showed that migratory and invasive cells require Vimentin overexpression to correctly migrate and invade, and not necessarily downregulate E-Cadherin expression (92). Moreover, this work demonstrated different EMT programs regulating invasion/migration and colony formation, with different EMT-TFs involved, which could be associated with distant tissue colonization. In the case of sEV-miRs, nowadays several studies

have demonstrated a role regulating the EMT in different contexts, including BC, However, most studies usually evaluate the effect of a miRNA on sEVs or exosomes by overexpressing the miRNA in the EVs-producing cell (e.g. by mimic transfection), then obtaining those EVs (115,118,227–229). This strategy does not always evaluate or compare the pro-EMT or pro-metastatic effect of the WT EVs, nor the effect of basal miRNA on these EVs; meaning that NT vs WT-EVs vs EVs-mimic comparisons are not made. Thus, the observable effect is clearly forced. Our results did consider the effect of a mix of possible "EMT-promoter" sEV-miRs and compared it with the effect of the complete sEVs (considering their complete cargo). Being a complex process, EMT can be induced by multiple molecules or stimulus besides miRNAs or sEV-miRs. EMT can also be studied by multiple approaches; from a cellular, molecular, morphological, or even spatial point of view (76,80,209). Each approach has different processes, molecules or changes that can be evaluated to have a better idea of the EMT as a whole. However, this complexity in the study of EMT is, at the same time, a blessing and a curse, as it is not often possible to go deeper in every field. In summary, our results showed that: i) sEVs secreted by a highly mesenchymal, metastatic, TNBC cell line, i.e. MDA-MB-231 (sEV-MDA231), can **promote pro-metastatic functional changes in less aggressive recipient cells *in vitro***, such as migration, colony formation (anchorage-independent growth), and tumoroid formation. They also **greatly promote the formation of malignant ascites and tumor micronodules *in vivo***, in a metastatic peritoneal carcinomatosis model

(specific aim 1); ii) sEV-MDA231 have a characteristic sEV-miRs profile, different from that of sEVs secreted by other BC cell lines, composed of several oncomiRs. **Twenty-seven sEV-miRs were enriched or selectively present in sEV-MDA231, which were associated with oncogenic and metastatic processes and pathways**, such as TGF-β, Hippo and estrogen signaling pathways, as well as adherens junction, cell cycle regulation, Wnt signaling, signaling by Rho GTPases and EMT. Of those twenty-seven, **six were experimentally validated** to investigate their role as candidate "EMT-promoter" sEV-miRs, **which are strongly associated with positive regulation of cell migration and EMT** (specific aim 2); iii) **the transfection of those 6 "EMT-promoter" sEV-miRs increase the expression of some EMT-markers in MCF10A "normal" non-tumorigenic mammary epithelial cells, but not in T47D BC cells**. Additionally, they also downregulate the expression of some predicted target genes in MCF10A cells, but they have opposite effects in T47D BC cells. These findings suggest that MCF10A cells, being non-tumorigenic, seems to be more responsive than T47D to the effect of the transfection of sEV-miRs. It may also suggest that each sEV-miR should be also analyzed separately to better dissect their role in the regulation of EMT-related markers expression (specific aim 3); iv) despite not having a great effect over the expression of EMT-related markers, the **co-transfection of the 6 "EMT-promoter" sEV-miRs increase the migration capacity of MCF10A normal cells and T47D BC cells** at levels even higher than that achieved by the incubation with sEV-MDA231. This suggest that other

pathways or processes than the EMT may be involved in that effect such as the mentioned above (e.g. Rac1/Cdc42, focal adhesion kinase, Wnt/beta-catenin, among others), which need further evaluation (specific aim 4).

In summary:

- sEVs secreted by metastatic, highly mesenchymal MDA-MB-231 TNBC cells (sEV-MDA231) promotes enhance pro-metastatic capacities in less aggressive recipient cells such as migration, anchorage-independent growth and tumoroid formation. Co-injection/inoculation/administration of MDA-MB-231 TNBC cell and sEV-MDA231 greatly promotes the formation of malignant ascites and tumor micronodules in mice.
- Twenty-seven candidate sEV-miRs enriched in sEV-MDA231 were identified as possible promoters of the EMT. Of those, the six miQPCR-validated “EMT-promoter” sEV-miRs enriched in sEV-MDA231 could participate in the regulation of cell migration, locomotion and cell junction.
- The co-transfection of the six “EMT-promoter” sEV-miRs slightly increased the expression of some EMT-related markers, both at the gene and protein levels in MCF10A “normal” mammary epithelial cells but not in T47D tumorigenic BC cells. They also caused a downregulation of some tumor suppressor predicted mRNA targets in MCF10A cells. Interestingly, they seemed to have opposite effects in T47D BC cells, causing an overexpression of some of the predicted targets evaluated.

- Despite not having an important effect over the expression of EMT-related markers, the co-transfection of “EMT-promoter” sEV-miRs increase the migration capacity of MCF10A and T47D cells, reaching similar levels than that achieved by two doses of sEV-MDA231 (**Figure 25**).

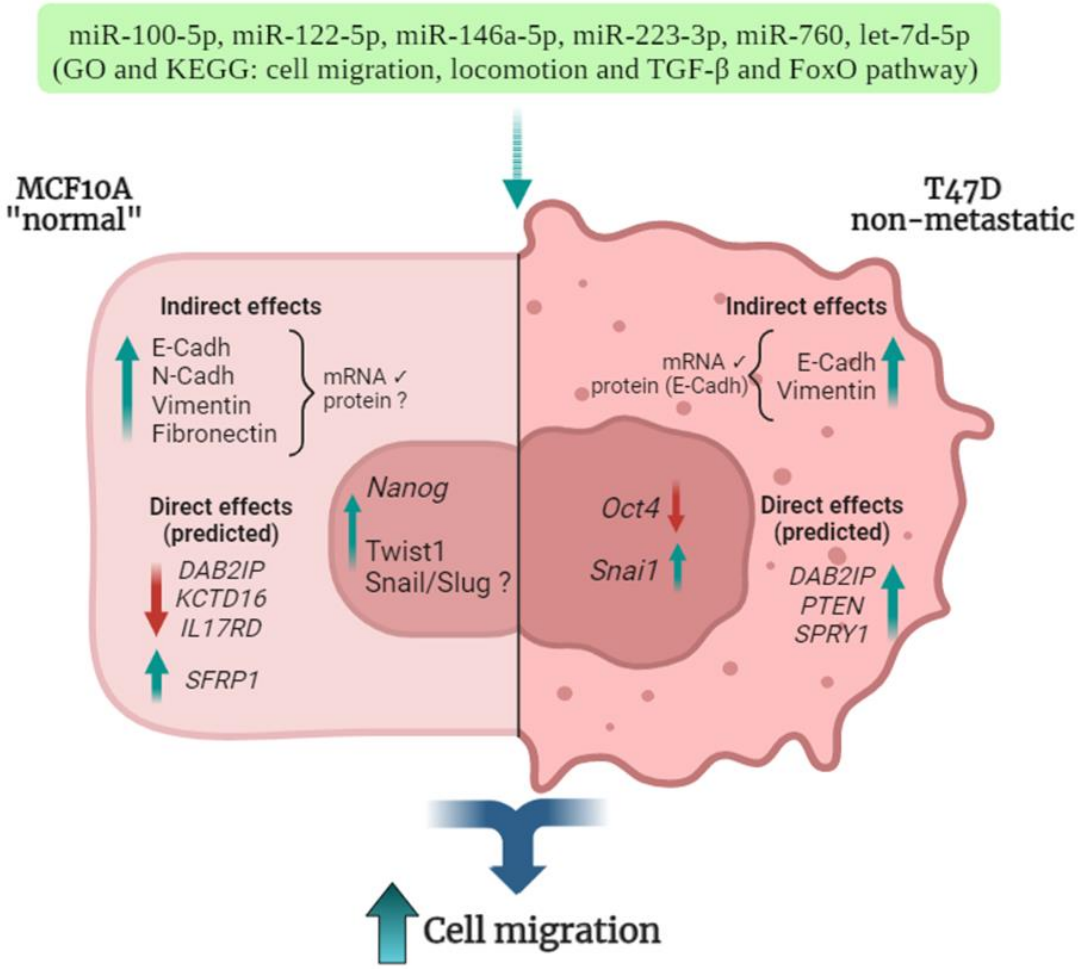

Figure 25: Research graphical summary.

The co-transfection of the 6 “EMT-promoter” sEV-miRs enriched in sEV-MDA231 increase the migration capacity of MCF10A normal mammary epithelial cells and T47D BC cells, but they caused different molecular changes in each cell line. **(left)** The co-transfection of the 6 “EMT-

promoter" sEV-miRs in MCF10A cells slightly increase gene expression and protein levels of some EMT-markers such as N-Cadherin (*CDH2*), Vimentin (*VIM*), Fibronectin (*FN*) and Twist1 and Snail/Slug EMT-TFs. Interestingly, they caused a simultaneous upregulation in the expression of E-Cadherin (*CHD1*). They also tend to decreased the expression of *DAB2IP*, *IL17RD* and *KCTD16* (yet, not statistically significant), which are tumor suppressor inhibitor of the EMT. **(right)** On the other hand, co-transfection of the six "EMT-promoter" sEV-miRs in T47D cells almost not alter the expression of EMT-related markers. Moreover, the expression of mRNA predicted targets such as *DAB2IP*, *PTEN* and *SPRY1* increased after the co-transfection. Despite this, they increased the migratory capacity of T47D BC cells. In both cell lines, the co-transfection of the 6 "EMT-promoter" sEV-miRs increased the migration capacity at levels similar to that achieved by two doses of sEV-MDA231. Thus, it suggests that other signaling pathways may be involved in the increase of migration in co-transfected/treated MCF10A and T47D cells, such as focal adhesion kinase (FAK/pFAK), small GTPases (Rac1/Cdc42) or Wnt signaling pathways, which need to be evaluated. Image created in Biorender.

7. BIBLIOGRAPHY

1. Sung H, Ferlay J, Siegel RL, Laversanne M, Soerjomataram I, Jemal A, et al. Global Cancer Statistics 2020: GLOBOCAN Estimates of Incidence and Mortality Worldwide for 36 Cancers in 185 Countries. CA Cancer J Clin. 2021 May;71(3):209–49.
2. Guías Clínicas AUGE Cáncer de Mama. 2015.
3. Seyfried TN, Huysentruyt LC. On the Origin of Cancer Metastasis. 2013.
4. Guan X. Cancer metastases: Challenges and opportunities. Vol. 5, Acta Pharmaceutica Sinica B. Chinese Academy of Medical Sciences; 2015. p. 402–18.
5. Siegel RL, Miller KD, Fuchs HE, Jemal A. Cancer statistics, 2022. CA Cancer J Clin. 2022 Jan;72(1):7–33.
6. Chaffer CL, Weinberg RA. A Perspective on Cancer Cell Metastasis [Internet]. 2011. Available from: http://science.sciencemag.org/
7. Dillekås H, Rogers MS, Straume O. Are 90% of deaths from cancer caused by metastases? Cancer Med. 2019 Sep 1;8(12):5574–6.
8. Wolf P. The Nature and Significance of Platelet Products in Human Plasma. 1967.
9. Anderson HC. VESICLES ASSOCIATED WITH CALCIFICATION IN THE MATRIX OF EPIPHYSEAL CARTILAGE. 1969.
10. György B, Szabó TG, Pásztói M, Pál Z, Misják P, Aradi B, et al. Membrane vesicles, current state-of-the-art: Emerging role of extracellular vesicles. Vol. 68, Cellular and Molecular Life Sciences. 2011. p. 2667–88.
11. Teng F, Fussenegger M. Shedding Light on Extracellular Vesicle Biogenesis and Bioengineering. Vol. 8, Advanced Science. John Wiley and Sons Inc; 2021.
12. Mathieu M, Martin-Jaular L, Lavieu G, Théry C. Specificities of secretion and uptake of exosomes and other extracellular vesicles for cell-to-cell communication. Vol. 21, Nature Cell Biology. Nature Publishing Group; 2019. p. 9–17.
13. Latifkar A, Hur YH, Sanchez JC, Cerione RA, Antonyak MA. New insights into extracellular vesicle biogenesis and function. Vol. 132, Journal of Cell Science. Company of Biologists Ltd; 2019.
14. Souza-Schorey C, Schorey JS. Regulation and mechanisms of extracellular vesicle biogenesis and secretion. Vol. 62, Essays in Biochemistry. Portland Press Ltd; 2018. p. 125–33.
15. Syn N, Wang L, Sethi G, Thiery JP, Goh BC. Exosome-Mediated Metastasis: From Epithelial-Mesenchymal Transition to Escape from Immunosurveillance. Vol. 37, Trends in Pharmacological Sciences. Elsevier Ltd; 2016. p. 606–17.
16. Becker A, Thakur BK, Weiss JM, Kim HS, Peinado H, Lyden D. Extracellular Vesicles in Cancer: Cell-to-Cell Mediators of Metastasis. Vol. 30, Cancer Cell. Cell Press; 2016. p. 836–48.
17. Lobb RJ, Lima LG, Möller A. Exosomes: Key mediators of metastasis and pre-metastatic niche formation. Vol. 67, Seminars in Cell and Developmental Biology. Elsevier Ltd; 2017. p. 3–10.
18. Jella KK, Nasti TH, Li Z, Malla SR, Buchwald ZS, Khan MK. Exosomes, their biogenesis and role in inter-cellular communication, tumor microenvironment and cancer immunotherapy. Vol. 6, Vaccines. MDPI AG; 2018.
19. Tkach M, Théry C. Communication by Extracellular Vesicles: Where We Are and Where We Need to Go. Vol. 164, Cell. Cell Press; 2016. p. 1226–32.

20. Théry C, Amigorena S, Raposo G, Clayton A. Isolation and Characterization of Exosomes from Cell Culture Supernatants and Biological Fluids. Curr Protoc Cell Biol. 2006 Mar;30(1).
21. van Niel G, D'Angelo G, Raposo G. Shedding light on the cell biology of extracellular vesicles. Vol. 19, Nature Reviews Molecular Cell Biology. Nature Publishing Group; 2018. p. 213–28.
22. Bebelman MP, Smit MJ, Pegtel DM, Baglio SR. Biogenesis and function of extracellular vesicles in cancer. Vol. 188, Pharmacology and Therapeutics. Elsevier Inc.; 2018. p. 1–11.
23. Liu Y, Gu Y, Han Y, Zhang Q, Jiang Z, Zhang X, et al. Tumor Exosomal RNAs Promote Lung Pre-metastatic Niche Formation by Activating Alveolar Epithelial TLR3 to Recruit Neutrophils. Cancer Cell. 2016 Aug 8;30(2):243–56.
24. Harris DA, Patel SH, Gucek M, Hendrix A, Westbroek W, Taraska JW. Exosomes released from breast cancer carcinomas stimulate cell movement. PLoS One. 2015 Mar 23;10(3).
25. Zhang X, Yuan X, Shi H, Wu L, Qian H, Xu W. Exosomes in cancer: Small particle, big player. Vol. 8, Journal of Hematology and Oncology. BioMed Central Ltd.; 2015.
26. Mateescu B, Kowal EJK, van Balkom BWM, Bartel S, Bhattacharyya SN, Buzás EI, et al. Obstacles and opportunities in the functional analysis of extracellular vesicle RNA - An ISEV position paper. J Extracell Vesicles. 2017;6(1).
27. Veerman RE, Teeuwen L, Czarnewski P, Güclüler Akpinar G, Sandberg AS, Cao X, et al. Molecular evaluation of five different isolation methods for extracellular vesicles reveals different clinical applicability and subcellular origin. J Extracell Vesicles. 2021 Jul 1;10(9).
28. Willms E, Cabañas C, Mäger I, Wood MJA, Vader P. Extracellular vesicle heterogeneity: Subpopulations, isolation techniques, and diverse functions in cancer progression. Vol. 9, Frontiers in Immunology. Frontiers Media S.A.; 2018.
29. Willms E, Johansson HJ, Mäger I, Lee Y, Blomberg KEM, Sadik M, et al. Cells release subpopulations of exosomes with distinct molecular and biological properties. Sci Rep. 2016 Mar 2;6.
30. Bobrie A, Colombo M, Krumeich S, Raposo G, Théry C. Diverse subpopulations of vesicles secreted by different intracellular mechanisms are present in exosome preparations obtained by differential ultracentrifugation. J Extracell Vesicles. 2012;1(1).
31. Crescitelli R, Lässer C, Jang SC, Cvjetkovic A, Malmhäll C, Karimi N, et al. Subpopulations of extracellular vesicles from human metastatic melanoma tissue identified by quantitative proteomics after optimized isolation. J Extracell Vesicles. 2020 Jan 1;9(1).
32. Tkach M, Kowal J, Théry C. Why the need and how to approach the functional diversity of extracellular vesicles. Philosophical Transactions of the Royal Society B: Biological Sciences. 2018 Jan 5;373(1737).
33. Van Deun J, Mestdagh P, Sormunen R, Cocquyt V, Vermaelen K, Vandesompele J, et al. The impact of disparate isolation methods for extracellular vesicles on downstream RNA profiling. J Extracell Vesicles. 2014;3(1).
34. Hoshino A, Costa-Silva B, Shen TL, Rodrigues G, Hashimoto A, Tesic Mark M, et al. Tumour exosome integrins determine organotropic metastasis. Nature. 2015 Nov 19;527(7578):329–35.
35. Webber J, Steadman R, Mason MD, Tabi Z, Clayton A. Cancer exosomes trigger fibroblast to myofibroblast differentiation. Cancer Res. 2010 Dec 1;70(23):9621–30.
36. Webber JP, Spary LK, Sanders AJ, Chowdhury R, Jiang WG, Steadman R, et al. Differentiation of tumour-promoting stromal myofibroblasts by cancer exosomes. Oncogene. 2015 Jan 15;34(3):319–33.

37. Campos A, Salomon C, Bustos R, Díaz J, Martínez S, Silva V, et al. Caveolin-1-containing extracellular vesicles transport adhesion proteins and promote malignancy in breast cancer cell lines. Nanomedicine. 2018;13(20):2597–609.
38. Lobos-González L, Bustos R, Campos A, Silva V, Silva V, Jeldes E, et al. Exosomes released upon mitochondrial ASncmtRNA knockdown reduce tumorigenic properties of malignant breast cancer cells. Sci Rep. 2020 Dec 1;10(1).
39. Gorczynski RM, Erin N, Zhu F. Serum-derived exosomes from mice with highly metastatic breast cancer transfer increased metastatic capacity to a poorly metastatic tumor. Cancer Med. 2016 Feb 1;5(2):325–36.
40. Reinhart BJ, Slack FJ, Basson M, Pasquinell AE, Bettinger JC, Rougvie AE, et al. 22. 2000 Reinhart B et al. The 21-nucleotide let-7 RNA regulates developmental timing in C. elegans. 2000;
41. Lee RC, Feinbaum RL, Ambros V. The C. elegans Heterochronic Gene lin-4 Encodes Small RNAs with Antisense Complementarity to lin-14 Ambros and Horvitz, 1987). Animals carrying a lin-4 loss-of-function (lf) mutation, lin-4(e912), display reiterations of early fates at inappropriately late developmental stages; cell lineage patterns normally specific for the L1 are reiter. Vol. 75, Cell. 1993.
42. Olsen PH, Ambros V. The lin-4 Regulatory RNA Controls Developmental Timing in Caenorhabditis elegans by Blocking LIN-14 Protein Synthesis after the Initiation of Translation [Internet]. 1999. Available from: http://www.idealibrary.com
43. Wightman B, Ha L, Ruvkun G. Posttranscriptional Regulation of the Heterochronic Gene lin-14 by W-4 Mediates Temporal Pattern Formation in C. elegans. Vol. 75. 1993.
44. Brodersen P, Voinnet O. Revisiting the principles of microRNA target recognition and mode of action. Vol. 10, Nature Reviews Molecular Cell Biology. 2009. p. 141–8.
45. Bartel DP. Review MicroRNAs: Genomics, Biogenesis, Mechanism, and Function. Vol. 116, Cell. 2004.
46. Calin GA, Croce CM. MicroRNA signatures in human cancers. Vol. 6, Nature Reviews Cancer. 2006. p. 857–66.
47. Liang Y, Ridzon D, Wong L, Chen C. Characterization of microRNA expression profiles in normal human tissues. BMC Genomics. 2007 Jun 16;8.
48. Lu M, Zhang Q, Deng M, Miao J, Guo Y, Gao W, et al. An analysis of human microRNA and disease associations. PLoS One. 2008 Oct 15;3(10).
49. Panwar B, Omenn GS, Guan Y. MiRmine: A database of human miRNA expression profiles. Bioinformatics. 2017 May 15;33(10):1554–60.
50. Bhattacharyya M, Nath J, Bandyopadhyay S. MicroRNA signatures highlight new breast cancer subtypes. Gene. 2015 Feb 10;556(2):192–8.
51. Kozomara A, Birgaoanu M, Griffiths-Jones S. MiRBase: From microRNA sequences to function. Nucleic Acids Res. 2019 Jan 8;47(D1):D155–62.
52. Lowery AJ, Miller N, Devaney A, McNeill RE, Davoren PA, Lemetre C, et al. MicroRNA signatures predict oestrogen receptor, progesterone receptor and HER2/neu receptor status in breast cancer. Breast Cancer Research. 2009 May 11;11(3).
53. Krell J, Frampton AE, Jacob J, Castellano L, Stebbing J. MiRNAs in breast cancer: Ready for real time? Vol. 13, Pharmacogenomics. 2012. p. 709–19.
54. Mulrane L, McGee SF, Gallagher WM, O'Connor DP. miRNA dysregulation in breast cancer. Vol. 73, Cancer Research. 2013. p. 6554–62.
55. Kurozumi S, Yamaguchi Y, Kurosumi M, Ohira M, Matsumoto H, Horiguchi J. Recent trends in microRNA research into breast cancer with particular focus on the associations between microRNAs and intrinsic subtypes. Vol. 62, Journal of Human Genetics. Nature Publishing Group; 2017. p. 15–24.

56. Loh HY, Norman BP, Lai KS, Rahman NMANA, Alitheen NBM, Osman MA. The regulatory role of microRNAs in breast cancer. Vol. 20, International Journal of Molecular Sciences. MDPI AG; 2019.
57. Søkilde R, Persson H, Ehinger A, Pirona AC, Fernö M, Hegardt C, et al. Refinement of breast cancer molecular classification by miRNA expression profiles. BMC Genomics. 2019 Jun 17;20(1).
58. Gebert LFR, MacRae IJ. Regulation of microRNA function in animals. Vol. 20, Nature Reviews Molecular Cell Biology. Nature Publishing Group; 2019. p. 21–37.
59. Treiber T, Treiber N, Meister G. Regulation of microRNA biogenesis and its crosstalk with other cellular pathways. Vol. 20, Nature Reviews Molecular Cell Biology. Nature Publishing Group; 2019. p. 5–20.
60. McGuire A, Brown JAL, Kerin MJ. Metastatic breast cancer: the potential of miRNA for diagnosis and treatment monitoring. Cancer and Metastasis Reviews. 2015 Mar 1;34(1):145–55.
61. Jin T, Kim HS, Choi SK, Hwang EH, Woo J, Ryu HS, et al. microRNA-200c/141 upregulates SerpinB2 to promote breast cancer cell metastasis and reduce patient survival. Oncotarget. 2017;8(20):32769–82.
62. Gong C, Yao Y, Wang Y, Liu B, Wu W, Chen J, et al. Up-regulation of miR-21 mediates resistance to trastuzumab therapy for breast cancer. Journal of Biological Chemistry. 2011 May 27;286(21):19127–37.
63. Najjary S, Mohammadzadeh R, Mokhtarzadeh A, Mohammadi A, Kojabad AB, Baradaran B. Role of miR-21 as an authentic oncogene in mediating drug resistance in breast cancer. Vol. 738, Gene. Elsevier B.V.; 2020.
64. Petrović N. miR-21 Might be Involved in Breast Cancer Promotion and Invasion Rather than in Initial Events of Breast Cancer Development. Vol. 20, Molecular Diagnosis and Therapy. Springer International Publishing; 2016. p. 97–110.
65. Vannini I, Fanini F, Fabbri M. Emerging roles of microRNAs in cancer. Vol. 48, Current Opinion in Genetics and Development. Elsevier Ltd; 2018. p. 128–33.
66. Pichler M, Calin GA. MicroRNAs in cancer: from developmental genes in worms to their clinical application in patients. Br J Cancer. 2015 Aug 11;113(4):569–73.
67. Zhang G, Zhang W, Li B, Stringer-Reasor E, Chu C, Sun L, et al. MicroRNA-200c and microRNA- 141 are regulated by a FOXP3-KAT2B axis and associated with tumor metastasis in breast cancer. Breast Cancer Research. 2017 Jun 21;19(1).
68. Fkih M'hamed I, Privat M, Ponelle F, Penault-Llorca F, Kenani A, Bignon YJ. Identification of miR-10b, miR-26a, miR-146a and miR-153 as potential triple-negative breast cancer biomarkers. Cellular Oncology. 2015 Dec 1;38(6):433–42.
69. Neves R, Scheel C, Weinhold S, Honisch E, Iwaniuk KM, Trompeter HI, et al. Role of DNA methylation in miR-200c/141 cluster silencing in invasive breast cancer cells [Internet]. 2010. Available from: http://www.biomedcentral.com/1756-0500/3/219
70. Bahena-Ocampo I, Espinosa M, Ceballos-Cancino G, Lizarraga F, Campos-Arroyo D, Schwarz A, et al. miR-10b expression in breast cancer stem cells supports self-renewal through negative PTEN regulation and sustained AKT activation. EMBO Rep. 2016 May;17(5):648–58.
71. Tang YT, Huang YY, Li JH, Qin SH, Xu Y, An TX, et al. Alterations in exosomal miRNA profile upon epithelial-mesenchymal transition in human lung cancer cell lines. BMC Genomics. 2018 Nov 6;19(1).
72. Yu D dan, Wu Y, Zhang X hui, Lv M meng, Chen W xian, Chen X, et al. Exosomes from adriamycin-resistant breast cancer cells transmit drug resistance partly by delivering miR-222. Tumor Biology. 2016 Mar 1;37(3):3227–35.

73. Chen WX, Liu XM, Lv MM, Chen L, Zhao JH, Zhong SL, et al. Exosomes from drug-resistant breast cancer cells transmit chemoresistance by a horizontal transfer of MicroRNAs. PLoS One. 2014 Apr 1;9(4).
74. Santos JC, Lima NDS, Sarian LO, Matheu A, Ribeiro ML, Derchain SFM. Exosome-mediated breast cancer chemoresistance via miR-155 transfer. Sci Rep. 2018 Dec 1;8(1).
75. Zhong S, Chen X, Wang D, Zhang X, Shen H, Yang S, et al. MicroRNA expression profiles of drug-resistance breast cancer cells and their exosomes. Oncotarget. 2016 Apr 12;7(15):19601–9.
76. Nieto MA, Huang RYYJ, Jackson RAA, Thiery JPP. EMT: 2016. Vol. 166, Cell. Cell Press; 2016. p. 21–45.
77. Kalluri R, Weinberg RA. The basics of epithelial-mesenchymal transition. Vol. 119, Journal of Clinical Investigation. 2009. p. 1420–8.
78. Thiery JP, Acloque H, Huang RYJ, Nieto MA. Epithelial-Mesenchymal Transitions in Development and Disease. Vol. 139, Cell. 2009. p. 871–90.
79. Ye X, Weinberg RA. Epithelial-Mesenchymal Plasticity: A Central Regulator of Cancer Progression. Vol. 25, Trends in Cell Biology. Elsevier Ltd; 2015. p. 675–86.
80. Yang J, Antin P, Berx G, Blanpain C, Brabletz T, Bronner M, et al. Guidelines and definitions for research on epithelial–mesenchymal transition. Vol. 21, Nature Reviews Molecular Cell Biology. Nature Research; 2020. p. 341–52.
81. Ye X, Tam WL, Shibue T, Kaygusuz Y, Reinhardt F, Ng Eaton E, et al. Distinct EMT programs control normal mammary stem cells and tumour-initiating cells. Nature. 2015 Sep 10;525(7568):256–60.
82. Tran HD, Luitel K, Kim M, Zhang K, Longmore GD, Tran DD. Transient SNAIL1 expression is necessary for metastatic competence in breast cancer. Cancer Res. 2014 Nov 1;74(21):6330–40.
83. Beerling E, Seinstra D, de Wit E, Kester L, van der Velden D, Maynard C, et al. Plasticity between Epithelial and Mesenchymal States Unlinks EMT from Metastasis-Enhancing Stem Cell Capacity. Cell Rep. 2016 Mar 15;14(10):2281–8.
84. Wu HT, Zhong HT, Li GW, Shen JX, Ye QQ, Zhang ML, et al. Oncogenic functions of the EMT-related transcription factor ZEB1 in breast cancer. Vol. 18, Journal of Translational Medicine. BioMed Central Ltd.; 2020.
85. Mohammadi Ghahhari N, Sznurkowska MK, Hulo N, Bernasconi L, Aceto N, Picard D. Cooperative interaction between ERα and the EMT-inducer ZEB1 reprograms breast cancer cells for bone metastasis. Nat Commun. 2022 Dec 1;13(1).
86. Li QQ, Xu J Da, Wang WJ, Cao XX, Chen Q, Tang F, et al. Twist1-mediated adriamycin-induced epithelial-mesenchymal transition relates to multidrug resistance and invasive potential in breast cancer cells. Clinical Cancer Research. 2009 Apr 15;15(8):2657–65.
87. AlAhmari MM, Al-Khalaf HH, Al-Mohanna FH, Ghebeh H, Aboussekhra A. AUF1 promotes stemness in human mammary epithelial cells through stabilization of the EMT transcription factors TWIST1 and SNAIL1. Oncogenesis. 2020 Aug 1;9(8).
88. Kar R, Jha NK, Jha SK, Sharma A, Dholpuria S, Asthana N, et al. A “NOTCH” deeper into the epithelial-to-mesenchymal transition (EMT) program in breast cancer. Vol. 10, Genes. MDPI AG; 2019.
89. Serej ZA, Ebrahimi A, Kazemi T, Najafi S, Amini M, Nastarin P, et al. NANOG gene suppression and replacement of let-7 modulate the stemness, invasion, and apoptosis in breast cancer. Gene. 2021 Oct 30;801.
90. Roy S, Sunkara RR, Parmar MY, Shaikh S, Waghmare SK. 238 EMT imparts cancer stemness and plasticity: new perspectives and therapeutic potential. Vol. 26, Frontiers in Bioscience. 2021.

91. Wilson MM, Weinberg RA, Lees JA, Guen VJ. Emerging Mechanisms by which EMT Programs Control Stemness. Vol. 6, Trends in Cancer. Cell Press; 2020. p. 775–80.
92. Grasset EM, Dunworth M, Sharma G, Loth M, Tandurella J, Cimino-Mathews A, et al. Triple-negative breast cancer metastasis involves complex epithelial-mesenchymal transition dynamics and requires vimentin [Internet]. Vol. 14, Sci. Transl. Med. 2022. Available from: https://www.science.org
93. Loh CY, Chai JY, Tang TF, Wong WF, Sethi G, Shanmugam MK, et al. The e-cadherin and n-cadherin switch in epithelial-to-mesenchymal transition: Signaling, therapeutic implications, and challenges. Vol. 8, Cells. MDPI; 2019.
94. Bhandari A, Zheng C, Sindan N, Sindan N, Quan R, Xia E, et al. COPB2 is up-regulated in breast cancer and plays a vital role in the metastasis via N-cadherin and Vimentin. J Cell Mol Med. 2019 Aug 1;23(8):5235–45.
95. Balanis N, Wendt MK, Schiemann BJ, Wang Z, Schiemann WP, Carlin CR. Epithelial to mesenchymal transition promotes breast cancer progression via a fibronectin-dependent STAT3 signaling pathway. Journal of Biological Chemistry. 2013 Jun 21;288(25):17954–67.
96. Li CL, Yang D, Cao X, Wang F, Hong DY, Wang J, et al. Fibronectin induces epithelial-mesenchymal transition in human breast cancer MCF-7 cells via activation of calpain. Oncol Lett. 2017 May 1;13(5):3889–95.
97. Kumar A, Golani A, Dinesh Kumar L. 979 EMT in breast cancer metastasis: an interplay of microRNAs, signaling pathways and circulating tumor cells. Vol. 25, Frontiers in Bioscience. 2020.
98. Wright JA, Richer JK, Goodall GJ. MicroRNAs and EMT in mammary cells and breast cancer. Vol. 15, Journal of Mammary Gland Biology and Neoplasia. 2010. p. 213–23.
99. Pan G, Liu Y, Shang L, Zhou F, Yang S. EMT-associated microRNAs and their roles in cancer stemness and drug resistance. Vol. 41, Cancer Communications. John Wiley and Sons Inc; 2021. p. 199–217.
100. Wu H, Wang Q, Zhong H, Li L, Zhang Q, Huang Q, et al. Differentially expressed microRNAs in exosomes of patients with breast cancer revealed by next-generation sequencing. Oncol Rep. 2020;43(1):240–50.
101. Han M, Wang Y, Liu M, Bi X, Bao J, Zeng N, et al. MiR-21 regulates epithelial-mesenchymal transition phenotype and hypoxia-inducible factor-1α expression in third-sphere forming breast cancer stem cell-like cells. Cancer Sci. 2012 Jun;103(6):1058–64.
102. Ma F, Li W, Liu C, Li W, Yu H, Lei B, et al. MiR-23a promotes TGF-β1-induced EMT and tumor metastasis in breast cancer cells by directly targeting CDH1 and activating Wnt/β-catenin signaling [Internet]. 2017. Available from: www.impactjournals.com/oncotarget
103. Zhao M, Ang L, Huang J, Wang J. MicroRNAs regulate the epithelial–mesenchymal transition and influence breast cancer invasion and metastasis. Vol. 39, Tumor Biology. SAGE Publications Ltd; 2017. p. 1–8.
104. Gee HE, Camps C, Buffa FM, Colella S, Sheldon H, Gleadle JM, et al. MicroRNA-10b and breast cancer metastasis. Vol. 455, Nature. Nature Publishing Group; 2008.
105. Title AC, Hong SJ, Pires ND, Hasenöhrl L, Godbersen S, Stokar-Regenscheit N, et al. Genetic dissection of the miR-200–Zeb1 axis reveals its importance in tumor differentiation and invasion. Nat Commun. 2018 Dec 1;9(1).
106. Stevanato L, Thanabalasundaram L, Vysokov N, Sinden JD. Investigation of content, stoichiometry and transfer of miRNA from human neural stem cell line derived exosomes. PLoS One. 2016 Jan 11;11(1).
107. Ferguson S, Yang KS, Weissleder R. Single extracellular vesicle analysis for early cancer detection. Vol. 28, Trends in Molecular Medicine. Elsevier Ltd; 2022. p. 681–92.

108. Chevillet JR, Kang Q, Ruf IK, Briggs HA, Vojtech LN, Hughes SM, et al. Quantitative and stoichiometric analysis of the microRNA content of exosomes. Proc Natl Acad Sci U S A. 2014 Oct 14;111(41):14888–93.
109. Das S, Halushka MK. Extracellular vesicle microRNA transfer in cardiovascular disease. Vol. 24, Cardiovascular Pathology. Elsevier Inc.; 2015. p. 199–206.
110. Martellucci S, Orefice NS, Angelucci A, Luce A, Caraglia M, Zappavigna S. Extracellular vesicles: New endogenous shuttles for mirnas in cancer diagnosis and therapy? Vol. 21, International Journal of Molecular Sciences. MDPI AG; 2020. p. 1–24.
111. Sueta A, Yamamoto Y, Tomiguchi M, Takeshita T, Yamamoto-Ibusuki M, Iwase H. Differential expression of exosomal miRNAs between breast cancer patients with and without recurrence [Internet]. 2017. Available from: www.impactjournals.com/oncotarget
112. Ozawa PMM, Vieira E, Lemos DS, Souza ILM, Zanata SM, Pankievicz VC, et al. Identification of miRNAs enriched in extracellular vesicles derived from serum samples of breast cancer patients. Biomolecules. 2020 Jan 1;10(1).
113. Sun Z, Shi K, Yang S, Liu J, Zhou Q, Wang G, et al. Effect of exosomal miRNA on cancer biology and clinical applications. Vol. 17, Molecular Cancer. BioMed Central Ltd.; 2018.
114. Kinoshita T, Yip KW, Spence T, Liu FF. MicroRNAs in extracellular vesicles: Potential cancer biomarkers. Vol. 62, Journal of Human Genetics. Nature Publishing Group; 2017. p. 67–74.
115. Sun X, Lin F, Sun W, Zhu W, Fang D, Luo L, et al. Exosome-transmitted miRNA-335-5p promotes colorectal cancer invasion and metastasis by facilitating EMT via targeting RASA1. Mol Ther Nucleic Acids. 2021 Jun 4;24:164–74.
116. Naseri Z, Oskuee RK, Jaafari MR, Moghadam MF. Exosome-mediated delivery of functionally active miRNA-142-3p inhibitor reduces tumorigenicity of breast cancer in vitro and in vivo. Int J Nanomedicine. 2018;13:7727–47.
117. Li C, Li R, Hu X, Zhou G, Jiang G. Tumor-promoting mechanisms of macrophage-derived extracellular vesicles-enclosed microRNA-660 in breast cancer progression. Breast Cancer Res Treat. 2022 Apr 1;192(2):353–68.
118. Wang H, Wei H, Wang J, Li L, Chen A, Li Z. MicroRNA-181d-5p-Containing Exosomes Derived from CAFs Promote EMT by Regulating CDX2/HOXA5 in Breast Cancer. Mol Ther Nucleic Acids. 2020 Mar 6;19:654–67.
119. Donnarumma E, Fiore D, Nappa M, Roscigno G, Adamo A, Iaboni M, et al. Cancer-associated fibroblasts release exosomal microRNAs that dictate an aggressive phenotype in breast cancer [Internet]. 2017. Available from: www.impactjournals.com/oncotarget
120. Mills J, Capece M, Cocucci E, Tessari A, Palmieri D. Cancer-derived extracellular vesicle-associated microRNAs in intercellular communication: One cell's trash is another cell's treasure. Vol. 20, International Journal of Molecular Sciences. MDPI AG; 2019.
121. Munir J, Yoon JK, Ryu S. Therapeutic miRNA-Enriched Extracellular Vesicles: Current Approaches and Future Prospects. Vol. 9, Cells. NLM (Medline); 2020.
122. Visan KS, Lobb RJ, Moller A. The role of exosomes in the promotion of epithelial-to-mesenchymal transition and metastasis. Vol. 25, Frontiers in Bioscience. 2020.
123. Franzen CA, Blackwell RH, Todorovic V, Greco KA, Foreman KE, Flanigan RC, et al. Urothelial cells undergo epithelial-to-mesenchymal transition after exposure to muscle invasive bladder cancer exosomes. Oncogenesis. 2015 Aug 17;4(8).
124. Greening DW, Gopal SK, Mathias RA, Liu L, Sheng J, Zhu HJ, et al. Emerging roles of exosomes during epithelial-mesenchymal transition and cancer progression. Vol. 40, Seminars in Cell and Developmental Biology. Academic Press; 2015. p. 60–71.
125. Xiao D, Barry S, Kmetz D, Egger M, Pan J, Rai SN, et al. Melanoma cell-derived exosomes promote epithelial-mesenchymal transition in primary melanocytes through

paracrine/autocrine signaling in the tumor microenvironment. Cancer Lett. 2016 Jul 1;376(2):318–27.
126. Garnier D, Magnus N, Lee TH, Bentley V, Meehan B, Milsom C, et al. Cancer cells induced to express mesenchymal phenotype release exosome-like extracellular vesicles carrying tissue factor. Journal of Biological Chemistry. 2012 Dec 21;287(52):43565–72.
127. Jeppesen DK, Nawrocki A, Jensen SG, Thorsen K, Whitehead B, Howard KA, et al. Quantitative proteomics of fractionated membrane and lumen exosome proteins from isogenic metastatic and nonmetastatic bladder cancer cells reveal differential expression of EMT factors. Proteomics. 2014;14(6):699–712.
128. Ji H, Greening DW, Barnes TW, Lim JW, Tauro BJ, Rai A, et al. Proteome profiling of exosomes derived from human primary and metastatic colorectal cancer cells reveal differential expression of key metastatic factors and signal transduction components. Proteomics. 2013 May;13(10–11):1672–86.
129. Qiao Z, Zhang Y, Ge M, Liu S, Jiang X, Shang Z, et al. Cancer cell derived small extracellular vesicles contribute to recipient cell metastasis through promoting HGF/c-Met pathway*□S. Molecular and Cellular Proteomics. 2019;18(8):1619–29.
130. Ying X, Sun Y, He P. MicroRNA-137 inhibits BMP7 to enhance the epithelial-mesenchymal transition of breast cancer cells [Internet]. 2017. Available from: www.impactjournals.com/oncotarget
131. Brena D, Huang MB, Bond V. Extracellular vesicle-mediated transport: Reprogramming a tumor microenvironment conducive with breast cancer progression and metastasis. Vol. 15, Translational Oncology. Neoplasia Press, Inc.; 2022.
132. Kogure A, Kosaka N, Ochiya T. Cross-talk between cancer cells and their neighbors via miRNA in extracellular vesicles: An emerging player in cancer metastasis. Vol. 26, Journal of Biomedical Science. BioMed Central Ltd.; 2019.
133. Singh R, Pochampally R, Watabe K, Lu Z, Mo YY. Exosome-mediated transfer of miR-10b promotes cell invasion in breast cancer. Mol Cancer. 2014 Nov 26;13(1).
134. Sung BH, Ketova T, Hoshino D, Zijlstra A, Weaver AM. Directional cell movement through tissues is controlled by exosome secretion. Nat Commun. 2015 May 13;6.
135. Spugnini EP, Logozzi M, di Raimo R, Mizzoni D, Fais S. A role of tumor-released exosomes in paracrine dissemination and metastasis. Vol. 19, International Journal of Molecular Sciences. MDPI AG; 2018.
136. Lobos-González L, Silva V, Araya M, Restovic F, Echenique J, Oliveira-Cruz L, et al. Targeting antisense mitochondrial ncRNAs inhibits murine melanoma tumor growth and metastasis through reduction in survival and invasion factors [Internet]. Vol. 7, Oncotarget. 2016. Available from: www.impactjournals.com/oncotarget/
137. Aparicio-Puerta E, Gómez-Martín C, Giannoukakos S, Medina JM, Scheepbouwer C, García-Moreno A, et al. sRNAbench and sRNAtoolbox 2022 update: accurate miRNA and sncRNA profiling for model and non-model organisms. Nucleic Acids Res. 2022 Jul 5;50(W1):W710–7.
138. Aparicio-Puerta E, Lebrón R, Rueda A, Gómez-Martín C, Giannoukakos S, Jaspez D, et al. SRNAbench and sRNAtoolbox 2019: intuitive fast small RNA profiling and differential expression. Nucleic Acids Res. 2019 Jul 1;47(W1):W530–5.
139. Robinson MD, McCarthy DJ, Smyth GK. edgeR: A Bioconductor package for differential expression analysis of digital gene expression data. Bioinformatics. 2009 Nov 11;26(1):139–40.
140. Ding J, Li X, Hu H. TarPmiR: A new approach for microRNA target site prediction. Bioinformatics. 2016 Sep 15;32(18):2768–75.

141. Sticht C, de La Torre C, Parveen A, Gretz N. Mirwalk: An online resource for prediction of microrna binding sites. PLoS One. 2018 Oct 1;13(10).
142. Szklarczyk D, Gable AL, Lyon D, Junge A, Wyder S, Huerta-Cepas J, et al. STRING v11: Protein-protein association networks with increased coverage, supporting functional discovery in genome-wide experimental datasets. Nucleic Acids Res. 2019 Jan 8;47(D1):D607–13.
143. Mi H, Muruganujan A, Casagrande JT, Thomas PD. Large-scale gene function analysis with the panther classification system. Nat Protoc. 2013;8(8):1551–66.
144. Thomas PD, Ebert D, Muruganujan A, Mushayahama T, Albou LP, Mi H. PANTHER: Making genome-scale phylogenetics accessible to all. Vol. 31, Protein Science. John Wiley and Sons Inc; 2022. p. 8–22.
145. Mi H, Thomas P. PANTHER pathway: an ontology-based pathway database coupled with data analysis tools. Methods Mol Biol. 2009;563:123–40.
146. Benes V, Collier P, Kordes C, Stolte J, Rausch T, Muckentaler MU, et al. Identification of cytokine-induced modulation of microRNA expression and secretion as measured by a novel microRNA specific qPCR assay. Sci Rep. 2015 Jun 25;5.
147. Andersen CL, Jensen JL, Ørntoft TF. Normalization of real-time quantitative reverse transcription-PCR data: A model-based variance estimation approach to identify genes suited for normalization, applied to bladder and colon cancer data sets. Cancer Res. 2004 Aug 1;64(15):5245–50.
148. Yang SS, Ma S, Dou H, Liu F, Zhang SY, Jiang C, et al. Breast cancer-derived exosomes regulate cell invasion and metastasis in breast cancer via miR-146a to activate cancer associated fibroblasts in tumor microenvironment. Exp Cell Res. 2020 Jun 15;391(2).
149. Guo L, Zhu Y, Li L, Zhou S, Yin G, Yu G, et al. Breast cancer cell-derived exosomal miR-20a-5p promotes the proliferation and differentiation of osteoclasts by targeting SRCIN1. Cancer Med. 2019 Sep 1;8(12):5687–701.
150. Gomes FG, Sandim V, Almeida VH, Rondon AMR, Succar BB, Hottz ED, et al. Breast-cancer extracellular vesicles induce platelet activation and aggregation by tissue factor-independent and -dependent mechanisms. Thromb Res. 2017 Nov 1;159:24–32.
151. Kaur J, Saul D, Doolittle ML, Rowsey JL, Vos SJ, Farr JN, et al. Identification of a suitable endogenous control miRNA in bone aging and senescence. Gene. 2022 Aug 15;835.
152. Donati S, Ciuffi S, Brandi ML. Human circulating miRNAs real-time qRT-PCR-based analysis: An overview of endogenous reference genes used for data normalization. Vol. 20, International Journal of Molecular Sciences. MDPI AG; 2019.
153. Occhipinti G, Giulietti M, Principato G, Piva F. The choice of endogenous controls in exosomal microRNA assessments from biofluids. Vol. 37, Tumor Biology. Springer Science and Business Media B.V.; 2016. p. 11657–65.
154. Peltier HJ, Latham GJ. Normalization of microRNA expression levels in quantitative RT-PCR assays: Identification of suitable reference RNA targets in normal and cancerous human solid tissues. RNA. 2008 May;14(5):844–52.
155. Crossland RE, Norden J, Bibby LA, Davis J, Dickinson AM. Evaluation of optimal extracellular vesicle small RNA isolation and qRT-PCR normalisation for serum and urine. J Immunol Methods. 2016 Feb 1;429:39–49.
156. Damanti CC, Gaffo E, Lovisa F, Garbin A, di Battista P, Gallingani I, et al. MiR-26a-5p as a reference to normalize microrna QRT-PCR levels in plasma exosomes of pediatric hematological malignancies. Cells. 2021 Jan 1;10(1):1–10.
157. Liu L, Xu C, Hsieh JT, Gong J, Xie D. DAB2IP in cancer [Internet]. Vol. 7. 2015. Available from: www.impactjournals.com/oncotarget

158. Chang WH, Cerione RA, Antonyak MA. Extracellular Vesicles and Their Roles in Cancer Progression. In: Methods in Molecular Biology. Humana Press Inc.; 2021. p. 143–70.
159. Xu R, Rai A, Chen M, Suwakulsiri W, Greening DW, Simpson RJ. Extracellular vesicles in cancer — implications for future improvements in cancer care. Vol. 15, Nature Reviews Clinical Oncology. Nature Publishing Group; 2018. p. 617–38.
160. Leal-Orta E, Ramirez-Ricardo J, Garcia-Hernandez A, Cortes-Reynosa P, Salazar EP. Extracellular vesicles from MDA-MB-231 breast cancer cells stimulated with insulin-like growth factor 1 mediate an epithelial–mesenchymal transition process in MCF10A mammary epithelial cells. J Cell Commun Signal. 2022 Dec 1;16(4):531–46.
161. Amorim C, Docasar CL, Guimarães-Bastos D, Frony AC, Barja-Fidalgo C, Renovato-Martins M, et al. Extracellular Vesicles Derived from MDA-MB-231 Cells Trigger Neutrophils to a Pro-Tumor Profile. Cells. 2022 Jun 1;11(12).
162. Leal-Orta E, Ramirez-Ricardo J, Cortes-Reynosa P, Galindo-Hernandez O, Salazar EP. Role of PI3K/Akt on migration and invasion of MCF10A cells treated with extracellular vesicles from MDA-MB-231 cells stimulated with linoleic acid. J Cell Commun Signal. 2019 Jun 6;13(2):235–44.
163. Papaccio G, Desiderio V. Cancer Stem Cells Methods and Protocols Methods in Molecular Biology 1692 [Internet]. Available from: http://www.springer.com/series/7651
164. Borowicz S, Van Scoyk M, Avasarala S, Karuppusamy Rathinam MK, Tauler J, Bikkavilli RK, et al. The soft agar colony formation assay. Journal of Visualized Experiments. 2014 Oct 27;(92).
165. Franken NAP, Rodermond HM, Stap J, Haveman J, van Bree C. Clonogenic assay of cells in vitro. Nat Protoc. 2006 Dec;1(5):2315–9.
166. Modi U, Makwana P, Vasita R. Molecular insights of metastasis and cancer progression derived using 3D cancer spheroid co-culture in vitro platform. Vol. 168, Critical Reviews in Oncology/Hematology. Elsevier Ireland Ltd; 2021.
167. Eguchi T, Sheta M, Fujii M, Calderwood SK. Cancer extracellular vesicles, tumoroid models, and tumor microenvironment. Vol. 86, Seminars in Cancer Biology. Academic Press; 2022. p. 112–26.
168. Nizamudeen ZA, Xerri R, Parmenter C, Suain K, Markus R, Chakrabarti L, et al. Low-power sonication can alter extracellular vesicle size and properties. Cells. 2021 Sep 1;10(9).
169. Lamichhane TN, Jeyaram A, Patel DB, Parajuli B, Livingston NK, Arumugasaamy N, et al. Oncogene Knockdown via Active Loading of Small RNAs into Extracellular Vesicles by Sonication. Cell Mol Bioeng. 2016 Sep 1;9(3):315–24.
170. Pomatto MAC, Bussolati B, D'Antico S, Ghiotto S, Tetta C, Brizzi MF, et al. Improved Loading of Plasma-Derived Extracellular Vesicles to Encapsulate Antitumor miRNAs. Mol Ther Methods Clin Dev. 2019 Jun 14;13:133–44.
171. Pottash AE, Levy D, Jeyaram A, Kuo L, Kronstadt SM, Chao W, et al. Combinatorial microRNA Loading into Extracellular Vesicles for Increased Anti-Inflammatory Efficacy. Noncoding RNA. 2022 Oct 1;8(5).
172. Sukreet S, Vieira B, Silva RE, Adamec J, Cui J, Zempleni J. Sonication and Short-term Incubation Alter the Content of Bovine Milk Exosome Cargos and Exosome Bioavailability (OR26-08-19).
173. Pchelintsev NA, Adams PD, Nelson DM. Critical parameters for efficient sonication and improved chromatin immunoprecipitation of high molecular weight proteins. PLoS One. 2016 Jan 1;11(1).
174. Giusti I, Di Francesco M, Poppa G, Esposito L, D'Ascenzo S, Dolo V. Tumor-Derived Extracellular Vesicles Activate Normal Human Fibroblasts to a Cancer-Associated

Fibroblast-Like Phenotype, Sustaining a Pro-Tumorigenic Microenvironment. Front Oncol. 2022 Feb 23;12.
175. He C, Wang L, Li L, Zhu G. Extracellular vesicle-orchestrated crosstalk between cancer-associated fibroblasts and tumors. Vol. 14, Translational Oncology. Neoplasia Press, Inc.; 2021.
176. Naito Y, Yoshioka Y, Ochiya T. Intercellular crosstalk between cancer cells and cancer-associated fibroblasts via extracellular vesicles. Vol. 22, Cancer Cell International. BioMed Central Ltd; 2022.
177. Kuriyama N, Yoshioka Y, Kikuchi S, Azuma N, Ochiya T. Extracellular Vesicles Are Key Regulators of Tumor Neovasculature. Vol. 8, Frontiers in Cell and Developmental Biology. Frontiers Media S.A.; 2020.
178. Lakshmi S, Hughes TA, Priya S. Exosomes and exosomal RNAs in breast cancer: A status update. Vol. 144, European Journal of Cancer. Elsevier Ltd; 2021. p. 252–68.
179. Dai X, Cheng H, Bai Z, Li J. Breast cancer cell line classification and Its relevance with breast tumor subtyping. Vol. 8, Journal of Cancer. Ivyspring International Publisher; 2017. p. 3131–41.
180. Riaz M, van Jaarsveld MTM, Hollestelle A, Prager-van der Smissen WJC, Heine AAJ, Boersma AWM, et al. MiRNA expression profiling of 51 human breast cancer cell lines reveals subtype and driver mutation-specific miRNAs. Breast Cancer Research. 2013 Apr 19;15(2).
181. Iorio M V., Ferracin M, Liu CG, Veronese A, Spizzo R, Sabbioni S, et al. MicroRNA gene expression deregulation in human breast cancer. Cancer Res. 2005 Aug 15;65(16):7065–70.
182. Vychytilova-Faltejskova P, Kovarikova AS, Grolich T, Prochazka V, Slaba K, Machackova T, et al. MicroRNA biogenesis pathway genes are deregulated in colorectal cancer. Int J Mol Sci. 2019 Sep 2;20(18).
183. Zhu J, Zheng Z, Wang J, Sun J, Wang P, Cheng X, et al. Different miRNA expression profiles between human breast cancer tumors and serum. Front Genet. 2014;5(MAY).
184. Hata A, Kashima R. Dysregulation of microRNA biogenesis machinery in cancer. Vol. 51, Critical Reviews in Biochemistry and Molecular Biology. Taylor and Francis Ltd; 2016. p. 121–34.
185. Li G, Manning AC, Bagi A, Yang X, Gokulnath P, Spanos M, et al. Distinct Stress-Dependent Signatures of Cellular and Extracellular tRNA-Derived Small RNAs. Advanced Science. 2022 Jun 1;9(17).
186. Chiou NT, Kageyama R, Ansel KM. Selective Export into Extracellular Vesicles and Function of tRNA Fragments during T Cell Activation. Cell Rep. 2018 Dec 18;25(12):3356-3370.e4.
187. Weng Q, Wang Y, Xie Y, Yu X, Zhang S, Ge J, et al. Extracellular vesicles-associated tRNA-derived fragments (tRFs): biogenesis, biological functions, and their role as potential biomarkers in human diseases. Vol. 100, Journal of Molecular Medicine. Springer Science and Business Media Deutschland GmbH; 2022. p. 679–95.
188. Tosar JP, Witwer K, Cayota A. Revisiting Extracellular RNA Release, Processing, and Function. Vol. 46, Trends in Biochemical Sciences. Elsevier Ltd; 2021. p. 438–45.
189. Sarver AL, Sarver AE, Yuan C, Subramanian S. OMCD: OncomiR Cancer Database. BMC Cancer. 2018 Dec 6;18(1).
190. Hurst DR, Edmonds MD, Welch DR. Metastamir: The field of metastasis-regulatory microRNA is spreading. Vol. 69, Cancer Research. 2009. p. 7495–8.

191. Zhao H, Kang X, Xia X, Gu X, Hu Y, Xie X, et al. miR-145 suppresses breast cancer cell migration by targeting FSCN-1 and inhibiting epithelial-mesenchymal transition [Internet]. Vol. 8, Am J Transl Res. 2016. Available from: www.ajtr.org
192. Wang S, Bian C, Yang Z, Bo Y, Li J, Zeng L, et al. miR-145 inhibits breast cancer cell growth through RTKN. Int J Oncol. 2009;34(5):1461–6.
193. Tang W, Zhang X, Tan W, Gao J, Pan L, Ye X, et al. miR-145-5p Suppresses Breast Cancer Progression by Inhibiting SOX2. Journal of Surgical Research. 2019 Apr 1;236:278–87.
194. Sun Z, Ou C, Liu J, Chen C, Zhou Q, Yang S, et al. YAP1-induced MALAT1 promotes epithelial–mesenchymal transition and angiogenesis by sponging miR-126-5p in colorectal cancer. Oncogene. 2019 Apr 4;38(14):2627–44.
195. Miao Y, Lu J, Fan B, Sun L. MicroRNA-126-5p Inhibits the Migration of Breast Cancer Cells by Directly Targeting CNOT7. Technol Cancer Res Treat. 2020;19.
196. van Solingen C, Oldebeken SR, Salerno AG, Wanschel ACBA, Moore KJ. High-Throughput Screening Identifies MicroRNAs Regulating Human PCSK9 and Hepatic Low-Density Lipoprotein Receptor Expression. Front Cardiovasc Med. 2021 Jul 12;8.
197. Creighton CJ, Benham AL, Zhu H, Khan MF, Reid JG, Nagaraja AK, et al. Discovery of novel MicroRNAs in female reproductive tract using next generation sequencing. PLoS One. 2010 Mar 10;5(3).
198. Johnstone RM. The Jeanne Manery-Fisher La conference a la memoire de Memorial Lecture Maturation of reticulocytes: formation of exosomes as a mechanism for shedding membrane proteins [Internet]. Available from: www.nrcresearchpress.com
199. Kita S, Shimomura I. Extracellular Vesicles as an Endocrine Mechanism Connecting Distant Cells. Vol. 45, Molecules and Cells. Korean Society for Molecular and Cellular Biology; 2022. p. 771–80.
200. Johnstone RM, Adam M, Hammond JR, Orr L, Turbide C. Vesicle formation during reticulocyte maturation. Association of plasma membrane activities with released vesicles (exosomes). Journal of Biological Chemistry. 1987 Jul 5;262(19):9412–20.
201. Farahani M, Rubbi C, Liu L, Slupsky JR, Kalakonda N. CLL exosomes modulate the transcriptome and behaviour of recipient stromal cells and are selectively enriched in MIR-202-3p. PLoS One. 2015 Oct 28;10(10).
202. Ostenfeld MS, Jeppesen DK, Laurberg JR, Boysen AT, Bramsen JB, Primdal-Bengtson B, et al. Cellular disposal of miR23b by RAB27-dependent exosome release is linked to acquisition of metastatic properties. Cancer Res. 2014 Oct 15;74(20):5758–71.
203. Kim H, Lee S, Shin E, Seong KM, Jin YW, Youn HS, et al. The Emerging Roles of Exosomes as EMT Regulators in Cancer. Vol. 9, Cells. NLM (Medline); 2020.
204. Jiang C, Zhang N, Hu X, Wang H. Tumor-associated exosomes promote lung cancer metastasis through multiple mechanisms. Vol. 20, Molecular Cancer. BioMed Central Ltd; 2021.
205. Chen Y, Lun AT, Mccarthy DJ, Ritchie ME, Phipson B, Hu YF, et al. Package “edgeR” Title Empirical Analysis of Digital Gene Expression Data in R. 2023.
206. Fillmore CM, Kuperwasser C. Human breast cancer cell lines contain stem-like cells that self-renew, give rise to phenotypically diverse progeny and survive chemotherapy. Breast Cancer Research. 2008 Mar 26;10(2).
207. Prat A, Parker JS, Karginova O, Fan C, Livasy C, Herschkowitz JI, et al. Phenotypic and molecular characterization of the claudin-low intrinsic subtype of breast cancer [Internet]. 2010. Available from: http://breast-cancer-research.com/content/12/5/R68

208. Grigoriadis A, Mackay A, Noel E, Wu PJ, Natrajan R, Frankum J, et al. Molecular characterisation of cell line models for triple-negative breast cancers. BMC Genomics. 2012 Nov 14;13(1).
209. Jolly MK, Mani SA, Levine H. Hybrid epithelial/mesenchymal phenotype(s): The 'fittest' for metastasis? Vol. 1870, Biochimica et Biophysica Acta - Reviews on Cancer. Elsevier B.V.; 2018. p. 151–7.
210. Bahrami A, Jafari A, Ferns GA. The dual role of microRNA-9 in gastrointestinal cancers: oncomiR or tumor suppressor? Vol. 145, Biomedicine and Pharmacotherapy. Elsevier Masson s.r.l.; 2022.
211. Budd WT, Seashols-Williams SJ, Clark GC, Weaver D, Calvert V, Petricoin E, et al. Dual action of miR-125b as a tumor suppressor and OncomiR-22 promotes prostate cancer tumorigenesis. PLoS One. 2015 Nov 6;10(11).
212. Perez-Añorve IX, Gonzalez-De la Rosa CH, Soto-Reyes E, Beltran-Anaya FO, Del Moral-Hernandez O, Salgado-Albarran M, et al. New insights into radioresistance in breast cancer identify a dual function of miR-122 as a tumor suppressor and oncomiR. Mol Oncol. 2019 May 1;13(5):1249–67.
213. Xiang Y, Tian Q, Guan L, Niu SS. The Dual Role of miR-186 in Cancers: Oncomir Battling With Tumor Suppressor miRNA. Vol. 10, Frontiers in Oncology. Frontiers Media S.A.; 2020.
214. He C, Luo B, Jiang N, Liang Y, He Y, Zeng J, et al. OncomiR or antioncomiR: Role of miRNAs in Acute Myeloid Leukemia. Vol. 60, Leukemia and Lymphoma. Taylor and Francis Ltd; 2019. p. 284–94.
215. Ni Y, Lu C, Wang W, Gao W, Yu C. circBANP promotes colorectal cancer growth and metastasis via sponging let-7d-5p to modulate HMGA1/Wnt/β-catenin signaling. Mol Ther Oncolytics. 2021 Jun 25;21:119–33.
216. Chen YN, Ren CC, Yang L, Nai MM, Xu YM, Zhang F, et al. MicroRNA let-7d-5p rescues ovarian cancer cell apoptosis and restores chemosensitivity by regulating the p53 signaling pathway via HMGA1. Int J Oncol. 2019 Apr 1;54(5):1771–84.
217. Kolenda T, Przybyla W, Teresiak A, Mackiewicz A, Lamperska KM. The mystery of let-7d - A small RNA with great power. Vol. 18, Wspolczesna Onkologia. Termedia Publishing House Ltd.; 2014. p. 293–301.
218. De Santis C, Götte M. The role of microRNA let-7d in female malignancies and diseases of the female reproductive tract. Vol. 22, International Journal of Molecular Sciences. MDPI; 2021.
219. Gao X, Liu H, Wang R, Huang M, Wu Q, Wang Y, et al. Hsa-let-7d-5p Promotes Gastric Cancer Progression by Targeting PRDM5. J Oncol. 2022;2022.
220. Williams ED, Gao D, Redfern A, Thompson EW. Controversies around epithelial–mesenchymal plasticity in cancer metastasis. Nat Rev Cancer. 2019 Dec 1;19(12):716–32.
221. Dongre A, Weinberg RA. New insights into the mechanisms of epithelial–mesenchymal transition and implications for cancer. Vol. 20, Nature Reviews Molecular Cell Biology. Nature Publishing Group; 2019. p. 69–84.
222. Zhao X, Guan JL. Focal adhesion kinase and its signaling pathways in cell migration and angiogenesis. Vol. 63, Advanced Drug Delivery Reviews. 2011. p. 610–5.
223. Yamao M, Naoki H, Kunida K, Aoki K, Matsuda M, Ishii S. Distinct predictive performance of Rac1 and Cdc42 in cell migration. Sci Rep. 2015 Dec 4;5.
224. Johnson E, Seachrist DD, DeLeon-Rodriguez CM, Lozada KL, Miedler J, Abdul-Karim FW, et al. HER2/ErbB2-induced breast cancer cell migration and invasion require p120 catenin

activation of Rac1 and Cdc42. Journal of Biological Chemistry. 2010 Sep 17;285(38):29491–501.
225. Bilir B, Kucuk O, Moreno CS. Wnt signaling blockage inhibits cell proliferation and migration, and induces apoptosis in triple-negative breast cancer cells. J Transl Med. 2013 Nov 4;11(1).
226. VanderVorst K, Dreyer CA, Konopelski SE, Lee H, Ho HYH, Carraway KL. Wnt/PCP signaling contribution to carcinoma collective cell migration and metastasis. Vol. 79, Cancer Research. American Association for Cancer Research Inc.; 2019. p. 1719–29.
227. Zhang X, Sai B, Wang F, Wang L, Wang Y, Zheng L, et al. Hypoxic BMSC-derived exosomal miRNAs promote metastasis of lung cancer cells via STAT3-induced EMT. Mol Cancer. 2019 Mar 13;18(1).
228. Zeng Z, Li Y, Pan Y, Lan X, Song F, Sun J, et al. Cancer-derived exosomal miR-25-3p promotes pre-metastatic niche formation by inducing vascular permeability and angiogenesis. Nat Commun. 2018 Dec 1;9(1).
229. He Q, Ye A, Ye W, Liao X, Qin G, Xu Y, et al. Cancer-secreted exosomal miR-21-5p induces angiogenesis and vascular permeability by targeting KRIT1. Cell Death Dis. 2021 Jun 1;12(6).

ANNEXES

Table A. List of specific miRNA primers used

miRBase ID	Specific primer (Tm adj)	
hsa-let-7d-5p	GAGGTAGTAGGTTGCATAGTTGGC	
hsa-let-7i-5p	TGAGGTAGTAGTTTGTGCTGTTGG	
hsa-miR-1-3p	TGGAATGTAAAGAAGTATGTATGGC	
hsa-miR-10a-3p	CAAATTCGTATCTAGGGGAATAGG	
hsa-miR-100-5p	AACCCGTAGATCCGAACTTGTGG	
hsa-miR-122-5p	GAGTGTGACAATGGTGTTTGG	
hsa-miR-125b-1-3p	GGTTAGGCTCTTGGGAGCTG	
hsa-miR-126-5p	*CATTATTACTTTTGGTACGCGG*	
hsa-miR-1307-5p	GGACCTCGACCGGCTG	
hsa-miR-133a-3p	CCCCTTCAACCAGCTGG	
hsa-miR-143-3p	TGAGATGAAGCACTGTAGCTCG	
hsa-miR-145-5p	*AGTTTTCCCAGGAATCCCTG*	
hsa-miR-146a-5p	GAGAACTGAATTCCATGGGTTG	**Candidate EMT-promoters sEV-miRs enriched in sEV-MDA231**
hsa-miR-199a-3p	ACAGTAGTCTGCACATTGGTTAGG	
hsa-miR-199a-5p	CCAGTGTTCAGACTACCTGTTCG	
hsa-miR-199b-3p	ACAGTAGTCTGCACATTGGTTAGG	
hsa-miR-218-5p	TTGTGCTTGATCTAACCATGTG	
hsa-miR-223-3p	TGTCAGTTTGTCAAATACCCCAG	
hsa-miR-3689a-5p	*TGATATCATGGTTCCTGGGAG*	
hsa-miR-3689b-5p	*TGATATCATGGTTCCTGGGAG*	
hsa-miR-3689e	*TGATATCATGGTTCCTGGGAG*	
hsa-miR-432-5p	GGAGTAGGTCATTGGGTGGG	
hsa-miR-499a-5p	TTAAGACTTGCAGTGATGTTTGG	
hsa-miR-503-5p	CGGGAACAGTTCTGCAGG	
hsa-miR-522-3p	AAAATGGTTCCCTTTAGAGTGTG	
hsa-miR-760	CGGCTCTGGGTCTGTGGGGAG	
hsa-miR-891a-5p	AACGAACCTGAGCCACTGAG	
hsa-miR-16-5p	AGCACGTAAATATTGGCGG	**Candidate sEV-miRs normalizers**
hsa-miR-21-5p	GCTTATCAGACTGATGTTGAGGC	
hsa-miR-25-3p	TGCACTTGTCTCGGTCTGAG	
hsa-miR-125a-5p	CCTGAGACCCTTTAACCTGTGAG	
hsa-miR-148a-3p	CAGTGCACTACAGAACTTTGTGG	
hsa-miR-423-3p	GTCTGAGGCCCCTCAGTG	
hsa-miR-451a	AAACCGTTACCATTACTGAGTTGG	
hsa-miR-484	TCAGTCCCCTCCCGATG	

Upm2A	CCCAGTTATGGCCGTTTA	**Universal miQPCR primer**

sEV-miRs in italic indicates selectively detected only in sEV-MDA231 and not in the other sEVs.

Table B. List of specific primers used for EMT-markers gene expression evaluation

Genes	Forward (5'→3')	Reverse (5'→3')
ZEB1	AAGTGGCGGTAGATGGTAATG	AGGAAGACTGATGGCTGAAATAA
SNAIL (*SNAI1*)	CTTCCAGCAGCCCTACGAC	GACAGAGTCCCGATGAGCA
TWIST1	GCATCACTATGGACTTTCTCTATT	GCCAGTTTGATCCCAGTATT
E-CADHERIN (*CDH1*)	CGAGAGCTACACGTTCACGG	GGGTGTCGAGGGAAAAATAGG
N-CADHERIN (*CDH2*)	AGCCAACCTTAACTGAGGAGT	GGCAAGTTGATTGGAGGGATG
VIMENTIN (*VIM*)	CGGGAGAAATTGCAGGAGGA	AAGGTCAAGACGTGCCAGAG
FIBRONECTINA (*Fn*)	CGGTGGCTGTCAGTCAAAG	AAACCTCGGCTTCCTCCATAA
OCT4	AGGTATTCAGCCAAACGACCA	TCGATACTGGTTCGCTTTCTC
SOX2	AGCTACAGCATGATGCAGGA	GAGTAGGACATGCTGTAGGT
NANOG	CATGAGTGTGGATCCAGCTTG	CCTGAATAAGCAGATCCATGG
GAPDH	CTGGGCTACACTGAGCACC	AAGTGGTCGTTGAGGGCAATG

Table C. GO biological processes overrepresented by the targets (predicted and validated; miRWalk) of the 27 sEV-miRs enriched or selectively present in sEV-MDA231

GO Biological process	FC enrichment	Adjusted p value (FDR)
SMAD protein complex assembly	16.34	1.97E-2
Regulation of cardiac muscle cell differentiation	9.53	2.38E-2
DNA damage response, signal transduction by p53 class mediator resulting in cell cycle arrest	8.58	1.18E-2
Positive regulation by host viral transcription	8.41	3.32E-2
miRNA processing	8.41	2.26E-4
Small regulatory ncRNA processing	7.53	4.50E-4

DNA damage response, signal transduction by p53 class mediator	6.50	1.16E-3
Glandular epithelial cell development	5.92	4.35E-2
Negative regulation of cell-matrix adhesion	5.56	2.75E-2
Regulation of phosphatidylinositol 3-kinase activity	5.52	1.54E-3

GO Biological process	FC enrichment	Adjusted p value (Bonferroni)
miRNA processing	8.41	1.48E-2
Regulation of lipid kinase activity	5.39	3.25E-2
Response to hypoxia	3.1	1.95E-3
Mesenchyme development	2.99	3.50E-2
Apoptotic signaling pathway	2.71	2.42E-2
Gland development	2.57	4.94E-3
Positive regulation of cell migration	2.31	1.44E-2
Regulation of growth	2.28	2.11E-3
Positive regulation of cell motility	2.20	4.58E-2
Regulation of kinase activity	2.19	4.82E-4

Table D. GO molecular functions overrepresented by the targets (predicted and validated; miRWalk) of the 27 sEV-miRs enriched or selectively present in sEV-MDA231

GO Molecular function	FC enrichment	Adjusted p value (FDR)
RNA polymerase II CTD heptapeptide repeat kinase activity	11.00	2.73E-2
Transcription coactivator binding	6.65	2.26E-3
Transcription coregulator binding	3.76	5.33E-3
RNA polymerase II-specific DNA-binding transcription factor binding	2.40	4.75E-3
Transcription factor binding	2.39	2.75E-5
Ubiquitin protein ligase binding	2.38	1.77E-2
mRNA binding	2.37	1.15E-2
DNA-binding transcription factor binding	2.34	7.98E-4
Ubiquitin-like protein ligase binding	2.32	2.38E-2
Chromatin binding	2.08	2.69E-3
DNA-binding transcription activator activity	2.05	1.95E-2

DNA-binding transcription activator activity, RNA polymerase II-specific	2.00	3.78E-2
Protein domain specific binding	1.95	6.61E-3
Protein kinase activity	1.86	4.11E-2
Phosphotransferase activity, alcohol group as acceptor	1.82	2.69E-2
Kinase activity	1.79	2.42E-2
Protein kinase binding	1.78	4.05E-2
RNA polymerase II cis-regulatory region sequence-specific DNA binding	1.75	1.78E-3
Cis-regulatory region sequence-specific DNA binding	1.72	2.66E-3
Transferase activity, transferring phosphorus-containing groups	1.68	3.73E-2

Table E. Panther pathways overrepresented by the targets (predicted and validated; miRWalk) of the 27 sEV-miRs enriched or selectively present in sEV-MDA231

Panther pathway	FC enrichment	Adjusted p value (FDR)
Insulin/IGF pathway-protein kinase B signaling cascade	3.36	3.79E-2
Ionotropic glutamate receptor pathway	3.35	2.59E-2
p53 pathway feedback loops 2	3.22	2.40E-2
Alzheimer disease-amyloid secretase pathway	2.90	2.71E-2
Ras pathway	2.75	2.48E-2
p53 pathway	2.52	3.71E-2
Alzheimer disease-presenilin pathway	2.51	1.10E-2
TGF-beta signaling pathway	2.49	2.20E-2
Angiogenesis	2.39	3.79E-3
PDGF signaling pathway	2.37	1.51E-2

Table F. Reactome pathways overrepresented by the targets (predicted and validated; miRWalk) of the 27 sEV-miRs enriched or selectively present in sEV-MDA231

Reactome pathway	FC enrichment	Adjusted p value (FDR)
SMAD2/3 MH2 domain mutants in cancer	28.60	4.67E-2
SMAD4 MH2 domain mutants in cancer	28.60	4.55E-2
Loss of function of SMAD4 in cancer	28.60	4.44E-2
Signaling by TGF-beta receptor complex in cancer	20.43	4.14E-3
Loss of function of TGFBRI in cancer	19.06	2.50E-2
Loss of function of SMAD2/3 in cancer	19.06	2.40E-2
RUNX3 regulates CDKN1A transcription	16.34	3.38E-2
SMAD2/SMAD3:SMAD4 heterotrimer regulates transcription	9.83	8.12E-5
Oncogene induced senescence	8.67	2.88E-4
FOXO-mediated transcription of cell cycle genes	8.41	4.78E-2
Transcriptional activity of SMAD2/SMAD3:SMAD4 heterotrimer	7.46	1.80E-4
Signaling by TGF-beta receptor complex	5.80	1.38E-4
Intrinsic pathway for apoptosis	4.95	2.23E-2
Nuclear events (kinase and transcription factor activation)	4.22	4.01E-2
Signaling by TGFB family members	4.16	1.65E-3
MAP kinase activation	4.09	4.80E-2
TP53 regulates transcription of DNA repair genes	3.96	4.70E-2
FOXO-mediated transcription	3.96	4.60E-2
Signaling by FGFR2	3.96	4.50E-2
Interleukin-4 and interleukin-13 signaling	3.61	1.12E-2

Table G. EMT-regulating role of the 27 sEV-miRs enriched in metastatic sEV-MDA231

Mature sEV-miR	Fold Change			Role in EMT
	MDA231 vs ZR75	MDA231 vs T47D	MDA231 vs MCF10A	
miR-1-3p	118,2	1335,7	271,9	Supp
miR-10a-3p	3,2	28,6	82,1	Supp
miR-100-5p	**381,9**	**28,3**	**2,7**	**Prom/Supp**
miR-122-5p	**41,5**	**115,0**	**6,2**	**Prom**
miR-125b-1-3p	1248,3	931,1	3,2	Not reported (NR)
miR-126-5p	39,8	29,9	86,0	Prom/Supp
miR-133a-3p	55,7	41,7	19,0	Supp
miR-143-3p	20,3	7,0	10,9	Supp
miR-145-5p	20,4	15,5	43,6	Supp
miR-146a-5p	**57,5**	**51,6**	**148,8**	**Prom/Supp**
miR-199a-3p	5,7	2,6	2,8	Prom/Supp
miR-199a-5p	4,0	3,7	4,4	Supp
miR-199b-3p	4,9	2,6	2,6	Supp
miR-218-5p	29,2	22,0	2,7	Supp
miR-223-3p	**3,7**	**23,4**	**66,7**	**Prom**
miR-3689a-5p	NA	NA	NA	NR
miR-3689b-5p	NA	NA	NA	NR
miR-3689e	NA	NA	NA	NR
miR-432-5p	9,7	48,3	3,0	Supp-like
miR-499a-5p	39,8	3,2	3,2	Prom/Supp
miR-503-5p	207,2	154,7	3,6	Supp
miR-522-3p	2,6	15,5	10,8	Prom-like
miR-760	**3,1**	**48,6**	**2,6**	**Supp**
miR-891a-5p	20,4	15,5	9,6	NR
miR-1307-5p	3,2	9,3	3,2	NR
let-7d-5p	**2,5**	**2,3**	**4,4**	**Supp**
let-7i-5p	4,6	2,3	2,7	Supp

Table H. Variability among the candidate normalizers sEV-miRs evaluated by the NormFinder algorithm

Sample sEV-miR	MCF10A	T47D	ZR75	MDA231
miR-16-5p	22.77	18.60	23.12	23.69
miR-21-5p	23.17	19.23	25.42	23.10

miR-25-3p	25.75	20.16	24.12	24.32
miR-148a-3p	25.09	20.62	25.88	24.79
miR-423-3p	25.52	20.57	24.44	24.54
miR-484	26.15	21.35	26.61	26.26

Best sEV-miR: miR-16-5p

sEV-miR	Stability value	#
miR-16-5p	45478300905	3
miR-21-5p	37599177506	1
miR-25-3p	57187726640	4
miR-148a-3p	41000873062	2
miR-423-3p	73506652537	5
miR-484	154902779894	6

Best sEV-miR: miR-21-5p

sEV-miR	Stability value	#
miR-16-5p	0.023	3
miR-21-5p	0.042	5
miR-25-3p	0.032	4
miR-148a-3p	0.017	2
miR-423-3p	0.029	6
miR-484	0.003	1

Best sEV-miR: miR-484

sEV-miR	Stability value	Std. error	#
miR-16-5p	0.023	0.013	3
miR-21-5p	0.045	0.019	6
miR-25-3p	0.035	0.016	5

miR-148a-3p	0.004	0.022	1
miR-423-3p	0.025	0.013	4
miR-484	0.006	0.014	2

Best sEV-miR: miR-148a-3p

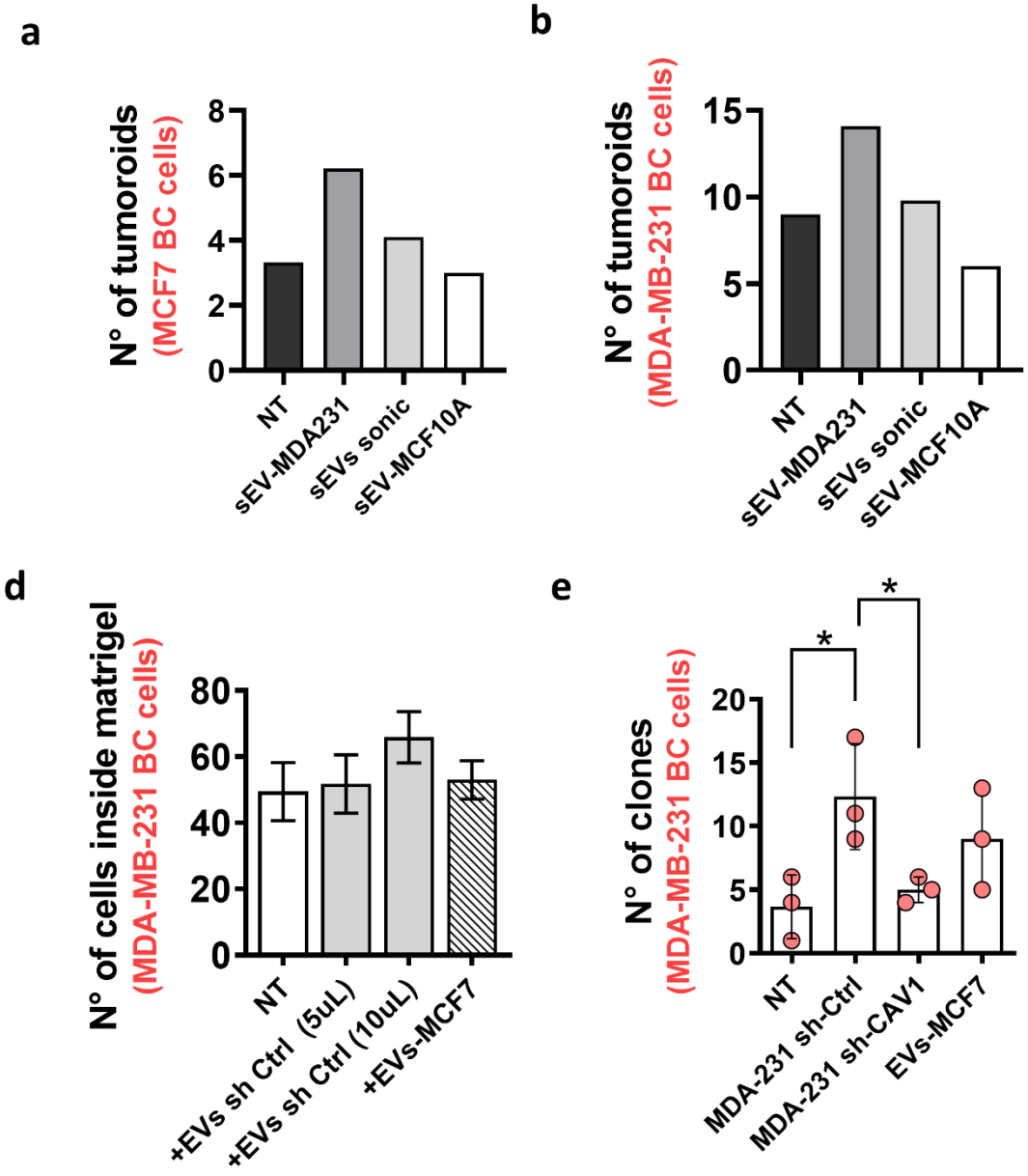

Figure S1. Effect of sEVs secreted by normal or non-metastatic BC cells over pro-metastatic capacities in BC recipient cells.

sEVs secreted by a normal MCF10A mammary epithelial cells or tumorigenic but non-metastatic BC does not promote pro-metastatic capacities in recipient cells. (a,b) sEVs secreted by a normal MCF10A mammary epithelial cells does not promote the tumoroid formation capacity of recipient

cells (MCF7 and MDA-MB-231). (c,d) sEVs secreted by MCF7 non-metastatic BC cells does not promote the invasion and colony formation capacity of recipient cells (MDA-MB-231) (preliminary results).

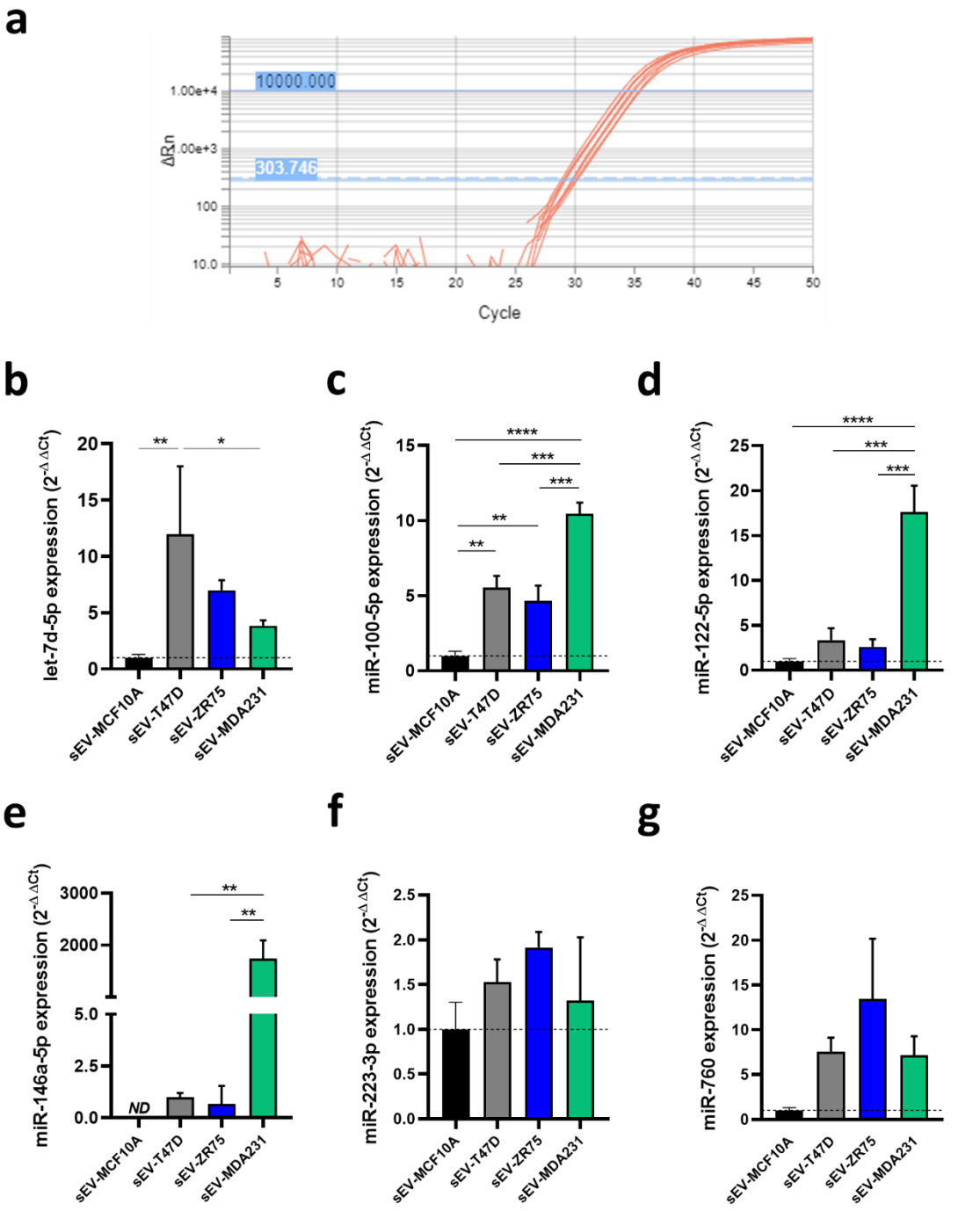

Figure S2. Validation of the presence and levels of "EMT-promoter" sEV-miRs in sEV-MDA231 through miQPCR using let-7i-5p as normalizer.

The twenty-seven candidate sEV-miRs enriched in sEV-MDA231 through the sRNA-seq analyses were experimentally tested by miQPCR and normalized against let-7i-5p levels. (a) Levels of let-7i-5p in the different BC cells-secreted sEVs. (b) miR-100-5p; (c) miR-122-5p; (d) miR 146a-5p; (e) let-7d-5p; (f) miR-223-3p and (g) miR-760. Graphs shows mean ± SD. All data is representative of 2-3 independent experiments.